EUROPEAID/139904/DH/SER/CN

'STRENGTHENING INTERNATIONAL OCEAN DATA THROUGH THE EU'S OCEAN DIPLOMACY WITH CHINA'

EMOD-PACE (EMODNET PARTNERSHIP FOR CHINA AND EUROPE)

Broad-scale habitat mapping in the Beibu Gulf, South China Sea. Final methodology report (D4.4 – M30 Report)

Work Package	Work-Package 4: Comparison of European and Chinese models for seabed habitat and ecosystem vulnerability
Lead Partners	Angel Borja (AZTI) and Eleonora Manca (JNCC)
Lead Author (Org)	Eleonora Manca (JNCC)
Contributing Author(s)	Lewis Castle (JNCC), Mickaël Vasquez (Ifremer), Susanna Kihlman (GTK), Kim Knauer (EOMAP); Lu Wenhai (NMDIS), Huang Haiyan (NMDIS), Zuo Guocheng (NMDIS); Fan Miao (NMDIS), Yu Jia (NMDIS), Ma Yong (NMDIS); Tao Yijun (NMDIS), Liu Chang (NMDIS), Xu Yan (NMDIS), Li Xiao (NMDIS), Yang Lu (NMDIS), Zhang Yujia (NMDIS); Li Qingyang (NMDIS), Wu Shuangquan (NMDIS), Yang Zhitong (NMDIS), Chen Qian (NMDIS); Thierry Schmitt (SHOM); Markus Lindh (SMHI); Angel Borja (AZTI)
Reviewers	NMDIS

The project "International Ocean Governance: Strengthening international ocean data through the EU's ocean diplomacy with China" is financed by the European Commission EuropeAid/139904/DH/SER/CN.

Due Date	19.12.2022, M33
Submission Date	16/11/22
Version	2

DISCLAIMER

This document contains information on EMOD-PACE project activities. Any reference to content in this document should clearly indicate the authors, source, organisation, and publication date.

The content of this publication is the sole responsibility of the EMOD-PACE Consortium. The authors of this document have taken any available measure in order for its content to be accurate, consistent and lawful. The information and views set out in this report are those of the author(s) and do not necessarily reflect the official opinion of the European Commission. The European Commission does not guarantee the accuracy of the data included in this study. Neither the European Commission nor any person acting on the European Commission's behalf may be held responsible for the use which may be made of the information.

VERSIONING AND CONTRIBUTION HISTORY

Version	Date	Authors	Notes
01		Lewis Castle (JNCC) Eleonora Manca (JNCC) Mickaël Vasquez (Ifremer)	Initial draft- Literature review; Model guidance
0.4		Lewis Castle (JNCC) Eleonora Manca (JNCC), Mickael Vasquez (Ifremer), Susanna Kihlman (GTK), Kim Knauer (EOMAP); Huang Haynan (NMDIS), Zuo Guocheng (NMDIS); Fan Miao (NMDIS), Yu Jia (NMDIS); Thierry Schmitt (SHOM); Markus Lindh (SMHI); Angel Borja (AZTI)	Draft methods, draft results and preliminary discussions
1		Lewis Castle (JNCC), Eleonora Manca (JNCC), Mickaël Vasquez (Ifremer), Susanna Kihlman (GTK), Kim Knauer (EOMAP); Lu Wenhai (NMDIS), Huang Haiyan (NMDIS), Zuo Guocheng (NMDIS); Fan Miao (NMDIS), Yu Jia (NMDIS), Ma Yong (NMDIS); Tao Yijun (NMDIS), Liu Chang (NMDIS), Xu Yan (NMDIS), Li Xiao (NMDIS), Yang Lu (NMDIS), Zhang Yujia (NMDIS); Li	Final comments, edits and formatting

		Qingyang (NMDIS), Wu Shuangquan (NMDIS), Yang Zhitong (NMDIS), Chen Qian (NMDIS); Thierry Schmitt (SHOM); Markus Lindh (SMHI); Angel Borja (AZTI)	
1.2	26/07/22	Eleonora Manca (JNCC); Mickaël Vasquez (Ifremer),	First draft of final report – updated methodology
1.3	30/09/2022	Eleonora Manca (JNCC) Lewis Castle (JNCC), Mickaël Vasquez (Ifremer), Susanna Kihlman (GTK), Kim Knauer (EOMAP); Lu Wenhai (NMDIS), Huang Haiyan (NMDIS), Zuo Guocheng (NMDIS); Fan Miao (NMDIS), Yu Jia (NMDIS), Ma Yong (NMDIS); Tao Yijun (NMDIS), Liu Chang (NMDIS), Xu Yan (NMDIS), Li Xiao (NMDIS), Yang Lu (NMDIS), Zhang Yujia (NMDIS); Li Qingyang (NMDIS), Wu Shuangquan (NMDIS), Yang Zhitong (NMDIS), Chen Qian (NMDIS); Thierry Schmitt (SHOM); Markus Lindh (SMHI); Angel Borja (AZTI)	Updates to input layers, improved habitat map, confidence assessments, and final discussions
2	16/11/2022	Eleonora Manca (JNCC) Lewis Castle (JNCC), Mickaël Vasquez (Ifremer), Susanna Kihlman (GTK), Kim Knauer (EOMAP); Lu Wenhai (NMDIS), Huang Haiyan (NMDIS), Zuo Guocheng (NMDIS); Fan Miao (NMDIS), Yu Jia (NMDIS), Ma Yong (NMDIS); Tao Yijun (NMDIS), Liu Chang (NMDIS), Xu Yan (NMDIS), Li Xiao (NMDIS), Yang Lu (NMDIS), Zhang Yujia (NMDIS); Li Qingyang (NMDIS), Wu Shuangquan (NMDIS), Yang Zhitong (NMDIS), Chen Qian (NMDIS); Thierry Schmitt (SHOM); Markus Lindh (SMHI); Angel Borja (AZTI)	Final draft submitted for comments by Chief Scientist

Summary

This report details the collaborative effort between partners from Europe and China to deliver the first broad-scale habitat map for a Chinese sea basin, using the EUNIS (European Nature Information System) approach, as part of Task 4.1 of the joint EMOD-PACE/CEMDNET project.

Broad-scale habitat models can be useful in data poor regions and, provide a full spatial coverage dataset on the distribution of habitat types, for very large areas (basin wide, national water, European waters) for application such as marine spatial planning or marine protected sites network assessments. EUNIS (European Nature Information System) broad-scale habitat map provide a first general picture of the variety and general types of physical habitats at the seabed and should be based on good understanding of key physical variables that drive the distribution of characteristics benthic communities.

The present report introduces the first broad-scale habitat map in an Asian sea basin, based on the EMODnet habitat mapping approach, and associated confidence datasets. The case study site selected for this work covers part of the Beibu Gulf, located in the north-western parts of the South China Sea. We include a summary of the methodology used, as well as a presentation the habitat map, its input layers and associated confidence assessments. Furthermore, we discuss limitations of the approach, applicability to Chinese sea basins and propose the next steps to improve in this work.

Table of Contents

Table of illustrations

Figures

Tables

1 Introduction

1.1 Aims

This report details the collaborative effort between partners from Europe and China to deliver the first broad-scale habitat map for a Chinese sea basin, using the EUNIS (European Nature Information System) approach, as part of Task 4.1 of the joint EMOD-PACE/CEMDNET project.

The present report aims to introduce the first broad-scale habitat map covering part of the Beibu Gulf, located in the north-western parts of the South China Sea. The report describes the methodology used and present and discuss the maps.

The habitat map and key layers produced as part of this project are made available through the map viewer of the EMODpace/CEMDNET portal [1]

1.2 EUNIS Broad-Scale Habitat Mapping in Europe

The concept of mapping seabed habitats using marine geophysical data was first formulated by Roff and Taylor (2000), and subsequently put in practice by Roff et al. (2003) for Canadian waters. Considering that mapping benthic animal and plant communities over extensive areas by direct sampling is impractical due to prohibitive costs, the authors advocated the use of enduring and recurrent seabed geophysical (i.e., geologic and oceanographic) factors as surrogates for benthic communities. Their mapping approach comprised i) classifying the oceanographic spatial data layers into ecologically relevant broad categories (e.g., light penetration into 'photic' or 'aphotic'; exposure to water motion into 'exposed' or 'sheltered') and ii) overlaying via GIS techniques the classified geophysical layers in order to produce a map of what they defined as benthic 'seascapes' (e.g. 'Photic-Exposed-Gravel'). This study has since inspired many initiatives worldwide.

In Europe the concept was tested on an international level by two European projects: BALANCE (2005-2007), and MESH (2004-2008). BALANCE produced marine landscape maps for the entire Baltic Sea (BALANCE, 2008). MESH developed a prototype broad-scale seabed habitat map for North-West Europe, for which efforts were made to adapt the method to the marine section of the EUNIS (European Nature Information System) habitat hierarchical classification scheme, widely used across Europe by managers and scientists (Coltman et al, 2008). This EUNIS-compliant MESH approach gave a strong impetus to initiatives of broad-scale habitat mapping across Europe, among which, the EUSeaMap cartography. As part of ur-EMODnet (2009-2012), the Seabed Habitats EMODnet thematic lot harmonised the MESH and the BALANCE approaches to deliver a prototype predictive seabed habitat map in four trial basins (Greater North Sea, Celtic Seas, Baltic, Western Mediterranean). This map was named EUSeaMap (Cameron and Askew, 2011). In EMODnet Phase 2 (2012-2016), the consortium extended EUSeaMap coverage to all European regions (Populus et al, 2017). In phase 3 (2017-2021), a first version (2019) extended the spatial coverage further North in order to include the Barents Sea, developed better environmental data were incorporated, and substantially improved the spatial detail (Vasquez et al., 2020). A second version (2021) has been recently released (Vasquez et

[1] EMODnet/CEMDNET portal
https://emodnet.ec.europa.eu/geoviewer/?layer_collections=EMOD_PACE#!/.

al,. 2021) in order to account for new seabed substrate data published by EMODnet Geology in 2021 and translate EUSeaMap in the new version of the marine section of EUNIS, named EUNIS 2019.

1.3 Introduction to habitat mapping and marine management in China

In recent years, China has stepped up efforts in the sustainable utilization and management of marine resources. The Ministry of Natural Resources of the People's Republic of China has established a marine ecological environmental monitoring system and has initially grasped the distribution of major ecosystem types through the continuous surveying of China's coastal zone. In addition, these efforts have been supplemented by the development of a marine ecological classification guide in 2020, alongside further investigations into ecological zonation in the China Seas (and adjacent waters) in 2021. The latter investigations provide a strong foundation to be able to apply the same habitat mapping techniques adapted in Europe, to China, through technical co-ordination and knowledge exchange. As an international common tool, habitat mapping can describe habitat types and characteristics in detail and has the potential to enrich management practices in China by supporting decisions relating to marine ecosystem management, such as supporting marine spatial planning and designation of marine protected areas.

2 Creating a Broad-Scale Habitat Map for the Beibu Gulf

2.1 Choice and introduction to the study area

The study site was selected following a kick-off meeting held in May 2020. Colleagues from NMDIS proposed the Beibu Gulf to be a suitable case study for the application of EUNIS mapping in China for several reasons:

- There was a lack of knowledge relating to deep-sea benthic communities in the South China Seas, restricting the scope of the study area to coastal regions;
- NMDIS had selected the site for the development of a pilot national classification system hence data sourcing was already started;
- Availability of key physical (bathymetry and substrate) and biological datasets for the area;
- The relatively clear coastal waters of the gulf provided strong prospects for being able to utilise satellite data for determining light attenuation

The Beibu Gulf, also known as the Gulf of Tonkin, is located in the north-western parts of the South China Sea and is situated between China and Vietnam (Figure 1). It is a relatively shallow gulf covering an area of over 128,000km^2, with an average depth of ~40m and a maximum depth of less than 100m. It is considered a major estuarine system (Laio et al., 2018), containing over 200 rivers (Qiao et al., 2008) and is supplied with large quantities of terrigenous nutrients, resulting in high marine productivity (Wang et al., 2014). The productive waters are favourable to a number of commercially important fish stocks, making it one of the four main fish farming regions of China (Shen et al., 2018).

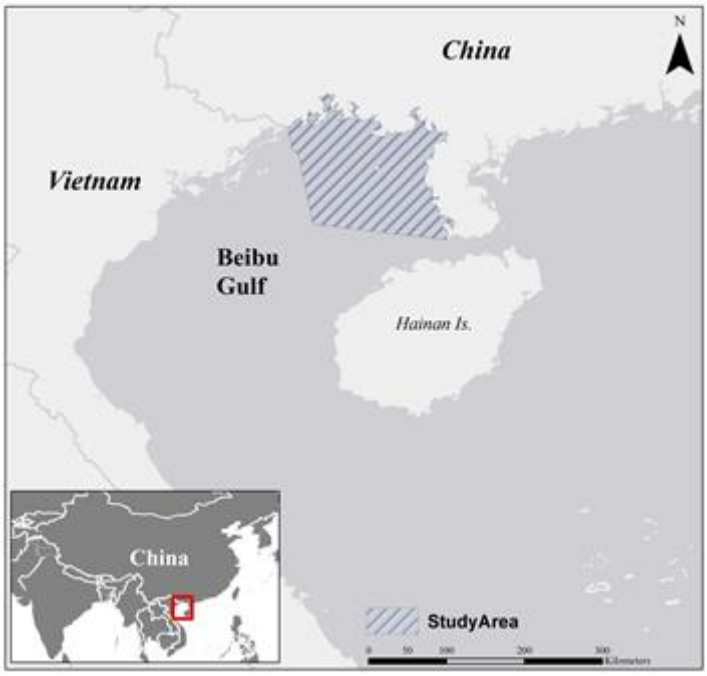

Figure 1. Location of the study area within the Beibu Gulf. Inset map shows the location of the Beibu Gulf in relation to China.

The gulf exhibits a sub-tropical climate and is largely influenced by the East Asian Monsoon system (Lai et al., 2014). Seafloor temperatures and salinities remain relatively uniform throughout the seasons, ranging between 33-34PSU and 24-27°C (Chen et al., 2011). Waves are generated by diurnal tides in the west and semidiurnal tides in the east, which propagate eastwards where they decrease in amplitude significantly (Shi et al., 2002). The distribution of sediments is heavily influenced by currents and circulation in the gulf, which is reportedly much stronger towards the coast. Soft sediments are dominant in the gulf, comprised mainly of well-sorted fine sand, fine sediment and gravel (Ma et al., 2019). Information on the distribution of hard substrates is limited to the presence of coral reefs along the east coast of the gulf and surrounding Weizhou and Xieyang Island (see Figure 19). Coastal habitats in the areas include mangroves, mudflats, sandflats, saltmarshes, tidal creeks, seagrass beds and coral reefs (Xie et al., 2020).

2.2 Principles and approach to EUNIS broad-scale habitat mapping

Due to the practical problems and high costs associated with direct mapping of the seabed, coupled with the vastness of the area being mapped, a fundamental principle in the creation of broad-scale habitat maps is that of Connor et al. (2006):

"[it is] recognised [that there is] strong correlation between environmental parameters and ecological character, such that mapping environmental parameters in an integrated manner can successfully be used to produce ecologically relevant maps."

In other words, it is possible to produce a 'predictive map' of expected seabed habitat types by combining a series of proxy measurements, such as water depth and light levels, and using statistical analysis and a set of rules for combining spatial information in a geographical information system (GIS).

Principal drivers for seabed habitat distributions depend on the biogeographic region but can include the type of movements, among others. To describe the variation in environmental conditions with depth, EUNIS divides subtidal habitats into zones: infralittoral, shallow circalittoral (or circalittoral), deep circalittoral, and deep sea (Figure 2), seabed substrate (rock, mud, mixed sediment, etc.), depth, light availability, oxygen, salinity and the energy of water.

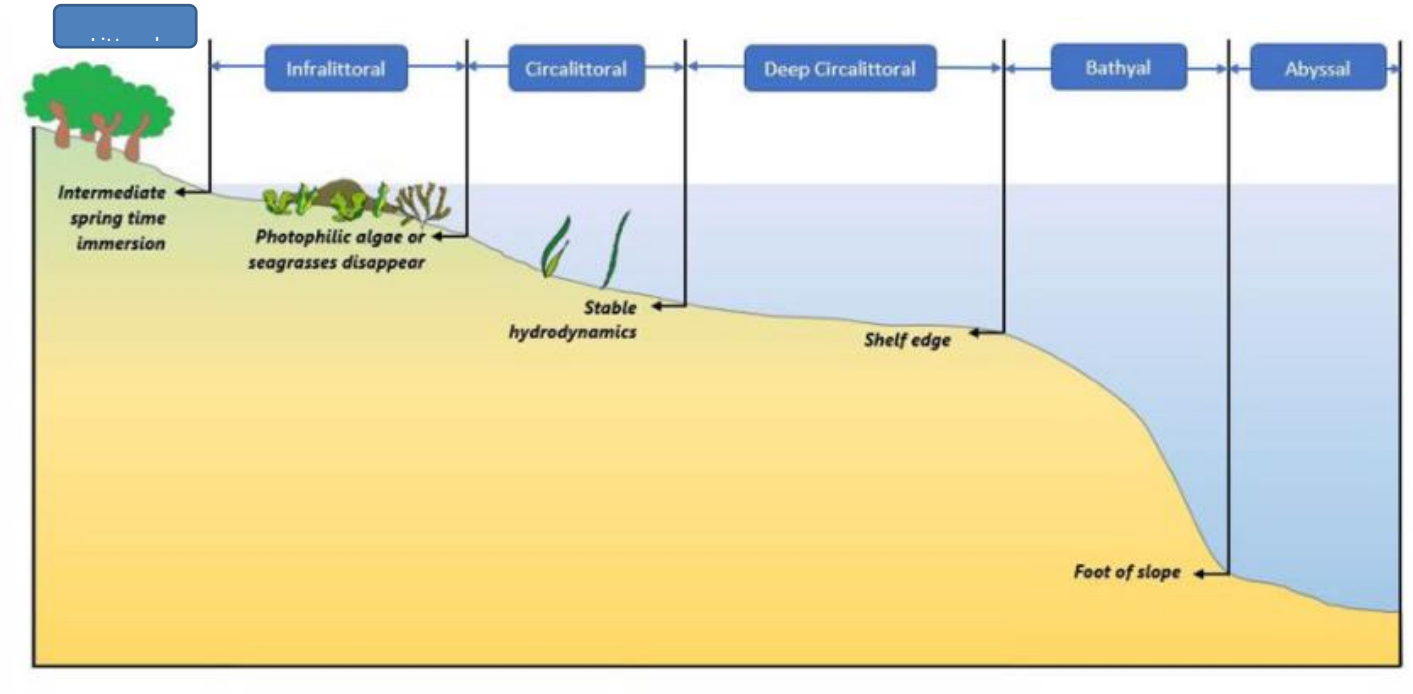

Figure 2. The division of marine sublittoral habitats into biological zones (©MESH Atlantic Blue Box, 2013).

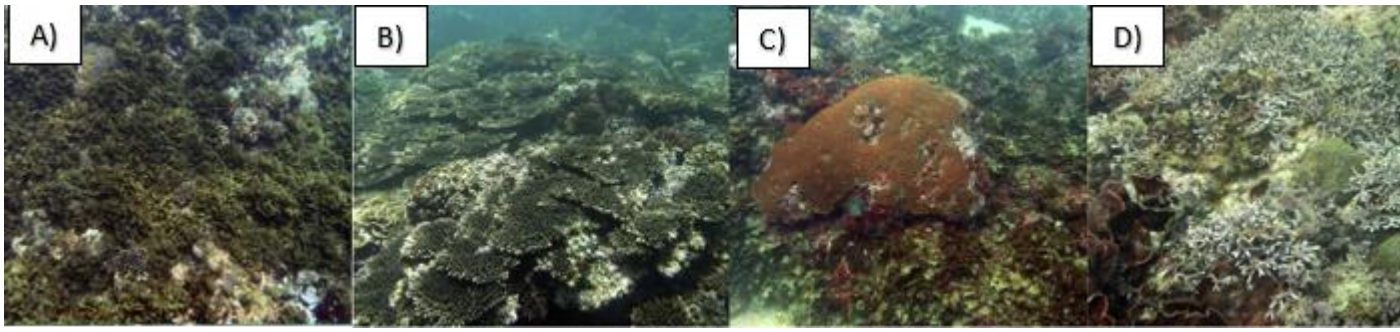

Figure 3. Examples of circalittoral biotopes within the Beibu Gulf, found south of Wengchang City, Hainan Island (see Figure 2. from Li et al., 2015). A) Communities of Loborphora variagata, B) Communities of Acropora c) Massive coral communities. d) Calcified algal communities.

Another factor that can be fundamental in driving habitat types is the degree of exposure to wave and water-current energy. For some basins that are more enclosed, other parameters, such as salinity, presence of large rivers, oxygen levels and temperature of water at the seabed, are also considered to be fundamental for habitat mapping. For example, the salinity regime is considered in the EUSeaMap habitat model of the Baltic Sea.

The broad-scale habitat mapping approach is normally applied to subtidal areas, as opposed to intertidal areas, because they are relatively data poor. Modelling is the most effective way to provide information on habitat types across very large areas, specifically where data availability is limited. Intertidal areas are generally more accessible and can be surveyed relatively accurately using satellite, LIDAR, aerial photography, or Drone images. Furthermore, the extent of intertidal habitats can be effectively estimated in large littoral habitats (see Figure 2) and are therefore not modelled for the Beibu Gulf, as we believe that there are better ways to gather data in this area.

2.3 Overview of the broad-scale habitats model

The broad scale habitat model for the Beibu Gulf, was developed in ESRI™ ArcGIS ModelBuilder, and can be saved and executed multiple times, which ensures the systems are repeatable and easily updated when new layers or methodologies are available.

The ArcGIS model applies a multicriteria evaluation to habitat mapping. This method is well-established in Europe, successfully producing four iterations of EMODnet's broad-scale predictive habitat map for Europe (EUSeaMap) since 2010 (Cameron and Askew, 2011, Populus et al., 2017, Vasquez et al., 2020, Vasquez et al., 2021). In general terms, the model stacks a suite of classified environmental variables on top of each other in a way that, when the values of each environmental variable are combined, a unique code is generated to correspond with a specific habitat type (Figure 4).

In more detail, the model first requires each environmental variable to be organised, manipulated, and classified into biologically meaningful classes in a way that mirrors how different habitat classes are separated in the EUNIS classification system. Typically, environmental variables are recorded as continuous values, so to separate values into a specific category, a threshold is applied (see section 2.6 for more details). The result is a set of categorised environmental data layers whose grid cell values are represented by a code. When each of the categorised environmental data layers are stacked on top of each other, the model combines the codes from each intersecting grid cells across all layers, to form a new unique code. The model then uses a look-up table to translate the unique model codes into different EUNIS habitat types (see SECTION 5.2 Appendix 2 for more details).

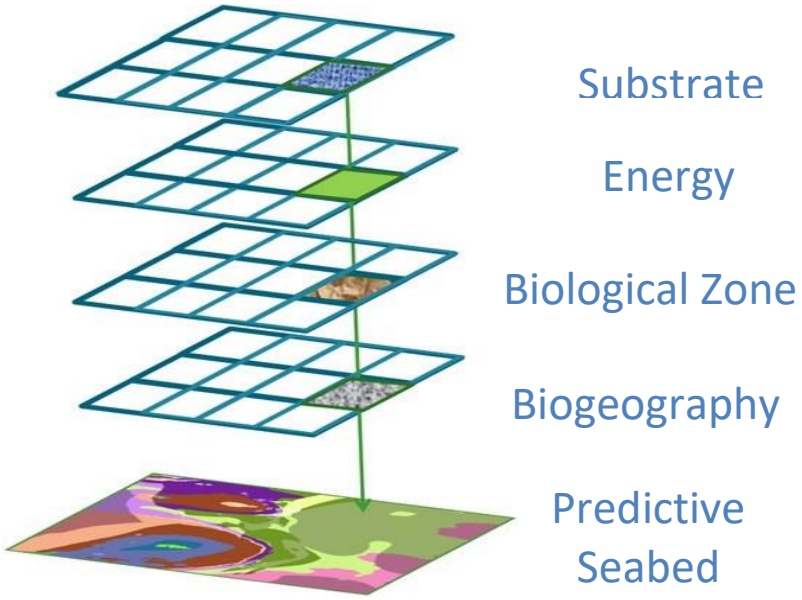

Figure 4. Illustration of how a typical broad scale habitat mapping ArcGIS model applies the multicriteria evaluation approach.

2.4 Confidence assessment

An instrumental part of the predictive habitat modelling process is being able to communicate the overall uncertainty of the habitat map to its users, achieved through the application of a confidence assessment. Confidence assessments are initially performed on the continuous physical datasets (e.g., kDPAR, Depth to the seabed), which informs the confidence in the classified habitat descriptors (e.g., biological zones), and in turn informs the overall confidence of the broad-scale habitat classes. It is important to mention that confidence scores are not a mathematical definition, such as sensitivity, specificity of kappa scores calculated in species distribution modelling, but are qualitative measure for users to readily compare the reliability of datasets – assigning labels of low, medium, or high. The confidence of continuous physical variables considers factors such as the number of remote sensing images used to generate the average values recorded in each grid cell. Confidence in the habitat descriptor classes considers the fuzziness in the thresholds used to delineate between two classes, accounting for the natural transition between one habitat descriptor, to another. The overall habitat classes' confidence is an aggregation of the confidence in threshold values and the confidence in values of continuous physical variables (see Figure 5).

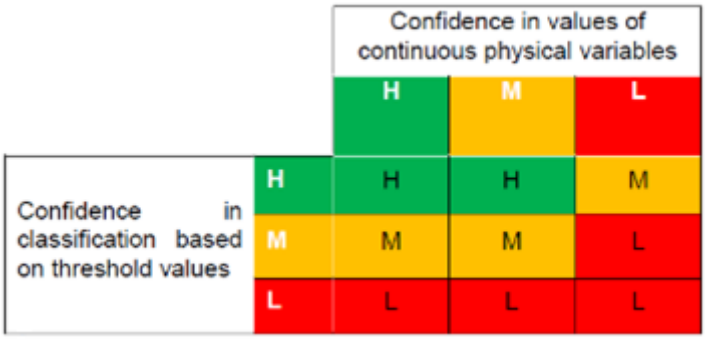

Figure 5 Logic used for combining confidence scores given to continuous physical variables and threshold values are aggregated and assigned to the overall habitat classes determined by the broad-scale model (Adapted from Populus et al,, 2017).

The confidence assessment includes confidence assessments for the input layers, classified habitat descriptors and confidence in the final habitat types. Detailed methods used to create each confidence layer are described in Section 5.2 (Appendix II: Model Guidance).

2.5 Selection of the input data

To fulfil the data needs of the EUNIS habitat modelling methods, a conceptual model (Figure 6) and an inventory of the physical and biological datasets held by project partners were produced. The properties of each dataset were reviewed, and datasets were selected, based on coverage, spatial resolution and quality and following NMDIS expert advice. The final list of datasets used as input to the model is shown in Table 1.

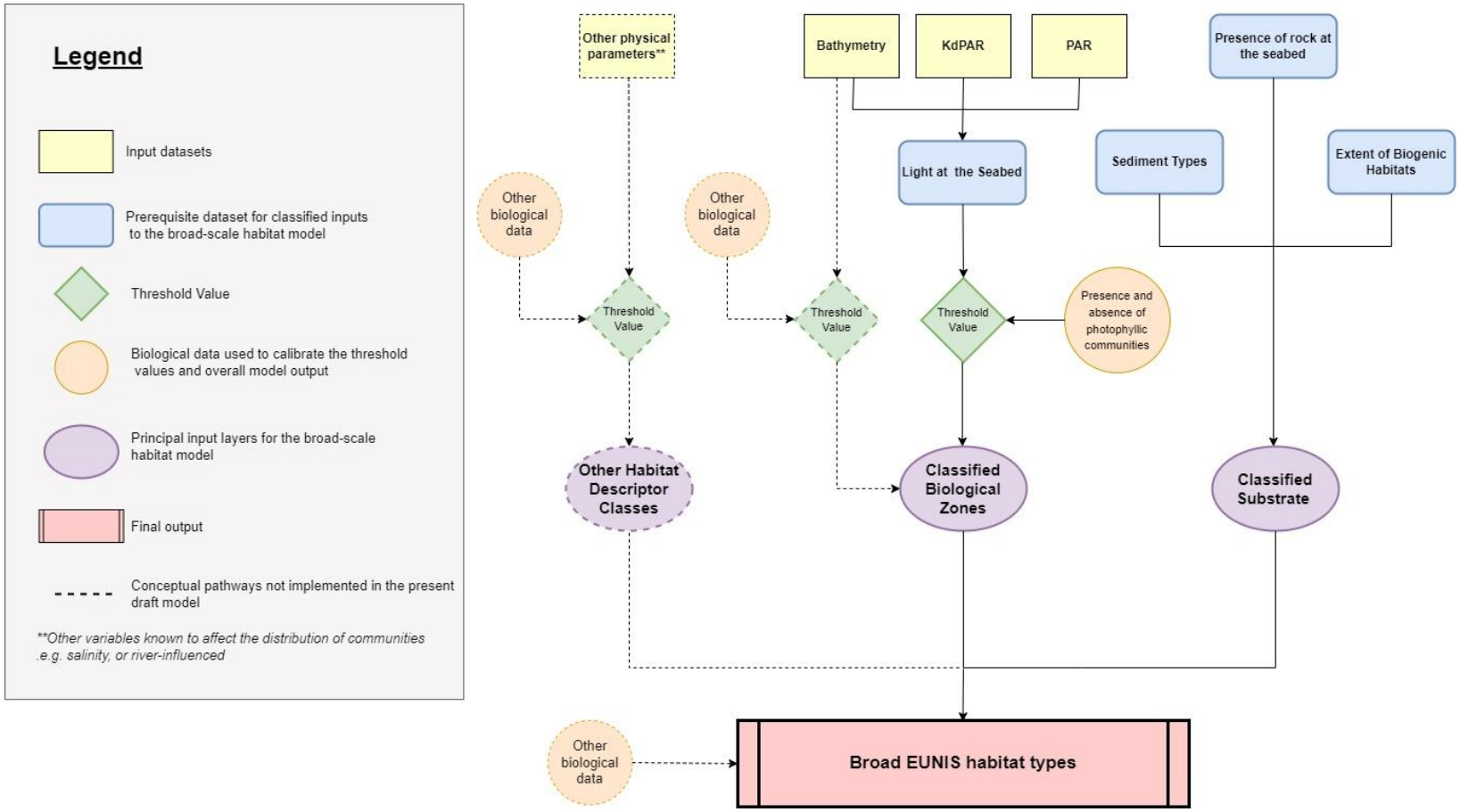

Figure 6. Conceptual model for the creation of the broad-scale habitat map of the Beibu Gulf. Dashed pathways are conceptual and could not be implemented in the present pilot model.

The project “International Ocean Governance: Strengthening international ocean data through the EU’s ocean diplomacy with China” is financed by the European Commission EuropeAid/139904/DH/SER/CN.

Table 1. Final list of datasets used to create all input layers for the broad-scale habitat model.

Dataset type	Data source	Parameter	Coverage	Spatial resolution	Temporal resolution	File type
Bathymetry	NMDIS Multibeam bathymetry dataset	Depth (m)	See Figure 7	50m	2008-2009	Geotiff and IMG (ERDAS IMAGINE format)
Bathymetry	Singlebeam bathymetry dataset	Depth (m)	See Figure 7	500m	2008-2009	Geotiff and IMG (ERDAS IMAGINE format)
Bathymetry	NMDIS Chart Soundings	Depth (m)	See Figure 8	Between 1:2000 to 1:500,000	2013-2020	Geotiff derived from shapefile
Bathymetry	General Bathymetric Chart of the Oceans (GEBCO) Global bathymetry map (Version 2020)	Depth (m)	Global	15 arc-sec	Version 2020	netcdf
Bathymetry	MSB_CHN_Beibu_EOMAP_2021_100m_CD Raster created by interpolating nautical chart points	Depth (m)	Sea Figure 7	100m	Unknown -2021	Geotiff
Substrate - sediment	NMDIS Special survey of China's offshore	Sediment classes (Folk Classification)	Full for study area	Polygon data - distance between sampling stations 5km	2007-2008	shapefile

The project “International Ocean Governance: Strengthening international ocean data through the EU’s ocean diplomacy with China” is financed by the European Commission EuropeAid/139904/DH/SER/CN.

Dataset type	Data source	Parameter	Coverage	Spatial resolution	Temporal resolution	File type
Substrate – rock	NMDIS Special survey of Guangxi province coast	Bedrock boundary	Guangxi Province	Polygon data	2006-2007	shapefile
Substrate - coral	NMDIS 2020 Coral reef survey	Extent of coral reefs/coral habitats	Available data in study area	Polygon data	2019-2020	shapefile
Substrate - coral and rock	Allen Coral Atlas	Benthic Habitat (Classes include Coral/Algae, Rock, Rubble, Sand, Seagrass)	Weizhou and Xieyang Island	3.125m	2018-2021	shapefile
Geomorphology layer	Geomorphology Map and Paper China offshore Marine Comprehensive Survey and Evalution Project	Geomorphology types	Beibu gulf	Polygon data	2017	shapefile
Optical properties	EU Copernicus Remote sensing imagery	PAR and KdPAR	Beibu Gulf	300m	Daily	Geotiff

2.5.1 The bathymetry layer

Typically, there is a marked zonation of communities that spans from the top of the shore, through the intertidal and down to the plains of the deep sea. Although zonation is not directly linked to depth, there are a number of other environmental factors which influence zonation that are linked to depth. For example, the amount of light reaching the seafloor decreases with depth, and so there will be a natural transition from communities dominated by photosynthetic organisms to communities that thrive under gloomy conditions. Therefore, having a full-coverage bathymetric dataset of the study area is an important first step in being able to determine the biological zones described in EUNIS.

A composite bathymetry layer covering the entire study area was created by combining data from five separate sources (See Table 1). Multibeam and singlebeam data were sourced from surveys between 2008 and 2009, the former covering the northern portion of the Beibu Gulf and the latter covering the central and eastern portion of the Gulf (Figure 7). Data obtained from these surveys were cleaned and validated using CARIS HIPS and SIPS software.

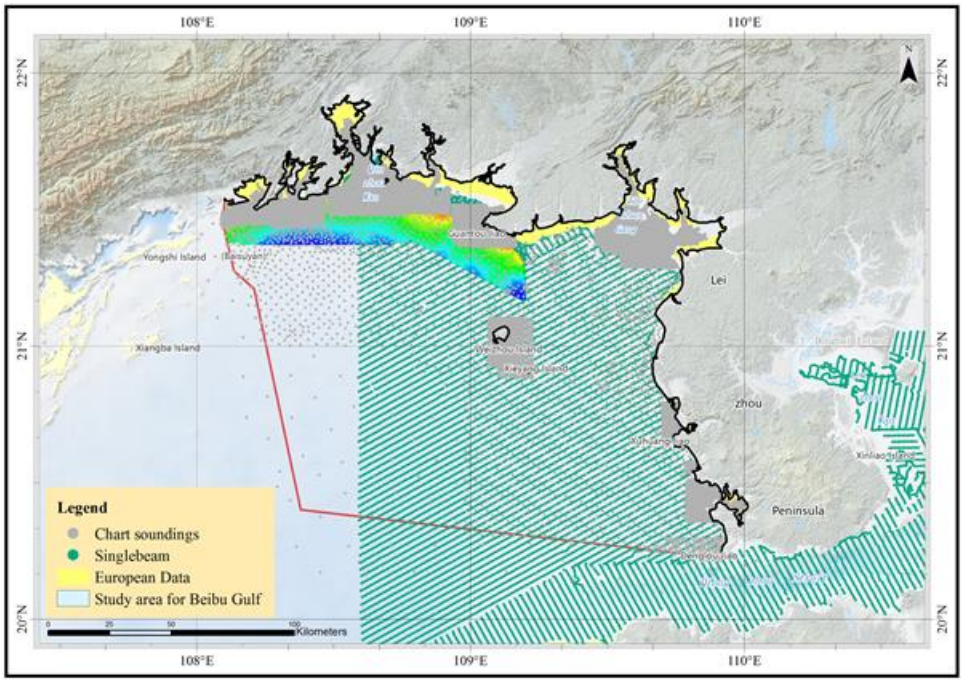

Figure 7. Distribution of bathymetry datasets within the study area. The coverage of multibeam data is indicated by the rainbow colour ramp, the coverage of single beam data is indicated by horizontal stripes. Chart soundings are indicated by grey points and yellow polygons shows coverage of European data (multisource bathymetry from soundings).

NMDIS sources Nautical chart soundings by China Authority in the shallow coastal areas of the Beibu Gulf which were not covered by the multibeam and singlebeam dataset. These data were obtained between the years 2013 and 2020, and at scales varying between 1:2000 to 1:500,000 (Figure 8). Additional sounding data was extracted from a global commercial repository and compared to the national depth sounding (see Figure 7) and showed significant differences. The global depth sounding were outdated compared to NMDIS national data, hence these were ultimately excluded from the harmonisation process. Vertical reference for all datasets was lowest normal low water.

In the estuarine areas, we compared SDB (Satellite derived bathymetry) data with the multisource batyhmetric data provided by EOMAP and created using soundings from a global repository (refer to as “European data” in Figure 7). EOMAP raster was more reliable than SDB raster, due to high load of sediment in the water.

Finally, the GEBCO global bathymetry data (version May 2020, 15 arc seconds resolution) datasets were used to cover the remaining South West sector of the study area.

The project “International Ocean Governance: Strengthening international ocean data through the EU’s ocean diplomacy with China” is financed by the European Commission EuropeAid/139904/DH/SER/CN.

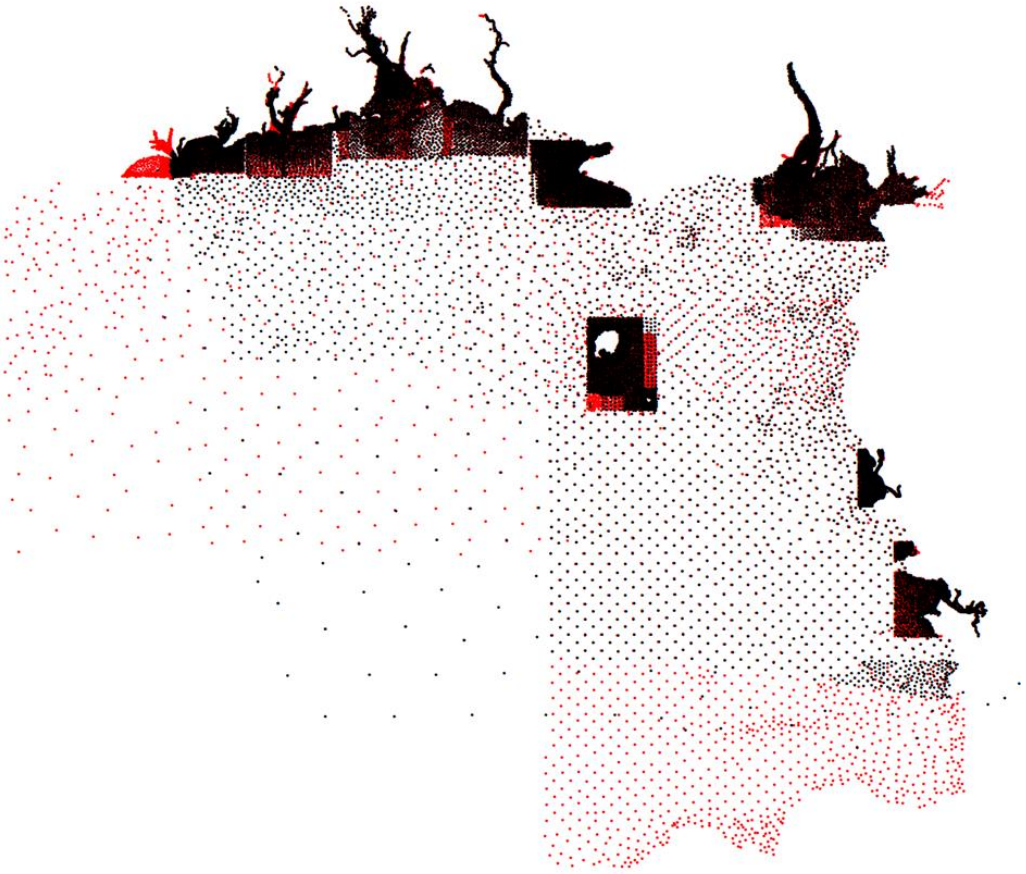

Figure 8. Comparison of the distribution of bathymetry sounding data in the Beibu Gulf. Red points represent national chart sounding data, whilst black dots represent depth sounding from a global repository.

To create the composite bathymetry layer, a single lower resolution bathymetry grid of 500m was first produced, using Generic Mapping Tools (GMT, https://www.generic-mapping-tools.org/). Here, a 'BlockMedian' function was performed on each of the datasets to interpolate results in areas containing low densities of chart soundings (Figure 8). Results were subsequently interpolated and gridded using a 'surface spline in tension' function and resampled to a higher resolution of 200m for use as a base grid.

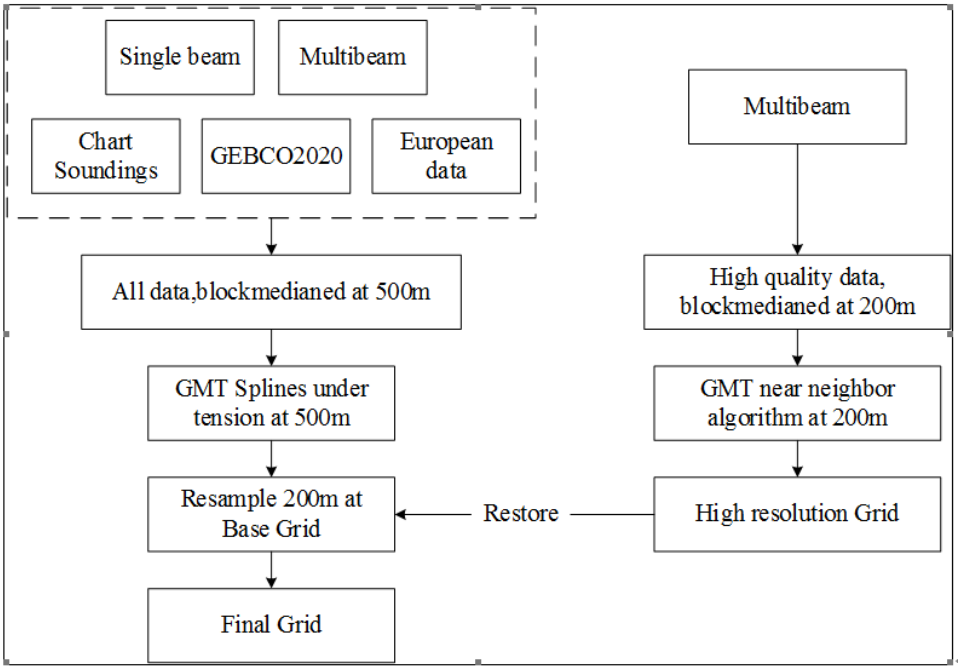

Figure 9. Flow diagram detailing the process by which the five bathymetry datasets were combined into a single layer. The left side represents the production of the low-resolution base layer, whilst the right side represents the production of supplementary high-resolution data.

A second grid of the same resolution (200m) was then produced in areas covered by denser soundings (multibeam), utilizing the same methods, however, applying the 'nearest neighbour' algorithm instead. The flow diagram in Figure 8 describes the data processing steps. The two layers were then combined using the remove-restore method, which retains details of the seafloor morphology in areas of higher data density and quality, whilst preventing the occurrence of artefacts in areas where data were sparse (Hell & Jakobsson, 2011). In detail, the differences in depth values between the two datasets were gridded using the 'surface spline under tension' function and values are then added on to the base layer. Overall, this process results in the smoother merging of a higher resolution dataset, with a lower resolution resampled dataset - producing a final grid for the entire study area at 200m resolution. The resulting bathymetry map shows good detail in shallow waters (Figure 10) and it is a clear improvement on the GEBCO 2020 grid.

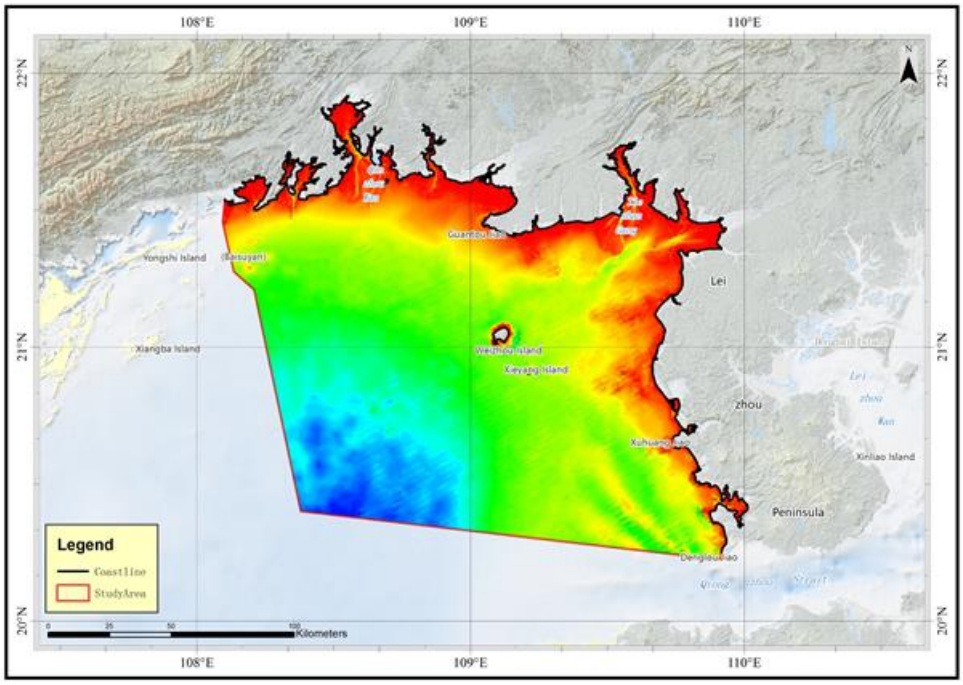

Figure 10 Composite bathymetry dataset covering the entire study area within the Beibu Gulf with a 200m resolution grid.

2.5.2 Confidence in the bathymetry layer

Confidence in the bathymetry layer (Figure 11) was assessed following Guidance document available from EMODnet Bathymetry[2], based on characteristics of the datasets such as age, sounding density and uncertainty of positioning. Scores were assigned to the various data sources as outlined in the table below.

Table 2 Bathymetry datasets confidence scores for the Beibu Gulf

Data type	Data source	EMODnet confidence score	Confidence class
Bathymetry	NMDIS Multibeam bathymetry dataset	76.9	High
Bathymetry	Singlebeam bathymetry dataset	53.8	Moderate
Bathymetry	Chart Soundings	92.3	High

[2] EMODnet Bathymetry guidance on DTM quality assessment available at https://www.emodnet-bathymetry.eu/media/emodnet_bathymetry/org/documents/emodnet_bathymetry_quality-index_application_version05022021.pdf

Bathymetry	General Bathymetric Chart of the Oceans (GEBCO) Global bathymetry map (Version 2020)	7.7	Low
Bathymetry	(European Data DTM) MSB_CHN_Beibu_EOMAP_2021_100m_CD	30.8	Low

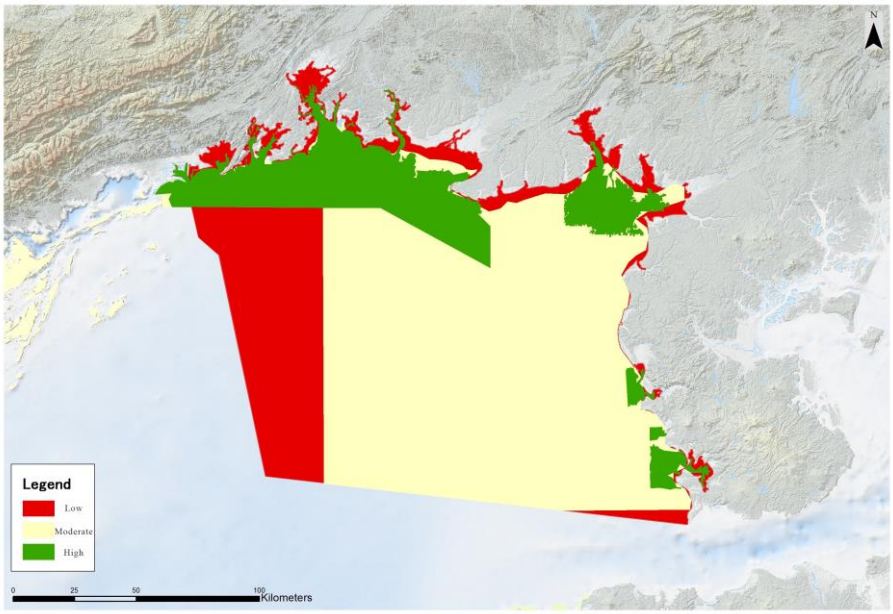

Figure 11 Bathymetry confidence map.

2.5.3 Fraction of light at the seabed layer

The availability of light at the seabed is used for the determination of the boundary between the infralittoral and circalittoral biological zones. The fraction of light reaching the seabed (Fr) is calculated using information on the depth to the seafloor (h) and the diffuse attenuation coefficient of photosynthetically available radiation in the water column (KdPAR), using the formula below:

$$\frac{I_h}{I_0} = Fr = e^{-h.Kd_{PAR}}$$

Light attenuation is usually quantified as the diffuse attenuation coefficient of the downwelling spectral irradiance at wavelength 490 nm (Kd490) or the photosynthetically available radiation (KdPAR). In this project, KdPAR was calculated from Kd490 using the approach proposed by Son & Wang (2015), which combines two different non-linear conversion formulae from Wang *et al.,* 2009 and Morel *et al.,* 2007. The two conversion formulae have differing levels of accuracy as they are designed for clearer and turbid waters respectively, however, this approach uses a weighted sum of

the two approaches (based on water leaving reflections at 490 nm and 670 nm) as a unified calculation that can be applied to sea basins with varying water clarity. The weighting factor is:

-1.175 + 4.512 * reflectance_670 / reflectance_490 for 0.2604 ≤reflectance_670 / reflectance_490 ≤ 0.4821. 0 if reflectance_670 / reflectance_490 < 0.2604 and 1 if reflectance_670 / reflectance_490 > 0.4821.

Kd490 values were obtained from absorption and scattering parameters of Sentinel-3 satellite data using the approach proposed by Heege et al., 2003, with a spatial resolution of 300m for the entire Beibu Gulf and the years 2017 to 2020 (Figure 12). Water ingredient data were downloaded automatically from Creodias and imported into EOMAP's Modular Inversion Program (MIP), which calculates the highest likelihood to explain the observed Top of Atmosphere (TOA) radiances of the satellite scene under consideration and water leaving reflectances. Several correction modules were applied such as a land and cloud masking, and the calculation of in-water absorption and scattering was derived before the actual KdPAR derivation as described above. Automatic quality checks and an aggregation to annual mean datasets were conducted subsequently. In addition to the annual means (Figure 12), uncertainty layers were derived to be able to calculate the error propagation for the final habitat map.

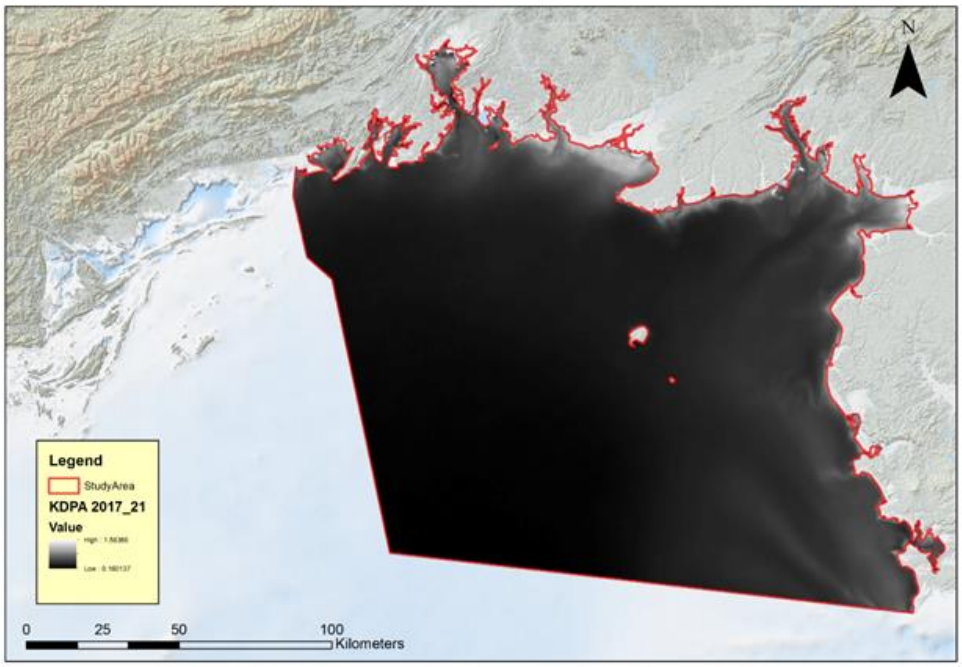

Figure 12. Diffuse attenuation coefficient of photosynthetically active radiation in the water column (KdPAR) within the study area. Values averaged for year 2017 to 2021 are in m^{-1}.

The resulting spatial datasets of Fraction of light reaching the seabed (Fr) is shown in Figure 13. Confidence in the Fr values (Figure 14) was calculated from information on the quality of KdPAR (number of satellite images) and confidence in the bathymetry data , with a method described in Section 5.2(Appendix II: Model Guidance).

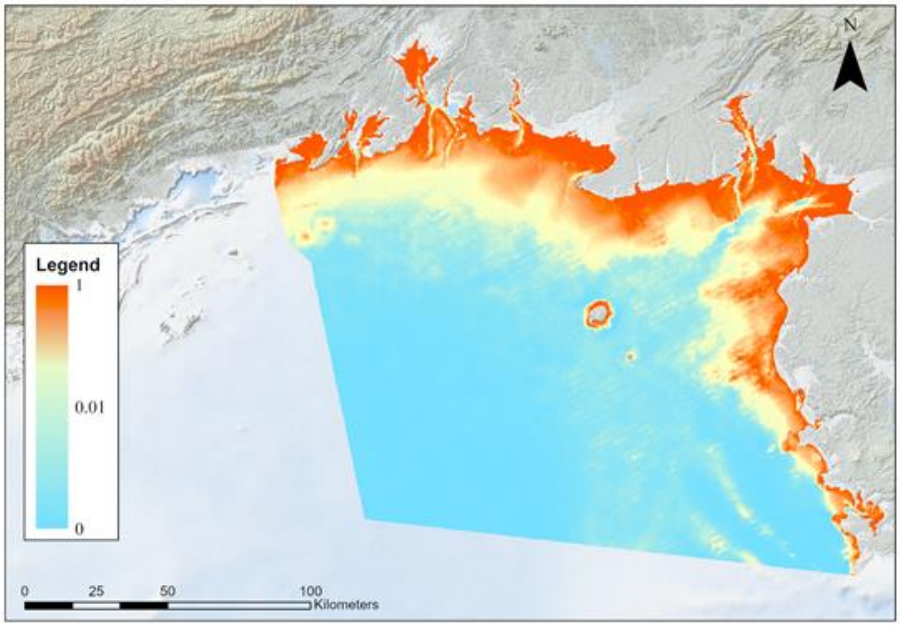

Figure 13. Fraction of light reaching the seabed (Fr) within the Beibu Gulf.

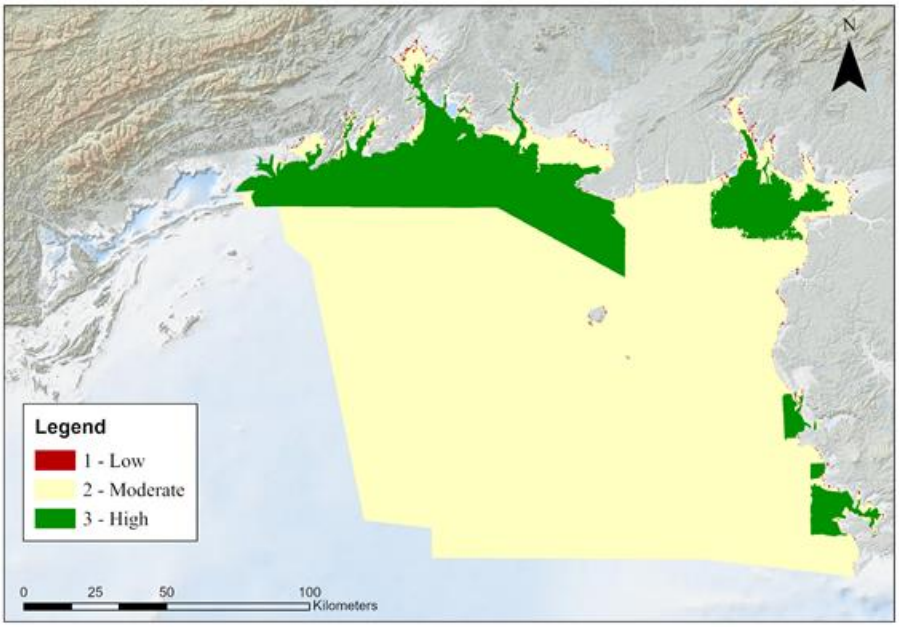

Figure 14 Confidence map in fraction of light reaching the seabed

2.5.4 The substrate layer

Benthic communities are generally divided by those living within the sediment (infauna) or on the surface of the sea floor (epifauna). The species composition of these communities are strongly

influenced by the substratum type, which can vary from rock, boulders, gravels, sands and muds. The EUNIS classification system places considerable emphasis on substratum in the early levels of the hierarchy, and so having a full coverage map of substrate classes is crucial.

A sediment sample dataset that was used to create the substrate layer of the Beibu Gulf, was obtained from three surveys implemented in 2007. The data covers most of the coastal and offshore areas and consists of surface sediment samples (0-20 cm depth) from evenly arranged 1000 sediment data stations, with an interval of 5km. Samples were collected by using box samplers or grab corers. Very shallow areas were surveyed independently using smaller boats and a grab corer was used for sampling. Diver surveys were not performed. Seismo-acoustic data, such as multi-beam echo sounder were collected for bathymetry in the Beibu Gulf area, but the backscatter data were either missing or of poor quality, so these data were not utilized in the Beibu Gulf substrate map.

Different methods were used to analyse and classify the sediment sample dataset. Grain size analysis was used to determine the particle size distribution of each sample: The laser particle size analysis for finer fractions, and sieving for the coarser, gravel size components. Analysis followed the grain size limits of Wentworth (1922), and the laser particle size analysis was repeated on 5% of the samples to ensure the quality of the data. Each datapoint was given a substrate type based on the grain size distribution and Folk (1970) classification. This point source dataset was then interpolated to a raster layer using kriging as a method. Finally, substrate polygons were drawn based on the spatial interpolation result, combined with bathymetry and a schematic layer of longshore current in the area as a reference. Achieved data layer was estimated to be sufficient for mapping at 1:100 000 scale. Other used methods and information included smear identification, physical and mechanical properties, sample description records and image data. Different sediment sources (land, biological, anthropogenic) were distinguished based on the marine field survey records. The sediment classification system (Folk et al., 1970), which was used to create the original Beibu Gulf substrate layer, is based on the ratios of different sediment grain size fractions Mud, Sand and Gravel. Additionally, ratios of Clay, Silt and Sand is used to classify further the fine-grained sediments if the gravel content is ≤ 0.01%. Altogether nine of these Folk (1970) substrate classes were present at the research area: Mud (M), Silt (Z), sandy Mud (sM), sandy Silt (sZ), muddy Sand (mS), silty Sand (zS), Sand (S), gravelly Sand (gS) and gravelly muddy Sand (gmS) (Figure 15).

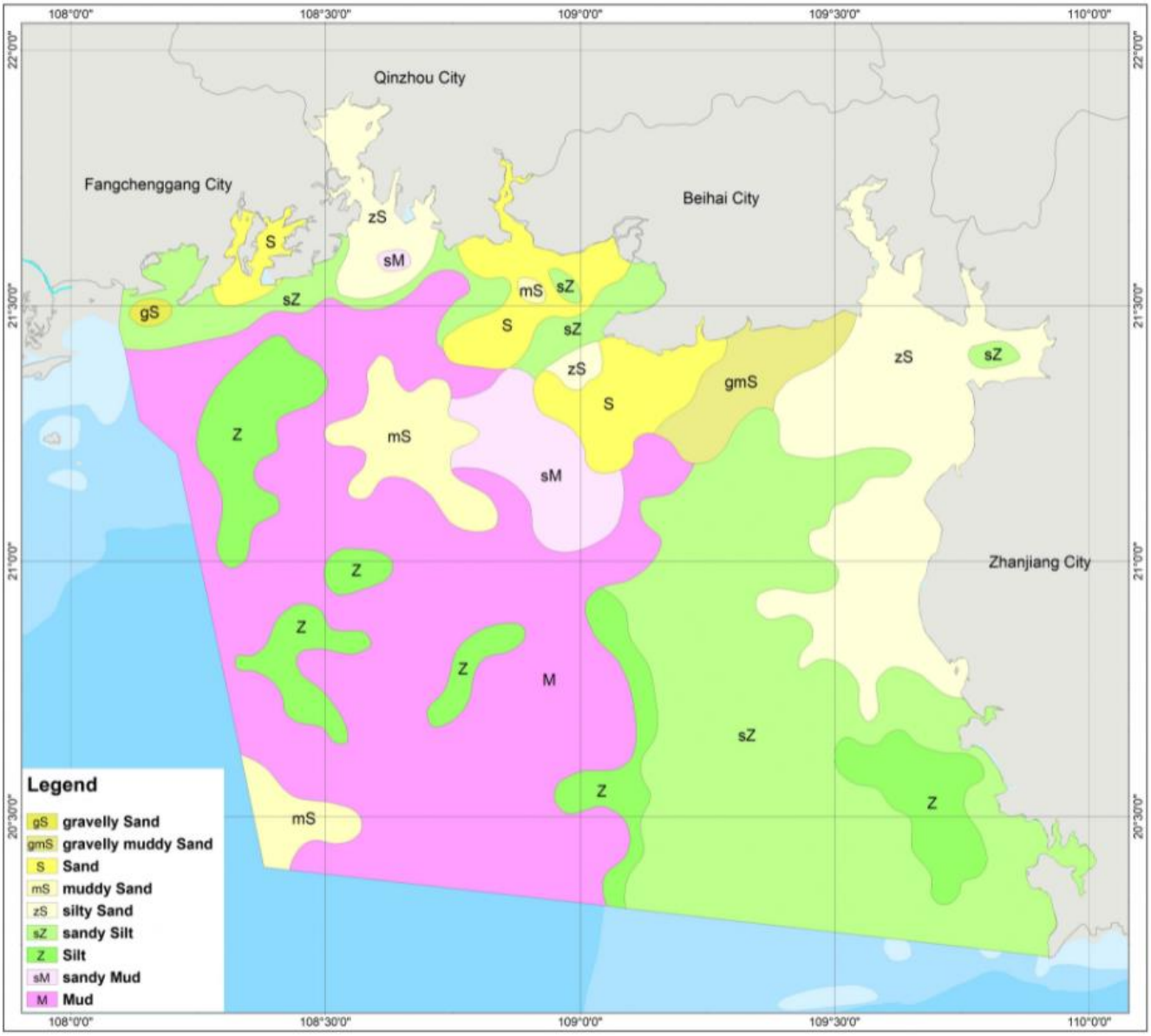

Figure 15. Sediment data in the Beibu Gulf in the original Folk classification.

To be suitable for the EUNIS classification, the original substrate data of the Beibu Gulf was reclassified into a modified EMODnet Folk substrate classification scheme (Kaskela et al., 2019). It is a grain-size based, uniform and simple, but ecologically relevant classification system developed within subsequent EMODnet Geology projects ongoing since 2009 (http://www.emodnet-geology.eu/). EMODnet Folk sediment classification system is based on the ratios of different sediment grain size fractions Mud, Sand and Gravel (Figure 16), and has either 15, 6 or 4 substrate classes, each supplemented with an additional class of rock and boulders. A simple hierarchy enables the straightforward union of 16 classes into 7 or 5 classes. The minimum level five classes are: 1. Mud to muddy sand, 2. Sand, 3. Coarse sediment, 4. Mixed sediment and an additional, 5. class, Rock and boulders.

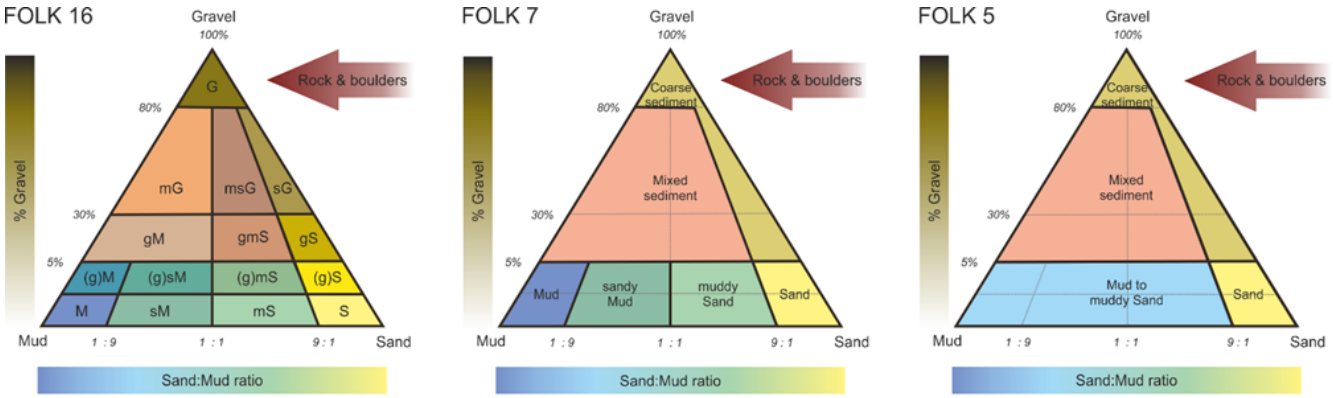

FOLK, 16 classes	FOLK, 7 classes	FOLK, 5 classes
Rock & Boulders	Rock & Boulders	Rock & Boulders
Gravel - G sandy Gravel - sG) gravelly Sand - gS	Coarse sediment	Coarse sediment *(Gravel >= 80% or (Gravel >= 5% and Sand >=90%)*
muddy Gravel - mG muddy sandy Gravel - msG gravelly Mud - gM gravelly muddy Sand - gmS	Mixed sediment	Mixed sediment *(Mud 95-10%; Sand < 90%; Gravel >= 5%)*
(gravelly) Mud - (g)M Mud - M	Mud *(Mud >= 90%; Sand < 10%; Gravel < 5%)*	Mud to muddy Sand *(Mud 100-10%; Sand < 90%; Gravel < 5%)*
(gravelly) sandy Mud – (g)sM sandy Mud - sM	sandy Mud *(Mud 50-90%; Sand 10-50%; Gravel < 5%)*	
(gravelly) muddy Sand – (g)mS muddy Sand - mS	muddy Sand *(Mud 10-50%; Sand 50-90%; Gravel <5%)*	
(gravelly) Sand – (g)S Sand	Sand *(Mud < 10%; Sand >= 90%; Gravel < 5%)*	Sand

Figure 16.The Folk sediment triangle and the hierarchy of Folk classification (15, 6 and 4 classes, plus an additional class "rock and boulders," indicated by the arrow) used in the EMODnet Geology project.

The classification of the original substrate data (Figure 15) is fully compatible with the EMODnet Folk classes, making the reclassification process a simple aggregation following the hierarchy of Folk triangles (Figure 16 and Table 3). Figure 17 shows the final sediment map classified in the FOLK5 classes.

Table 3 Reclassification of the original Beibu Gulf sediment classes to EMODnet Folk 5.

Original Beibu Gulf substrate class	Reclassified EMODnet Folk 5 class
Mud (M)	Mud to muddy Sand
Silt (Z)	Mud to muddy Sand
sandy Mud (sM)	Mud to muddy Sand
sandy Silt (sZ)	Mud to muddy Sand
silty Sand (zS)	Mud to muddy Sand
muddy Sand (mS)	Mud to muddy Sand

Sand (S)	Sand
gravelly Sand (gS)	Coarse sediment
gravelly muddy Sand (gmS)	Mixed sediment

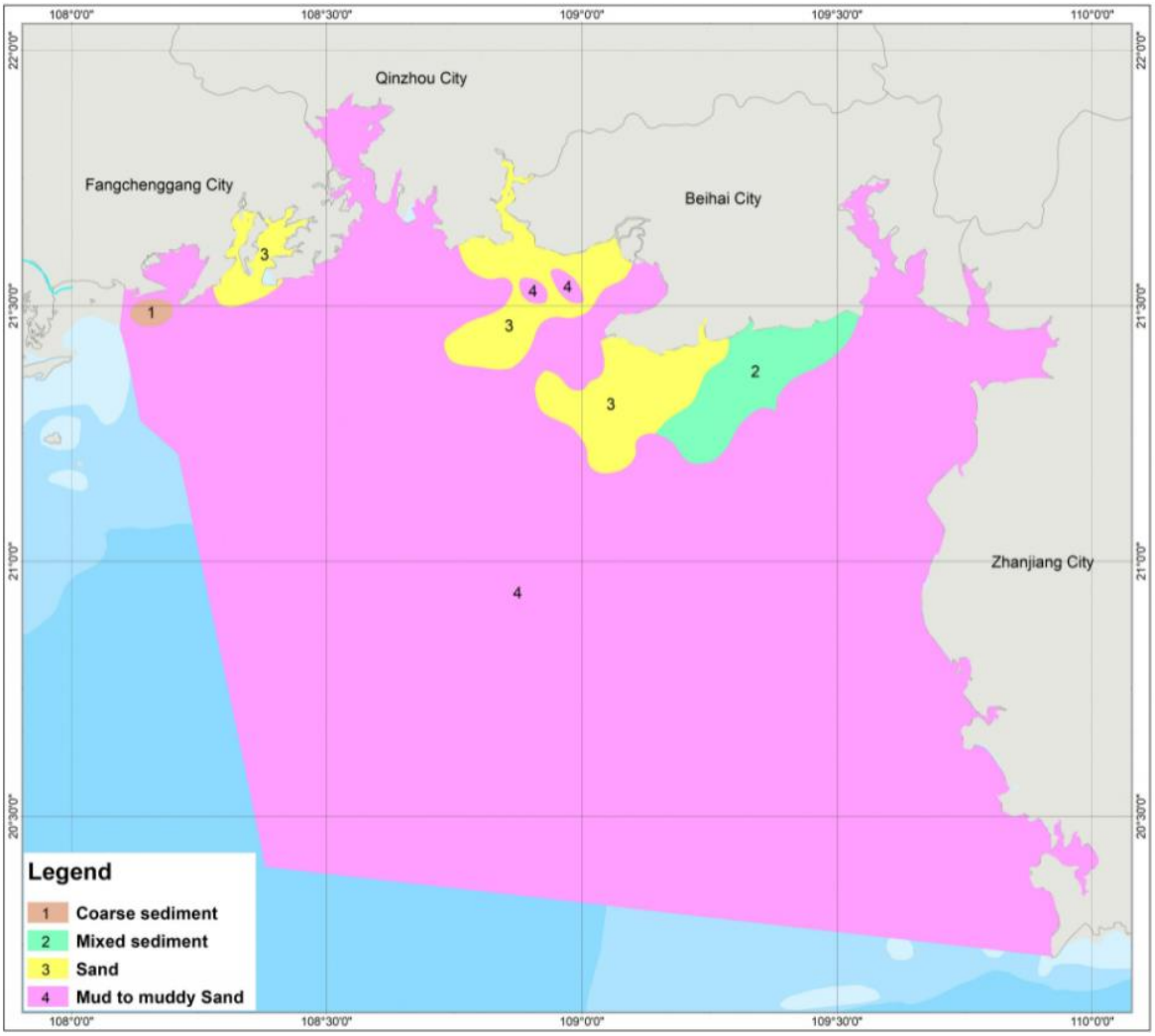

Figure 17. Classified sediment map of the Beibu Gulf in Folk 5 classes.

2.5.5 Biogenic substrate and rock

An important component in creating a substrate layer that follows a similar structure to the latest version of the EUNIS 2019 classification system (Schaminée et al., 2019), is the combination of grain-size-based substrate information with biogenic habitats. Biogenic habitats are defined in EUNIS as habitats formed by plants or animals that modify the nature of the underlying substrata and, include habitats such as coral reefs or oyster beds.

Data on the distribution of coral reefs in the study area were obtained from two sources. The first dataset was derived from dive surveys conducted between 2019 and 2020 (Figure 18), whilst the

second dataset used data obtained from the Allen Coral Atlas (Figure 19). The Allen Coral Atlas is a global-scale coral reef habitat mapping project that produces benthic habitat maps via machine learning random forest techniques (Allen Coral Atlas, 2022). Habitats observed in satellite images are classified by combining them with water depth data (which is also obtained via satellite), wave exposure and turbidity – and validated using ground-truthing from field surveys (see Lyons et al., 2020). Since data from the Allen Coral Atlas also included a category for rock and rubble, these polygons were also included into the final substrate layer, as rock.

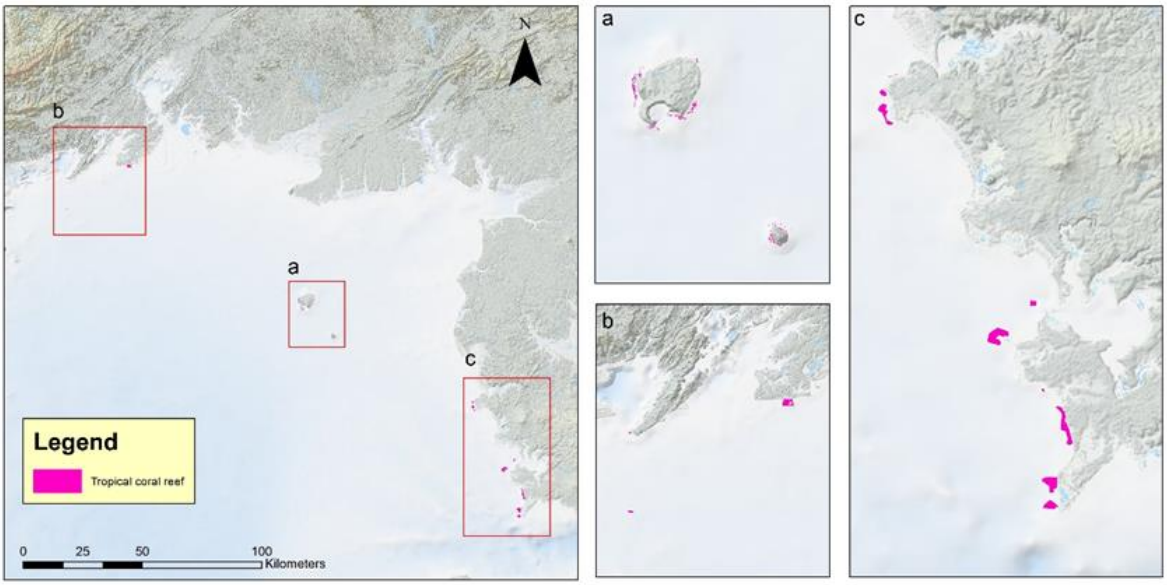

Figure 18. Distribution of coral reefs in the study area, obtained from the "National Coral Reef Ecological Status Survey" project (2019).

The Allen coral Atlas includes seagrass as habitat type. Seagrass species in the Beibu Gulf are small and generally are known to grow on muddy seabeds, They "do not substantially modify the nature of the underlying substrate" and hence areas covered by seagrass in the Atlas were not classified as biogenic substrate but as mud (in terms of broad-scale habitat type). In European waters, only the large Mediterranean seagrass *Posidonia oceanica* is considered as creating a biogenic substrate, which are these thick underwater terraces named "matte" composed of a mixture of plant roots and the sediment that fills in the interstices.

No other maps on other biogenic substrates known to occur in the area (E.g. Oyster and mussel beds) were found. Also no data on artificial hard substrate distribution were available to this study.

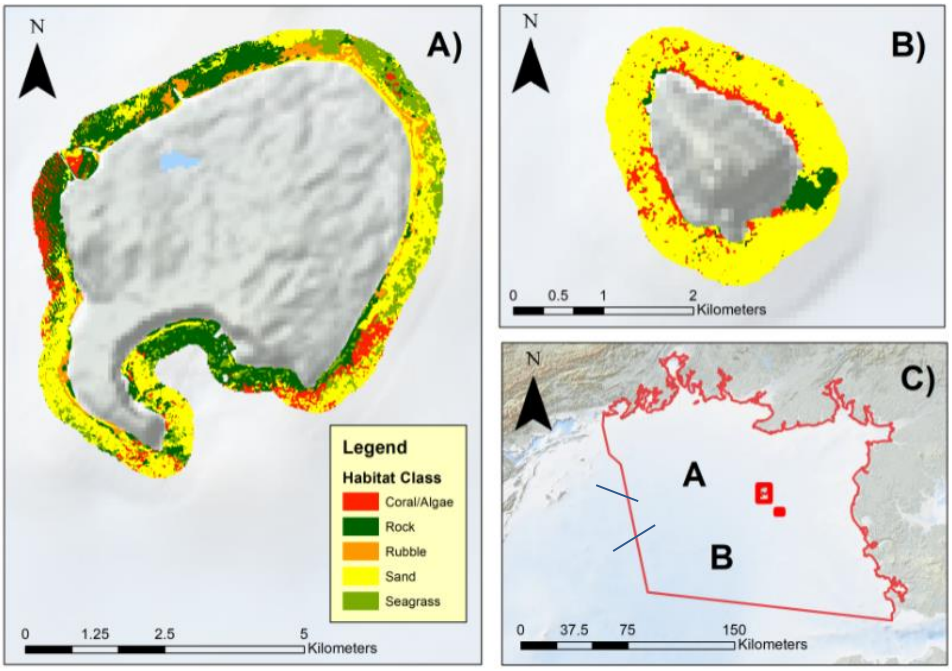

Figure 19. Distribution of marine habitat types around the two main islands of Weizhou and Xieyang in the Beibu Gulf, obtained from the Allen Coral Atlas (Allen Coral Atlas, 2022). A) Marine habitats surrounding Weizhou Island. B) Marine habitats surrounding Xieyang Island. C) Map of Weizhou and Xieyang islands within the Beibu Gulf study area. Allen Coral Atlas map © 2018-2022 Allen Coral Atlas Partnership and Arizona State University and licensed CC BY 4.0

Data on the distribution of exposed rock in the Beibu gulf were obtained from two datasets:

a) Datasets in intertidal area of Fangchenggang, Qinzhou and Beihai city (Figure 20a), obtained from the analysis of satellite remote sensing data ground-truthed using field data from a substrate survey project implemented in 2006-2007; and

a) An extract from the Allen Coral Atlas (as described in the previous paragraph) for the coastal zone (to 10m depth) of Weizhou island and Xieyang island (Figure 20b).

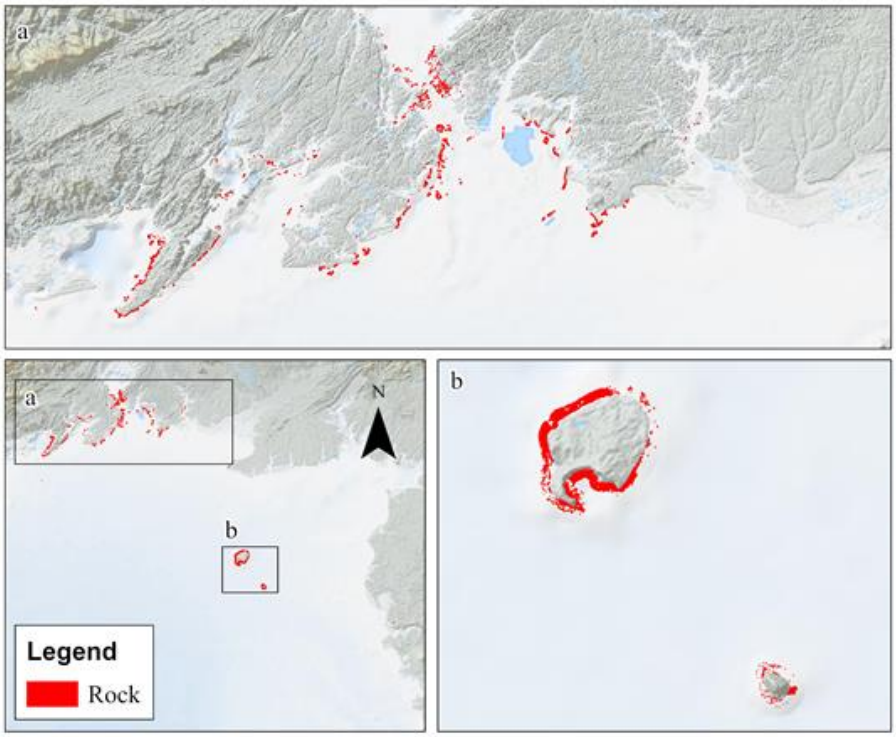

Figure 20 Distribution of exposed rock at the seabed in the Beibu gulf. a) the rock layer obtained from Guangxi province coast substrate survey (2006-2007). b) Predicted rock data obtained from the Allen Coral Atlas (Allen Coral Atlas, 2022).

2.5.6 Substrate confidence assessment

Confidence in the substrate layer was assessed using the approach developed by EMODnet Geology and JNCC (Kaskela et al., 2019). The method is based on the remote sensing coverage, amount of sampling and how distinctive is the boundary between substrate types. Score were assigned to the various data sources as outlined in Table 4.

Table 4 Breakdown of substrate confidence scores and justification for each input datasets into the substrate map. Conf_RS is confidence score for remote sensing coverage ; Conf_S is the confidence score related to the amount of sampling and Conf_D is a score assigned to the distinctness of class boundary.

Data type	Data source	EMODnet confidence score	Justification
Substrate - sediment	NMDIS Special survey of China's offshore	Conf_RS = 0, Conf_S = 1, Conf_D = -, **Conf_TOT = 1**	Remote sensing was not used. Large sample amount with evenly distributed grid of sampling points

			provided adequate amount of sampling to identify every polygon.
Substrate – rock	NMDIS Special survey of guangxi province coast	Conf_RS = 1, Conf_S = 1, Conf_D =0, **Conf_TOT = 2**	Remote sensing was used. every polygon was verified by sampling data or photo. Lack of remote sense data information.
Substrate - coral	NMDIS 2020 Coral reef survey	Conf_RS = 0, Conf_S = 1, Conf_D = -, **Conf_TOT = 1**	Remote sensing was not used. The dive survey data has been used to identify every polygon.
Substrate - coral seagrass and rock	Allen Coral Atlas	Conf_RS = 2, Conf_S = 0, Conf_D =0, **Conf_TOT = 2**	Remote sensing was used. No Field validation points in Beibu Gulf. Turbid water conditions so boundary distinctiveness poor

2.5.7 The geomorphology layer

A map of morphology of the seabed in the study area (Figure 21) was used to model biological zones, and in particular the base of the submerged slope was used as proxy boundary between circalittoral and deep circalittoral biological zone. The map was created using bathymetry, hydrological data and wave data. The Intertidal zone is the defined area where the ocean meets the land between high and low tides. The submerged coastal slope is located between low tide mark and 1/2 wavelength.

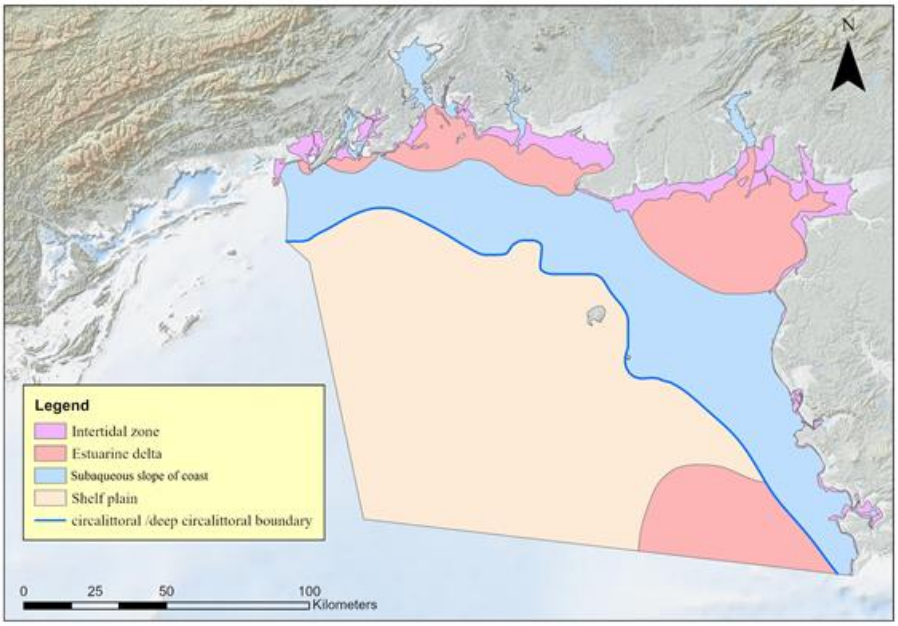

Figure 21 Seabed morphology map of the study area.

2.6 Benthic biodiversity data and biological zone threshold analysis

Benthic biodiversity data (observations of benthic biotopes or biotope-characterising species) are used in EUNIS broad-scale mapping in several ways (see Figure 6)

- When the species/biotopes form a biogenic substrate, and their extent is mapped (polygon data);
- To define ecologically meaningful thresholds between biological zones;
- To quality check the final habitat map

In order to gather suitable benthic biodiversity data for the study area we contacted authors of relevant papers and data owners, we extracted data from global data repositories (OBIS) and Atlases (UNEP Ocean Atlas) and NMDIS colleagues reviewed their internal biodiversity data holdings. It was clear that suitable benthic biodiversity data available for the study area very scarce or and those open and accessible were unsuitable for analysis.

A key step in the broad-scale modelling process is the selection of a suitable ecologically meaningful threshold that can be applied to the continuous light at the seabed layer, to delineate between the infralittoral and circalittoral biological zones. In the EUNIS classification system, these two zones are differentiated by the degree in which they are covered by vegetation cover. The infralittoral zone is dominated by photophilic algae and seagrasses, whilst the circalittoral zone is characterised by communities who thrive under darker conditions.

Ideally, this threshold is estimated using large quantities of ground-truthing data (i.e. observations of subtidal photosynthetic communities) with the depth values they were observed at, to determine the natural limits of these communities (in terms of the fraction of light reaching the seabed). Seagrass

beds were initially considered as a good potential candidate to help define the thresholds between circalittoral and infralittoral biological zones, given the lack of macroalgae or any other suitable species and/or biotope data in the Gulf. The literature review reported eight main seagrass species known to occur in the Beibu Gulf areas, these were: *Halophila ovalis, Halodule uninervis, Halophila beccarii, Zostera japonica, Enhalus acoroides, Thalassia hemperichii, Ruppia martime and Cymodocea rotundata* (Huang et al., 2006). Many of these species were reported to occupy a niche within the intertidal zone, however, four species in particular were suitable candidates for use in threshold analysis due to a confirmed subtidal presence: *H. uninervis, H. ovalis, Z. japonica* and *H. beccarii*. Subsequent investigations into the availability of seagrass data of these species, found that:

1) Data from the UNEP WCMC global seagrass monitoring database consisted of only a single observation in Hepu Bay, and did not specify which species was present or at what depth the record was observed at;

2) Data identified from literature searches could not be successfully obtained;

3) Data held by NMDIS lacked associated depth measurements.

Due to the lacking quantity of seagrass data containing associated depth measurements, an ecologically meaningful threshold could not be calibrated for the Beibu Gulf. As a result, the default threshold suggested by European literature of 1% of surface light levels reaching the seabed was applied (Figure 22).

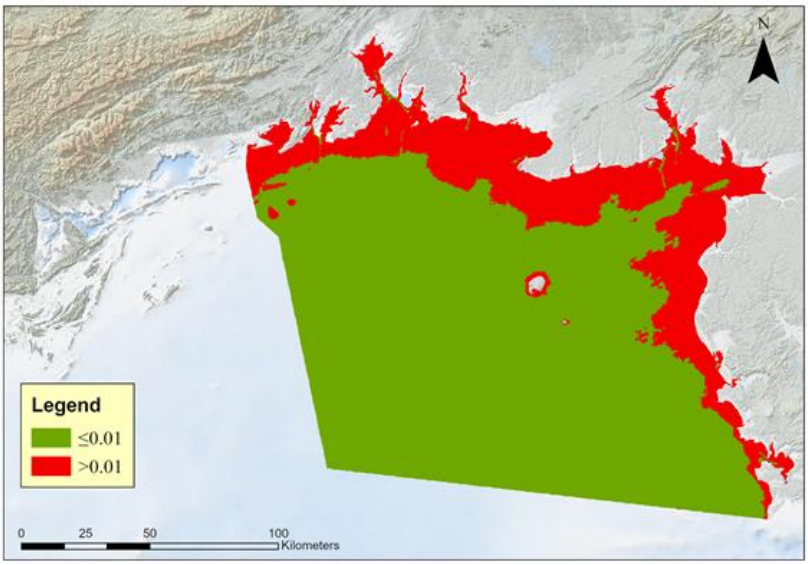

Figure 22. Percentage of surface light reaching the seabed, classified to > 1%, i.e. infralittoral (red) or ≤ 1% (green).

The EUNIS habitat classification describes the deep circalittoral zone (see Figure 2), as an area of relatively more stable conditions of physical parameters at the seabed, such as temperature, wave action and salinity. In EUSeaMap, the delineation of the boundary between the circalittoral and deep circalittoral zone is based on the ratio between wavelength and water depth (wave base), where these data are available. Suitable wave data was not available for the Beibu Gulf.

The -30m depth contour was considered as a proxy for the boundary, as it represents an ecologically significant depth, and the depth to which most living coral is found, according the US National Ocean Service Coastal and Marine Ecological Classification Standard (NOS, 2012).

Considering data availability and the location of the 30m depth contour in the Gulf, it was agreed that change in seabed slope to be a better representation of a change in physical conditions. A morphology map of the Gulf (Figure 21) shows the presence of a shallow slope and shelf plain, located slightly offshore the 30m depth contour. We made the assumption that conditions on the shelf plane are more stable for benthic communities than on the slope, and we used the slope deep edge as deep circalittoral/circalittoral boundary.

2.7 Applying the EUNIS classification to the Beibu Gulf

To be able to classify habitats from the model output, a look-up table was created to correlate the unique model codes with the predictive habitat classes (Table 5).

Table 5. Look-up table used to translate the unique model codes into EUNIS habitat classes.

Zone		Substrate					
		Hard / firm		Soft			
		Rock	Biogenic Habitats	Coarse	Mixed	Sand	Mud
Phytal gradient	Infralittoral	1070	1072	1030	1040	1020	1010
	Circalittoral	2070	2072	2030	2040	2020	2010
depth?? is this due to reduced light?	Deep circalittoral	3070	3072	3030	3040	3020	3010

3 Results and Discussion

3.1 The classified biological zone layer

The area chosen for the pilot application of the EUNIS broad-scale approach is located on the continental shelf and characterised by a maximum depth of about 60m and euhaline (fully marine) conditions. Three distinct biological zones are modelled in the study area: the infralittoral, circalittoral and deep circalittoral zones (Figure 23). As discussed in the previous section, the mapped infralittoral

area corresponds to the photic area where over 1% of light reaches the seabed, whilst the circalittoral area is characterised by darker conditions and photophilic communities are absent. Fuzzy limits of +-0.9% were defined based on expert judgement to reflect the uncertainty around the 1% threshold value.

The edge of the slope/shelf plain was used as a proxy for the deep circalittoral and circalittoral biological zone boundary.

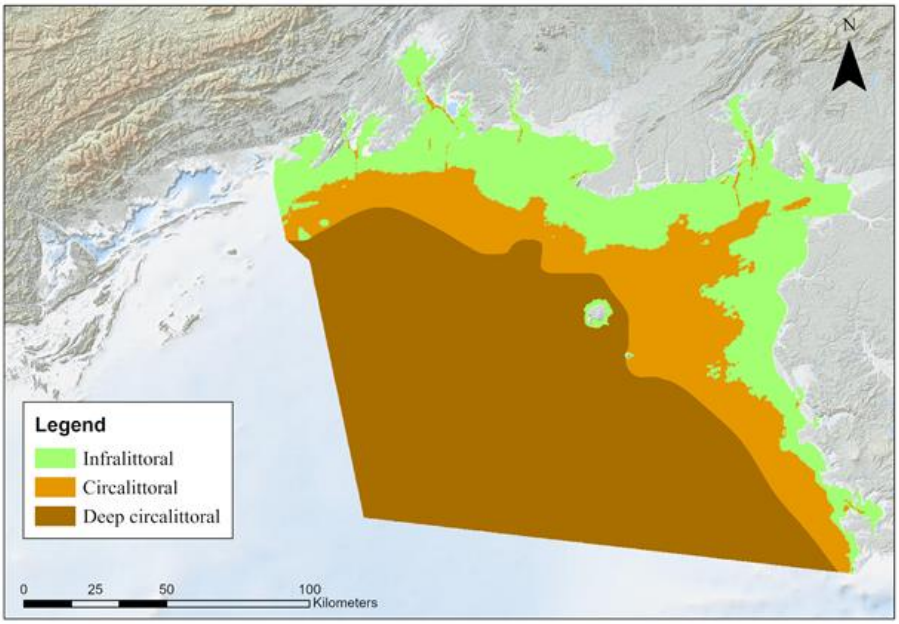

Figure 23. The biological zone map of the Beibu Gulf.

A map of confidence was produced by combining the confidence in the quality of the input layers (light at the seabed and seabed morphology) with the fuzziness in the thresholds used to delineate between two classes (see Guidance in Appendix 2 for more detail). A fixed buffer of 2.5 km either side of the shelf edge was used to create fuzzy boundaries and reflect uncertainty in the location of the circalittoral/deep circalittoral boundary (corresponding to the distance between single beam survey lines). The resulting confidence in the prediction of biological zones is high in most places and decreases at the boundary between biological zones (Figure 24).

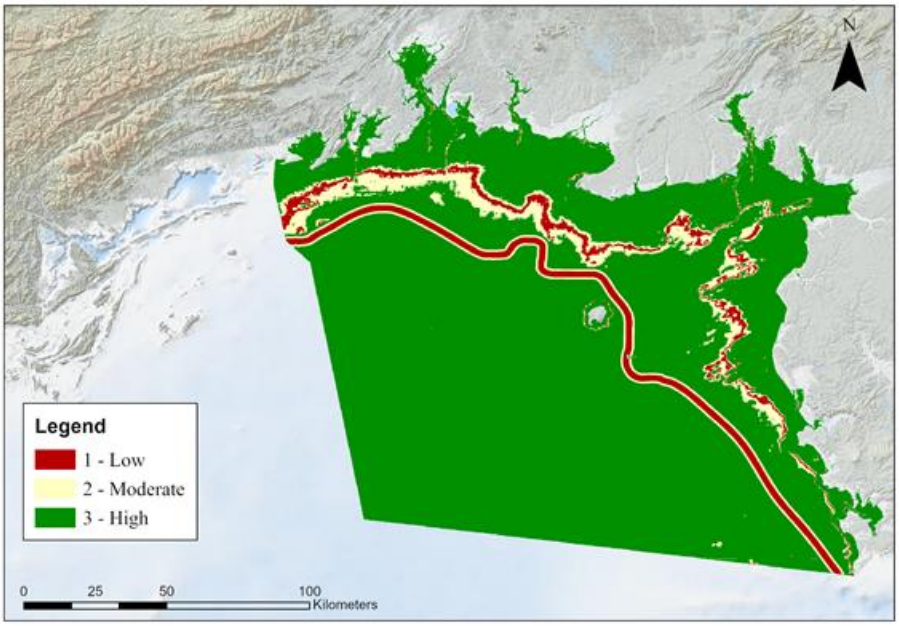

Figure 24 Map of confidence in the biological zone layer.

3.2 The classified substrate layer

The substrate layer used as input to the model is shown in Figure 25, combining the classified sediment map (Figure 17) with data on the presence of coral reefs (Figure 18 & Figure 19). The map includes sediments classified in Folk 5 classes, rock, and biogenic substrate (coral/algae). The vast majority of the study area is characterised by mud, with propagations of sand stemming offshore in the Beibu Bay and Pearl Bay. Substrates transition from sand to mixed sediments moving westwards towards the region of Hepu, and there is a small patch of coarse sediment towards the Vietnamese border in the North-East.

We were able to acquire data on rock at the seabed along the Guangxi province coast. We integrated these data with very small patches classed as rock around the offshore islands, derived from interpretation of satellite images (Allen Coral Atlas) where the seabed is mapped down to a relatively shallow 10m depth. However, it is important to note that rock at the seabed is not mapped as part of the main sediment survey (NMDIS Special survey of China's offshore), hence, we cannot exclude that patches of rock at the seabed (and associated biotopes) occur in other areas.

Tropical coral reef substrates are present in the very shallow areas around the 2 main islands and in the NE and SW corner of the study site, these sites are some of the furthest from the main estuaries that characterise the region.

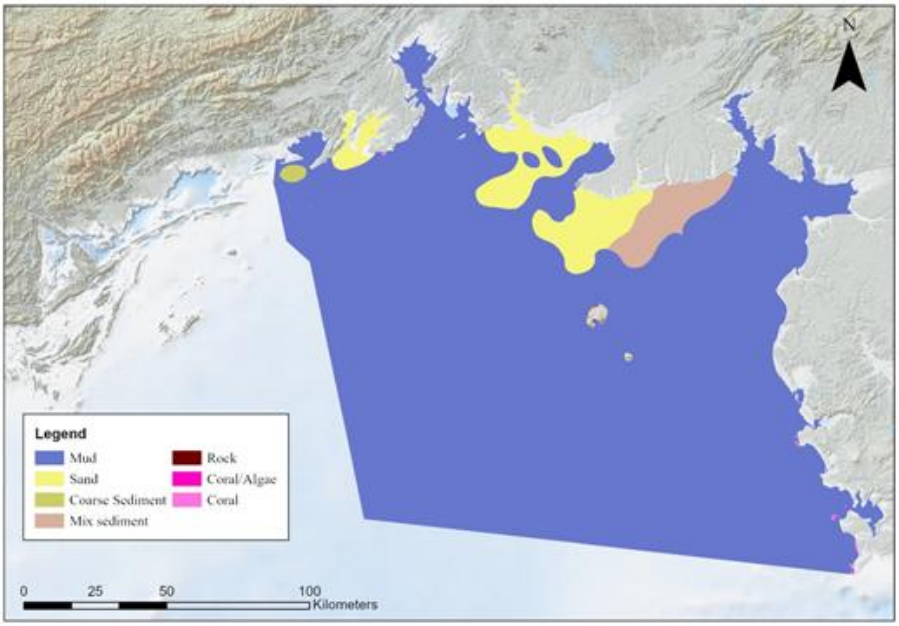

Figure 25. Classified substrate map of the Beibu Gulf, including sediments classes and biogenic substrates.

Confidence in the substrate (Figure 26) is mostly moderate, however low confidence is assigned to maps of the extent of coral as the coral polygon was derived from a few sparse observations by divers.

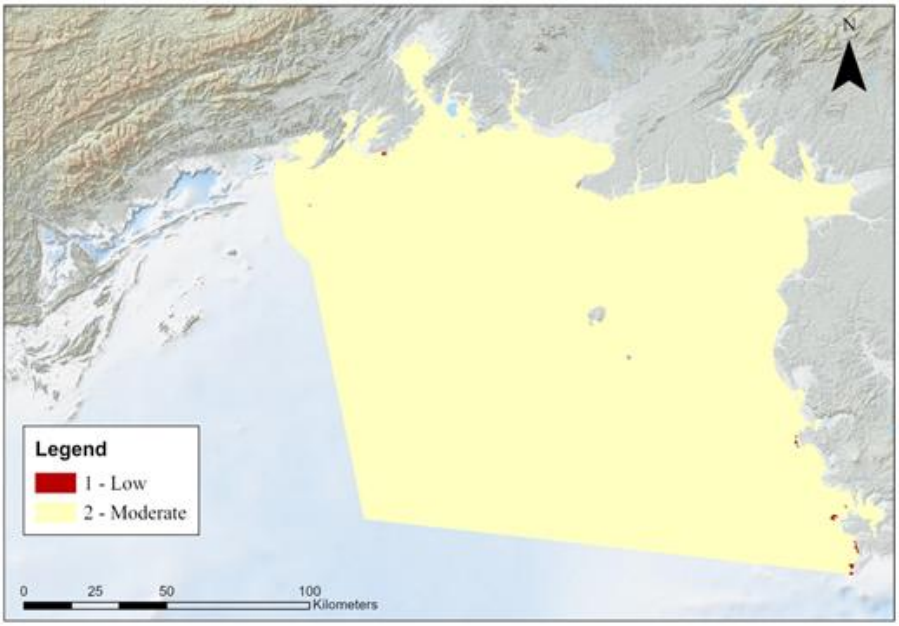

Figure 26 Confidence map in substrate class.

There are two main limitations related to the benthic habitat map used in the production of the rock and coral classes included in the final substrate layer, identifiable from the methods which are well documented online (https://allencoralatlas.org/methods/). Firstly, the methods are reliant on

optically shallow waters to obtain a reliable visual of the sea floor. Even in the clearest waters, satellite data is restricted to depths shallower than 20 meters, and with the coastal waters of the Beibu Gulf being relatively turbid in nature, obtaining somewhat clear satellite images are restricted to depths shallower than 10 meters. Secondly, the lack of ground-truthing points around Weizhou and Xieyang Island means that there is no direct validation of the model within the study area. Under these circumstances, the model relies on ground-truthing elsewhere to correctly assign habitat classes from the satellite imagery, reducing the overall reliability of the map. However, these were valuable datasets in the area on the extent of rock at the surface of seabed, as we understand rock is not routinely mapped as part of NMDIS offshore surveys.

3.3 The predictive habitat map

The broad-scale habitat model combines the classified biological zones with the classified substrate layer to describe 11 physical habitats within the study area (Figure 27) with generally moderate or low confidence (mainly at the boundaries between biological zones, Figure 28). Over half of the study area is characterised by deep circalittoral mud habitats (55%) with mud being the only substrate type occurring in the deep circalittoral zone, (see Table 6). Circalittoral muddy habitats are the second most dominant habitats in the study area (19%), followed by infralittoral mud (17%) and infralittoral sand (5%). Available data results in 9km^2 of infralittoral rock, and less than 1km^2 of circalittoral rock, but this is likely to be underestimated as rock substrate types are not routinely mapped. Additionally, the combination of coral/algae habitats from the Allen Coral Atlas and the coral identified from the National Coral Reef Ecological Status surveys resulted in the model mapping a total area of 12km^2 of infralittoral coral reef habitats. It is noted that all mapped coral reef data fell inside the infralittoral zone which is perhaps unsurprising as most species of coral thrive in well-lit areas. Further work is required to understand whether the species of coral found in the Beibu Gulf could be used to define the infralittoral area in the Gulf, in the absence of a robust seagrass or other suitable dataset.

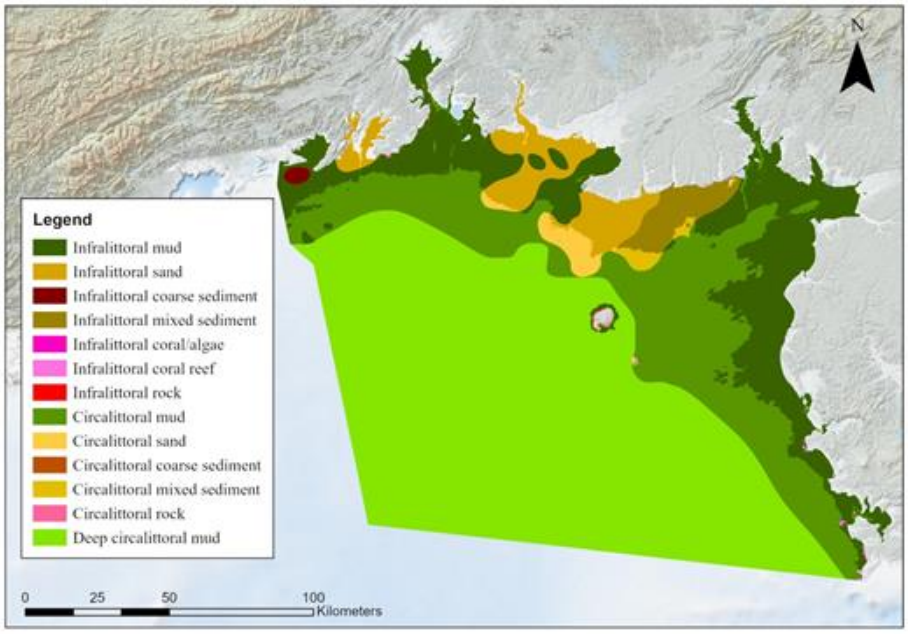

Figure 27. Distribution of physical broad-scale habitats within the Beibu Gulf study area.

Table 6. Area cover of every EUNIS classes represented in the Beibu Gulf study area, and their proportional representation.

EUNIS Class	Predicted area coverage (km²)	% of study area represented
Infralittoral mud	3756	17%
Infralittoral sand	1018	5 %
Infralittoral coarse sediment	42	<1%
Infralittoral mixed sediment	423	2%
Infralittoral coral/algae	1	<1%
Infralittoral coral reef	11	<1%
Infralittoral rock	9	<1%
Infralittoral total	**5260**	**24%**
Circalittoral mud	4295	19%
Circalittoral sand	235	1%
Circalittoral coarse sediment	<1	<1%
Circalittoral mixed sediment	97	<1%
Circalittoral rock	<1	<1%
Circalittoral total	**4627**	**21 %**
Deep circalittoral mud	12224	55%
Deep Circalittoral Total	**12224**	**55%**

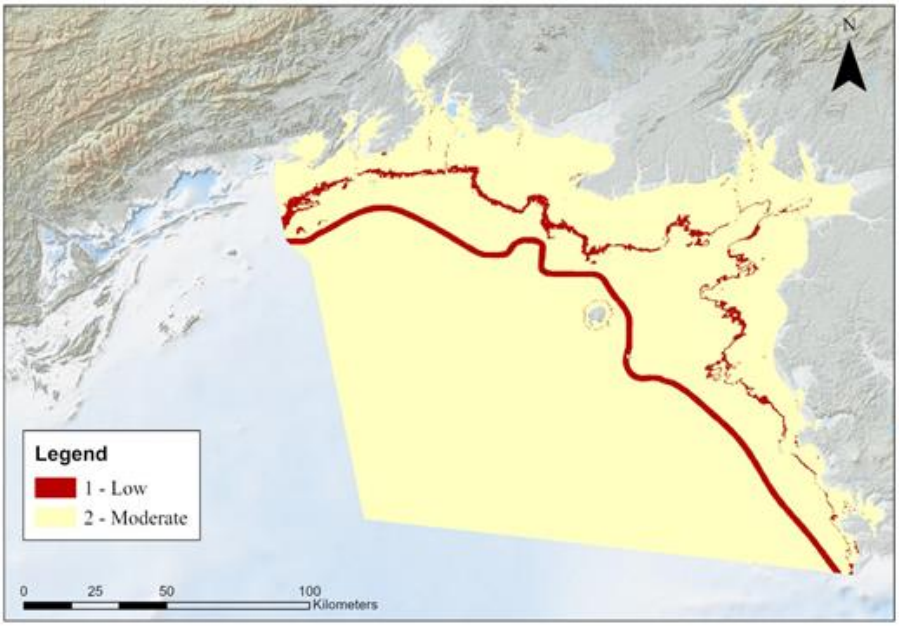

Figure 28 Map of confidence in habitat class.

3.4 Assessment of applicability and limitations of the EUNIS broad-scale map for China

3.4.1 Suitability and applicability of the approach to a Chinese sea basin

Applicability and suitability of the proposed approach for broad-scale habitat mapping in China was discussed during a joint CEMDNET/EMODpace remote workshop. We discussed positive aspects, as well as limitation of the approach, and considered some preliminary potential applications of the method in China.

We noted that the tools and knowledge shared, not only the final map, are useful in themselves and the tools could be easily adapted to extend coverage of the map to the full basin and other Chinese basins, provided input data and ecological understanding of the areas are available.

The process of creating the pilot EUNIS-style broad-scale habitat map has been very useful also in highlighting data gaps and knowledge gaps. The process focuses thinking on key drivers of community distribution and can support further development of habitat classifications in the region. Furthermore, the maps can be useful to target areas that required further sampling or details surveying, for example.

This first full coverage broad-scale habitat map would allow a first estimate of area covered by each broad habitat in the site. Area calculations are essential in various marine management applications: When estimating percentage of protected habitats or for estimation of value of habitat assets, for

example. These maps are usually particularly valuable when the map covers the full extent of the sea basin or an administration area.

NMDIS colleagues found the biological zone layer alone to be useful knowledge for the further development of a habitat classification and to improve understanding of habitat distribution.

3.4.2 Limitations

The broad-scale model was developed to predictively map the distribution of habitats at a larger spatial scale, rather than at the scale of this project's study area. By applying the model to a relatively small area, where there is also a shortage of access to suitable continuous physical datasets, the result has meant fewer environmental gradients have been observed (for example, temperature and salinity gradients) and, therefore, fewer habitat types being determined. From the habitat types that *have* been modelled, there is an element of uncertainty associated with the classification of biological zones within the study area. This is also attributed to the lack of open data, particularly on the Beibu Gulf's benthic communities within the sublittoral region, that are traditionally used to calibrate the thresholds between habitat descriptor classes. For example, the threshold between infralittoral and circalittoral of 1% fraction of light reaching the seabed (Fr) is a known approximate value recognised in the literature, but for better results, a threshold of Fr should be calculated using in-situ biodiversity and KdPAR data.

At the start of the project, it was decided that in line with the current European methods, the littoral (intertidal) habitats would not be modelled as these can be more accurately measured using remote sensing techniques (e.g., satellite, drone, or aerial images) (See also section Principles and approach to EUNIS broad-scale habitat mapping). We later realised, through more recent discussions with NMDIS colleagues, that there may be an interest in creating a broad-scale map covering the extent of these habitats. We suggest, however, the best method to achieve this would be to combine a modelled broad-scale map of subtidal habitats with maps of littoral habitats from survey – rather than apply a broad-scale map across the entire area.

3.5 Suggestions for improvement

Looking to the future of habitat mapping in a Chinese sea basin, there is a significant opportunity to up-scale the study area to generate biological zone layer and broad-scale habitat maps that covers a much wider area of an entire sea basin, where data are available. We considered extending the biological zone map to cover the whole Beibu Gulf but we decided against it as the quality of the available bathymetry data was not considered suitable for the task (particularly in shallow waters). Extending the broad-scale mapping area can assist in the development of the national classification systems for marine habitats.

Expanding the study area could also unlock the potential for new biological datasets to be sourced. Specifically, datasets on the distribution of photophilic communities with associated depth measurements that could be used to calibrate the threshold between the infralittoral and circalittoral biological zone. In general, the modelled habitat map can be improved as new physical and biological datasets are released or discovered or created.

Further studies into the environmental factors driving biotope distribution in the Beibu Gulf would assist in refining searches for additional continuous physical datasets and be used to describe

additional habitat classes (see dashed pathways in Figure 6). As an example, in Europe, biological assemblages in the deep sediments of the Black Sea are known to be affected by oxygen levels, and so oxygen regime is considered as an additional classified habitat descriptor to create an added level to the classification hierarchy. A comparison between the current habitat map and the national classification system being developed by NMDIS might uncover environmental parameters that could be used to improve the model further.

We recommend mapping exposed rock or other hard substrate (artificial and biogenic) because it is a very important aspect of habitat mapping because there is a clear distinction between communities on hard and soft sea bottoms.

Broad-scale habitat models can be useful in data poor regions and, provide a full coverage information for very large areas (basin wide, national water, European waters). They provide a first general picture of the variety and general types of physical habitats at the seabed, and should be based on good understanding of key physical drivers of broad communities distribution. They are not well suited to be used in small areas for application such as Marine protected sites designation or environmental impact assessments at site level, where detail habitat maps from survey (which include data on the communities present at the seabed) should be used for assessment.

If the perspective is to apply the EMODnet broad-scale seabed habitat mapping method tested in the Beibu Gulf to all Chinese waters, we recommend the development of a comprehensive EUNIS-like classification for China, i.e. a classification that would extensively describe habitats in a hierarchical manner from broad habitat types to communities of species. This would provide knowledge on i) the key environmental factors that determine the presence of habitats and communities and ii) which communities occupy which broad habitats. The latter is crucial for broad-scale seabed habitat map developers, as it provides information on the community observation data to be used to calibrate the thresholds that enable the classification of continuous environmental variable rasters into habitat descriptor classes. It is also crucial knowledge for policy makers, as it provides information on which communities of species are likely to be protected/endangered if broad habitat types are protected/endangered (e.g. if infralittoral rocks are well protected by Marine protected Areas, the communities that typically occupy that broad habitat, such as kelp forests and co-occurring species, are likely to be well protected).

4 References

Allen Coral Atlas (2022). Imagery, maps and monitoring of the world's tropical coral reefs. doi.org/10.5281/zenodo.3833242

BALANCE, 2008. BALANCE Technical Summary Report, part 2: Baltic Sea marine landscapes and habitats - mapping and modelling. Available online at: http://balance-eu.org/xpdf/balance-technical-summary-report-no-2-4.pdf

Cameron, A., Askew, N. (eds.), 2011. EUSeaMap - Preparatory Action for development and assessment of a European broad-scale seabed habitat map final report. Available online at http://jncc.gov.uk/euseamap.

Chen S, Li Y, Hu J, Zheng A, Huang L, Lin Y (2011a) Multiparameter cluster analysis of seasonal variation of water masses in the eastern Beibu Gulf. *Journal of oceanography*, 67(6), pp.709-718.

Coltman, N., Golding, N., Verling, E., 2008. Developing a broadscale predictive EUNIS habitat map for the MESH study area. 16 pp. Available online at http://www.searchmesh.net/pdf/MESH%20EUNIS%20model.pdf.

Connor D.W, Gilland P, Golding, N, Robinson P, Todd, D, Verling E. 2006. UKSeaMap: The Mapping of Seabed and Water Column Features of UK Seas. jncc.defra.gov.uk/page=3918

Folk, R.L, Andrews P.B, Lewis D.W. 1970, Detrital sedimentary rock classification and nomenclature for use in New Zealand: *New Zealand Journal of Geology and Geophys-ics*, 13, p. 937–968

Heege T, Häse C, Bogner A, Pinnel N (2003) Airborne multi-spectral sensing in shallow and deep waters. *Backscatter*, 14(1), pp.17-19.

Hell, B., and M. Jakobsson (2011), Gridding heterogeneous bathymetric data sets with stacked continuous curvature splines in tension, *Marine Geophysical Research*, 32(4), 493–501, doi:10.1007/s11001-011-9141-1.

Huang X, Huang L, Li Y, Xu Z, Fong C.W, Huang D, Han Q, Huang H, Tan Y, Liu S. 2006. Main seagrass beds and threats to their habitats in the coastal sea of South China. *Chinese Science Bulletin*, 51(2), pp.136-142.

Kaskela, A.M.; Kotilainen, A.T.; Alanen, U.; Cooper, R.; Green, S.; Guinan, J.; van Heteren, S.; Kihlman, S.; Van Lancker, V.; Stevenson, A.; the EMODnet Geology Partners. Picking Up the Pieces—Harmonising and Collating Seabed Substrate Data for European Maritime Areas. 2019 *Geosciences*, 9, 84. https://doi.org/10.3390/geosciences9020084

Lai J, Jiang F, Ke K, Xu M, Lei F, Chen B. 2014. Nutrients distribution and trophic status assessment in the northern Beibu Gulf, China. *Chinese journal of oceanology and limnology*, 32(5), pp.1128-1144.

Liao W, Hu J, Zhou H, Hu J, Peng P, Deng W. 2018. Sources and distribution of sedimentary organic matter in the Beibu Gulf, China: Application of multiple proxies. *Marine Chemistry*, 206, pp.74-83, ISSN 0304-4203, https://doi.org/10.1016/j.marchem.2018.09.006.

Lyons et al (2020) Mapping the world's coral reefs using a global multiscale earth observation framework. *Remote Sensing in Ecology and Evolution*. DOI:10.1002/rse2.157

Ma X, Yan, J, Song Y, Liu X., Zhang J, Traykovski P.A. 2019. Morphology and maintenance of steep dunes near dune asymmetry transitional areas on the shallow shelf (Beibu Gulf, northwest South China Sea). *Marine Geology*, 412, pp.37-52.

Morel A, Gentili B, Claustre H, Babin M, Bricaud A, Ras J, Tièche F. 2007. Optical properties of the "clearest" natural waters. Limnology and Oceanography – *Limnology and oceanography*. 52, pp. 217-229. 10.4319/lo.2007.52.1.0217.

Populus J, Vasquez M, Albrecht J, Manca E, Agnesi S, Al Hamdani Z, Andersen J, Annunziatellis A, Bekkby T, Bruschi A, Doncheva V, Drakopoulou V, Duncan G, Inghilesi R, Kyriakidou C, Lalli F, Lillis H, Mo G, Muresan M, Salomidi M, Sakellariou D, Simboura M, Teaca A, Tezcan D, Todorova V, Tunesi L (2017). EUSeaMap. A European broad-scale seabed habitat map. https://doi.org/10.13155/49975

Qiao Y, Chen Z, Lin Z. 2008. Changes of community structure of fishery species during spring and autumn in the Beibu Gulf. *Journal of Fishery Sciences of China (in Chinese*), 15(5), pp. 816–821

Roff J.C., Taylor, M.E., 2000. National frameworks for marine conservation — a hierarchical geophysical approach. *Aquatic Conservation: Marine and Freshwater Ecosystems* 10, pp. 209–223. doi:10.1002/1099-0755(200005/06)10:3<209::AID-AQC408>3.0.CO;2-J

Roff, J.C., Taylor, M.E., Laughren, J., 2003. Geophysical approaches to the classification, delineation and monitoring of marine habitats and their communities. *Aquatic Conservation: Marine and Freshwater Ecosystems* 13, 77–90. doi:10.1002/aqc.525

Schaminée, J.H., Chytrý, M., Hájek, M., Hennekens, S.M., Janssen, J.A. and Knollová, I., 2019. Updated crosswalks of the revised EUNIS Habitat Classification with the European Vegetation Classification and the European Red List Habitats for EUNIS coastal habitats and mires.

Shen C, Yan Y, Zhao H, Pan J, T. Devlin A. 2018. Influence of monsoonal winds on chlorophyll-α distribution in the Beibu Gulf. *PLoS ONE* 13(1): e0191051. https://doi.org/10.1371/journal.pone.0191051

Shi M, Chen C, Xu Q, Lin H, Liu G, Wang H, Wang F, Yan J .2002. The role of Qiongzhou Strait in the seasonal variation of the South China Sea circulation. *Journal of Physical Oceanography*, 32(1), pp.103-121.

Son SH, Wang M. 2015. Diffuse attenuation coefficient of the photosynthetically available radiation Kd(PAR) for global open ocean and coastal waters, *Remote Sensing of Environment*, 159, pp.250-258, ISSN 0034-4257, https://doi.org/10.1016/j.rse.2014.12.011

Vasquez, M., Allen, H., Manca, E., Castle, L., Lillis, H., Agnesi, S., Al Hamdani, Z., Annunziatellis, A., Askew, N., Bekkby, T., Bentes, L., Doncheva, V., Drakopoulou, V., Duncan, G., Gonçalves, J., Inghilesi, R., Laamanen, L., Loukaidi, V., Martin, S., McGrath, F., Mo, G., Monteiro, P., Muresan, M., Nikolova, C., O'Keeffe, E., Pesch, R., Populus, J., Pinder, J., Ridgeway, A., Sakellariou, D., Teaca, A., Tempera, F., Todorova, V., Tunesi, L. and Virtanen, E., 2021. EUSeaMap 2021, A European broad-scale seabed habitat map, Technical Report. https://doi.org/10.13155/83528

Vasquez, M., Manca, E., Inghilesi, R., Martin, S., Agnesi, S., Al Hamdani, Z., Annunziatellis, A., Bekkby, T., Pesch, R., Askew, N., Bentes, L., Castle, L., Doncheva, V., Drakopoulou, V., Gonçalves, J., Laamanen, L., Lillis, H., Loukaidi, V., McGrath, F., Mo, G., Monteiro, P., Muresan, M., O'Keeffe, E., Populus, J., Pinder, J., Ridgeway, A., Sakellariou, D., Simboura, M., Teaca, A., Tempera, F., Todorova, V., Tunesi, L. and Virtanen, E., 2020. EUSeaMap 2019, A European broad-scale seabed habitat map, Technical Report. https://doi.org/10.13155/74782

Wang M, Son S, Harding L.W (2009) Retrieval of diffuse attenuation coefficient in the Chesapeake Bay and turbid ocean regions for satellite ocean color applications, *Journal of Geophysical Research*, 114, C10011, doi:/10.1029/2009JC005286.

Wang Y, Zhang W, Lin Y, Cao W, Zheng L, Yang J (2014) Phosphorus, Nitrogen and Chlorophyll-a Are Significant Factors Controlling Ciliate Communities in Summer in the Northern Beibu Gulf, South China Sea. *PLoS ONE* 9(7): e101121. https://doi.org/10.1371/journal.pone.0101121

Wentworth, C.K., 1922, A scale of grade and class terms for clastic sediments: *Journal of Geology*, 30, pp. 377-392.

Xie X, Wu Z, Wang C.C, Fu Y, Wang, X, Xu P, Huang X, Liao Y, Huang S.L, Kwan K.Y (2020) Nursery habitat for Asian horseshoe crabs along the northern Beibu Gulf, China: Implications for conservation management under baseline gaps. *Aquatic Conservation: Marine and Freshwater Ecosystems*, 30(2), pp.260-272.

5 APPENDIXES

5.1 Appendix I: Literature Review of the Beibu Gulf

The aim of this literature review is to determine what seabed habitat mapping has occurred in the Beibu Gulf, to understand the physical environment and the ecology of the gulf, and in particular, which species and/or communities would be suitable for representing the transition from one broad habitat type to another. The latter would then be used to identify the most ecologically relevant thresholds for classifying different habitats. This review draws upon the information collected from the scientific literature in English language, the main findings are summarised in the conclusion.

5.1.1 Geographic Setting and Study Area

The Beibu Gulf, also known as the Gulf of Tonkin, is located in the north-western parts of the South China Sea and lies between China and Vietnam (Figure 24). It is a relatively shallow gulf, covering an area of over 128,000km^2 and with an average depth of 42m. The deepest portions of the gulf are towards the south where the mouth opens to the South China Sea. Here, the flat seabed plains begin to slope south-eastwards to maximum depths of ~100m (Chen et al., 2008). There is a secondary connection to the South China Sea at the Qiongzhou Strait, a narrow channel between Xuwen County and Hainan Island in the east (see Figure 25).

The gulf is considered a major estuarine system (Laio et al., 2018) with over 200 rivers flowing into it (Qiao et al., 2008). The largest rivers are: Red River, Fangcheng River, Nanliujiang River, Qinjiang River, Dafengjiang River, Beilunhe River and Changhuajiang River (Chen et al., 2008). Discharge from the rivers supply the gulf with large quantities of terrigenous nutrients, which drives marine productivity in the region (Wang et al., 2014). The productive waters are favourable to a number of commercially important fish stocks such as red snapper (Chen et al., 2011b), sardines (Yang et al., 2020) and Crimson Seabream (Wang et al., 2019), but are also ideal for shellfish aquaculture (Zhang[b] et al., 2020). The abundance of marine resources in the Beibu Gulf is of economic significance to both China and Vietnam and has been recognised as the fourth largest fish farming region of China (Shen et al., 2018).

The proposed study area covers the north-west portion of the Beibu Gulf (Figure 25). A rough boundary can be visualised at the intersection of a vertical line southward from the Vietnam/China border, and a horizontal line westward from the southern lip of the Xuwen County, mainland China. The study area includes two volcanic islands: Weizhou and Xieyang Island (Figure 26), measuring approximately 25km^2 and 2km^2 respectively (Xiaohua et al., 2019).

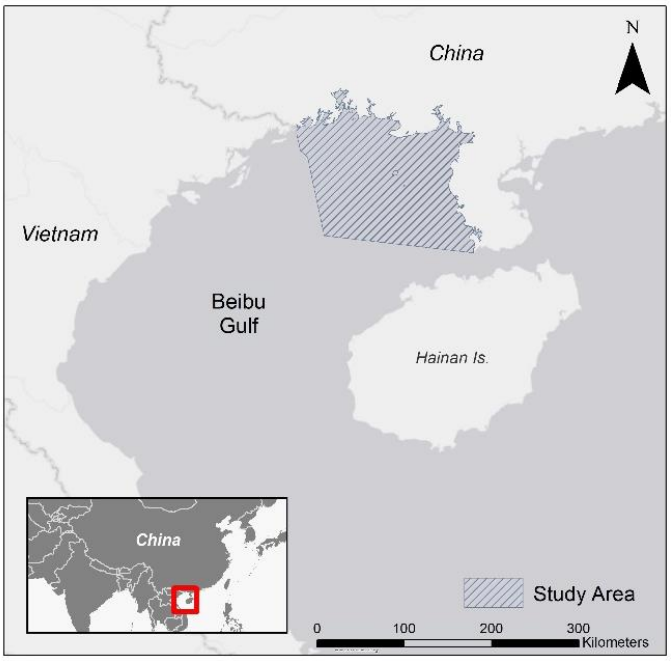

Figure 29. Location of the study area within the Beibu Gulf. Inset map shows the location of the Beibu Gulf in relation to China.

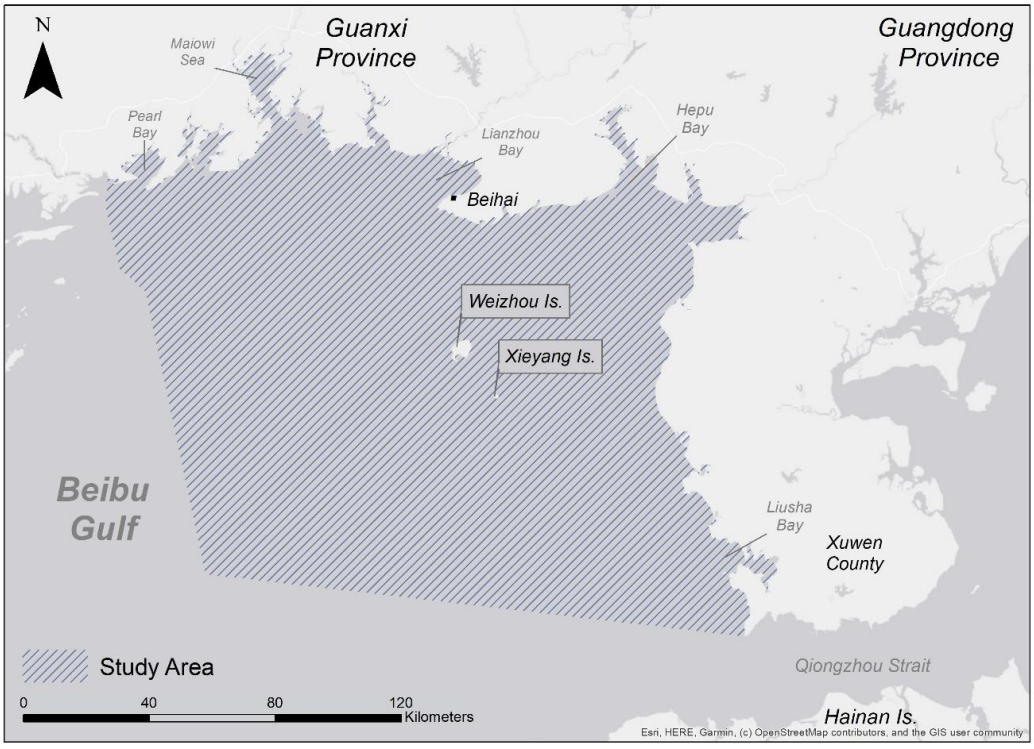

Figure 30. Close up of the project study area in the North-West of the Beibu Gulf. Figure annotated with locations referenced throughout the literature review.

5.1.2 Environmental Conditions

5.1.2.1 Seasonal Variability in Temperature and Salinity

The Beibu Gulf exhibits a sub-tropical climate and is largely influenced by the East Asian Monsoon system (Lai et al., 2014). During the winter months (December-February), salinity and water temperatures are relatively uniform and vertically well-mixed, with temperatures ranging from 20°C in the north and 24°C in the south (Chen et al., 2009). The winter mixing of the Beibu Gulf's mesotrophic waters generate favourable conditions for primary production and causes concentrations of chlorophyll-a to peak (Tang et al., 2003).

The portion of the gulf represented within our study area experiences greater temperature/salinity gradients during the summer months, whereby the dramatic increase in rainfall caused by monsoons results in greater volumes of freshwater being discharged by its estuaries (Bauer et al., 2013). Sea surface temperatures in the summer months range from around 27.5°C in the north and 30°C in the south, which become vertically stratified with weakening winds (Tang et al., 2003). The average temperature of the sea floor is around 19°C at this time (Bauer et al., 2013). Between March and June, the thermocline becomes so strong that it forces cold water to collect at the centre of the gulf, where the seafloor topology is concave (Chen et al., 2015). The cold-water mass remains trapped at the seabed until October, where lower atmospheric temperatures weaken the thermocline, generates mixing of the water column at the coast and the cold-water mass warms with the surrounding water (Chen et al., 2015).

Chen et al (2011a) gives a detailed overview of the seasonal salinities experienced by the gulf and characterises the area by five water masses: diluted water, mixed water, surface water, sub-surface water and bottom water (see Figure 27 and Table 5). The diluted water mass is formed from river discharge and runs along the Guangxi coast. The salinity of the diluted water mass remains relatively uniform across all seasons with an average of 32psu, but with a widening range between 29 and 32psu in the summer. The surface water mass is prominent in the central and southern areas of the gulf, whilst subsurface water exists south of Hainan Island near the mouth of the Gulf. Surface and subsurface water masses exhibit high salinities of >33psu, with peak salinities during springtime and oppositely during autumn. Subsurface water possesses slightly higher salinities than the surface water (no more than 1psu), particularly during spring and summer when the water column becomes more stratified but does not exist in winter months. The salinity ranges between 33.5-34.3psu for the surface water mass and 34.2-34.5psu for the subsurface water mass. The mixed water mass is described as a combination of the diluted water mass and the surface water mass, thus experiencing an intermediate of properties between the two. The mixed water mass dominates the northern portion of the gulf, and the study area of the project. Salinities within this water mass range from 32.4-33.4psu, with peaks in spring and troughs in autumn. The bottom water mass only occurs during summer and autumn, located towards the centre of the gulf, north-west of Hainan island. Salinities in this water mass are highest in autumn at around 34psu and slightly lower in summer at ~33.8psu.

Table 7. Parameter values for each water mass, as described in Chen et al., 2011a.

	Parameters	Diluted water	Mixed water	Surface water	Bottom water	Subsurface water
Spring	Salinity	31.88	33.40	34.24		34.52
	Temperature (°C)	20.51	21.64	25.90		20.66
	Dissolved oxygen (mg L^{-1})	7.88	7.38	6.87		5.74
	Reactive silicate (μmol L^{-1})	3.57	5.00	2.14		8.21
	Alkalinity (mmol L^{-1})	2.24	2.30	2.10		2.12
	Nitrite (μmol L^{-1})	0.043	1.114	0.086		0.143
	Chlorophyll *a* (μg L^{-1})	1.09	1.45	0.60		0.26
Summer	Salinity	30.67	33.22	33.89	33.82	34.47
	Temperature (°C)	30.27	30.41	28.37	26.71	19.90
	Dissolved oxygen (mg L^{-1})	6.09	5.90	6.38	5.03	4.94
	Reactive silicate (μmol L^{-1})	6.07	5.36	2.86	11.79	10.00
	Alkalinity (mmol L^{-1})	2.05	2.22	2.21	2.21	2.22
	Nitrite (μmol L^{-1})	0.221	0.236	0.093	0.550	0.314
	Chlorophyll *a* (μg L^{-1})	5.30	1.79	0.72	1.33	0.64
Autumn	Salinity	31.11	32.40	33.66	33.99	34.24
	Temperature (°C)	26.06	26.41	26.71	24.58	23.54
	Dissolved oxygen (mg L^{-1})	6.90	6.78	6.69	4.82	5.01
	Reactive silicate (μmol L^{-1})	8.21	6.79	3.93	10.71	11.43
	Alkalinity (mmol L^{-1})	2.17	2.25	2.29	2.30	2.31
	Nitrite (μmol L^{-1})	0.314	0.450	0.200	0.371	0.136
	Chlorophyll *a* (μg L^{-1})	2.39	2.22	0.82	1.16	0.44
Winter	Salinity	31.52	32.81	33.82		
	Temperature (°C)	17.85	20.65	23.83		
	Dissolved oxygen (mg L^{-1})	8.01	7.63	7.09		
	Reactive silicate (μmol L^{-1})	1.43	5.00	5.00		
	Alkalinity (mmol L^{-1})	2.21	2.30	2.36		
	Nitrite (μmol L^{-1})	0.000	0.257	0.114		
	Chlorophyll *a* (μg L^{-1})	1.94	2.01	1.14		

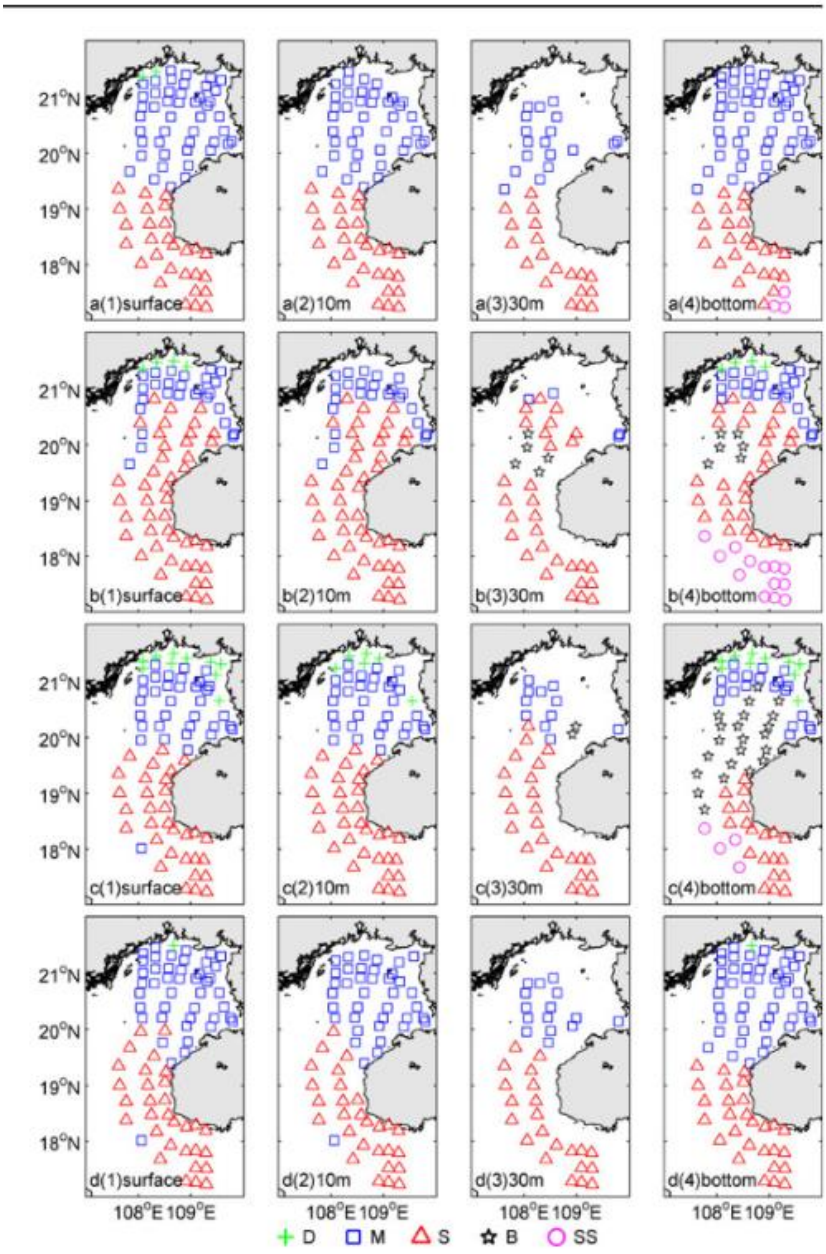

Figure 31. Excerpt from Chen et al., 2011a describing the location of each water mass across the seasons. A-d shows distributions of water mass in spring, summer, autumn, and winter respectively. 1-4 represents depth of water sampled. D represents diluted water mass, M refers to the mixed water mass, S relates to the surface water mass, SS denotes sub-surface water mass and B describes the bottom water mass.

Despite this detailed study, salinity values will realistically be much lower towards the gulf's coast. Local studies in Lianzhou Bay (see Figure 26 for location) show that surface salinities in tidal water can be relatively high at the coast, ranging from 22-26psu in the summer season (Fan et al., 2005) but increasing to 31psu in winter when there is less freshwater run-off in the estuaries (Sun et al., 2014). Other studies report far more extreme salinities along the coast during the peak monsoon season at 5psu (Chen et al., 2008).

5.1.2.2 Ocean Currents, Waves and Circulation

The Beibu Gulf is driven by complex physical processes. There are conflicting studies about the main driving forces behind ocean circulation in the Beibu Gulf during summer (Gao et al., 2017), however, it is known that north-easterly prevailing winds occur during the winter season, whilst south-westerly winds prevail during summer (Wu et al., 2008). This results in currents in the Qiongzhou Strait (see Figure 26 for location) flowing westerly in winter and easterly during summer (Wang et al., 2020). Waves are generated by diurnal tides in the west and semidiurnal tides in the east, which propagate from the gulf towards the Qiongzhou strait where they decrease in amplitude significantly (Shi et al., 2002).

The distribution of substrates is heavily influenced by currents and circulation in the gulf. Current velocity at the sea surface during springtime have an average recorded velocity of 30cm s^{-1}, whilst the central portions of the water column are predicted to be much slower between 5-10cm s^{-1} (Gao et al., 2017). Currents driven by the tide have a maximum velocity of ~60cm s^{-1} and 100cm s^{-1} near the surface (Ma et al., 2019). The spatio-temporal distribution of waves in the Beibu Gulf have been modelled by Zhou et al (2015) using the Simulated Waves Nearshore (SWAN) model at 0.5°x0.5° resolution. The model gives detail on the distribution of significant wave height, wave period and wave energy across the entire Beibu Gulf, excluding parts of the Guangdong Coast (Figure 32a, b and c respectively). The model predicts the highest wave energies to be located in the centre and southern areas of the gulf, with the strongest monthly wave energies from January to March at 2.5kW/m. With regards to the study area of the project, the model predicts annual average wave energies to not exceed 1kW/m.

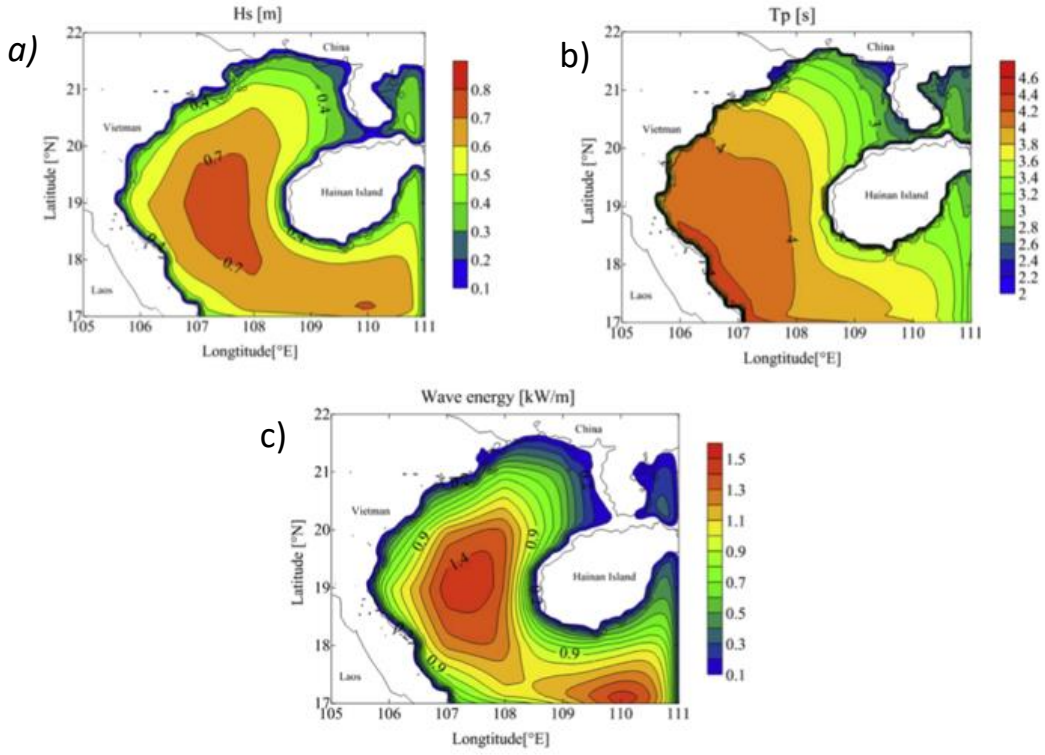

Figure 32. Spatial distribution of mean annual averaged a) significant wave height; b) wave period; c) wave energy in the Beibu Gulf. From Zhou et al., 2015

Current velocities are reported to be much higher closer to the coast. For example, a localised study on the accumulation of microplastics in mangrove ecosystems during flood/ebb tides report velocities ranging from 50-150cm s^{-1} (Zhang[a] et al., 2020). This is supported by other, more localised investigations which have also revealed strong tidal current velocities in winter (20cm s^{-1} vs 5cm s^{-1} in summer) (Sun et al., 2014).

5.1.2.3 Substrates and Geology

Soft sediments are dominant in the Beibu Gulf. The East and South-East portions of the gulf are described as a mixture of material deposited via coastal erosion and fine sediment deposited by oceanic currents from the South China Sea (Ma et al., 2014), comprised mainly of well-sorted fine sand, fine sediment and gravel (Ma et al., 2019).

Mudflats and sandflats are prominent in the north-east, particularly around the Shatian peninsula in the Guangxi Province. These tidal flats are characterised by sediments comprised of silty clay and sandy-silty clay (Meng et al., 2017). Deposition in the centre of the gulf is relatively slow at ~0.6 cm a^{-1} and is therefore described as a stable sedimentary environment (Kaiser et al., 2016). There is evidence that the composition of sediments can change seasonally, as reported in the Maowei Sea (see Figure 26 for location) where the sediments shift from silt to sandy silt sediments in the winter to sand to silty sand sediments in the summer (Figure 33; Yang et al., 2019).

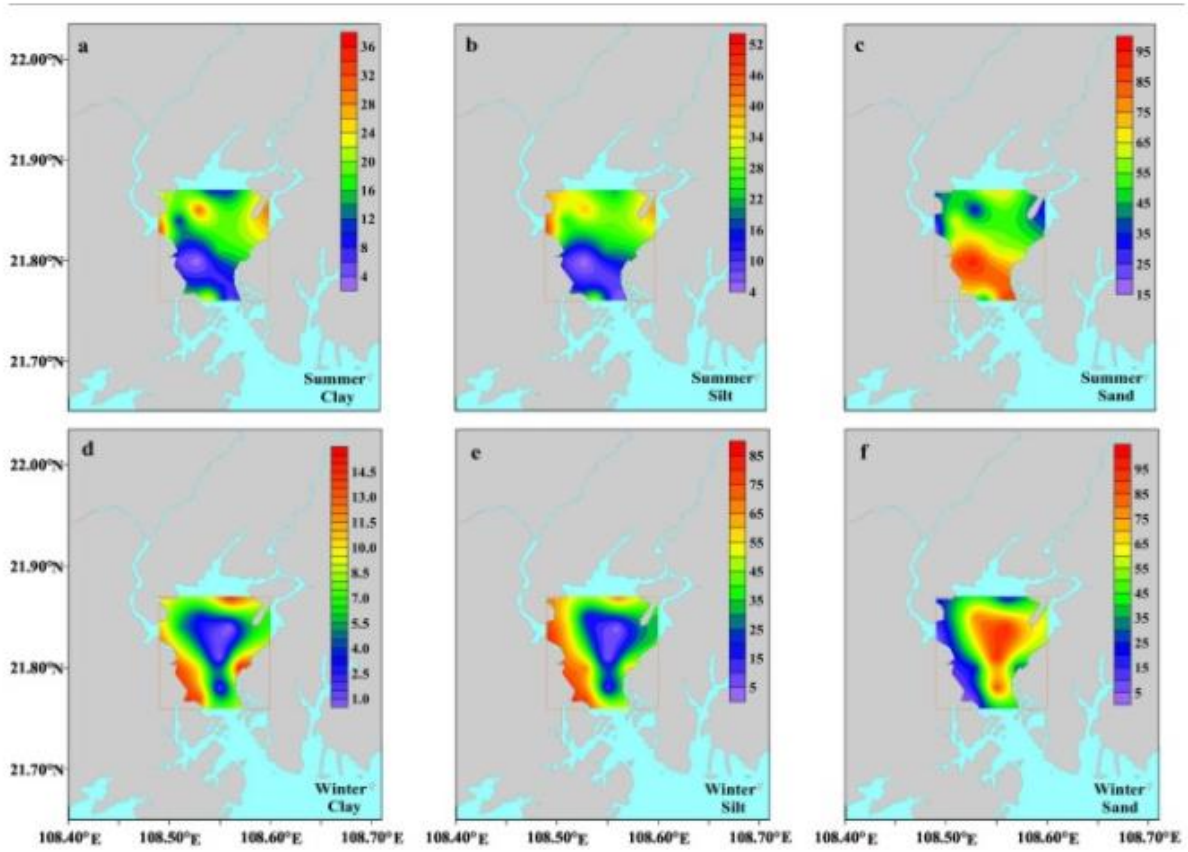

Figure 33. Seasonal changes in the sediment composition within the Maiowei Sea. The top row of figures show sediment compositions during the summer months, whilst the bottom row of figures show winter sediment compositions. Figures from left to right, read the percentage composition of clay, silt and sand respectively. Figure has been extracted from Yang et al., 2019.

5.1.3 Biological Setting

Literature on the types of biological communities found subtidally in the Beibu Gulf are extremely biased towards species distribution models for charismatic megafauna (e.g. Indo-Pacific humpback dolphin: Wu et al., 2017, Huang et al., 2019), intertidal mangrove studies (e.g. Tian et al. 2018) or fisheries resources (e.g. Xie et al., 2020). Papers are often complimentary on the gulf's biodiversity and species richness without any quantitative measures to support the claims. Perhaps the only exception being Yu & Mu (2006) who report the gulf possessing around 30 large kelp species, 200 shellfish, 20 cephalopod, 100 crustaceans and 240 fish species.

Although general biotope mapping seems absent in the study area and wider gulf, some studies give clues as to what habitat types occur in the gulf. For example. Xie et al., (2020) gives a general description of coastal regions of the gulf to contain a mosaic of different habitat types, including seagrass beds, coral reefs, mudflats, beaches and tidal creeks. Another study classified shoreline habitat for an oil spill response in the Vietnamese portion of the gulf (Figure 34), which could be indicative of habitats exhibited in the study area (Tri et al., 2014).

Figure 34. Examples of different shoreline habitats classified along the Vietnamese coast, taken from Tri et al (2014).

It seems that to get any spatial information about the different habitat types that occur in the gulf, search terms should include specific locations and specific biotopes.

5.1.3.1 Coral reefs

Weizhou Island (see Figure 26 for location) is a described as the northern limits of coral reef distribution within the South China Sea (Xiaohua et al., 2019) and is located south of Behai city in the centre of the project study area. It is estimated that the total area of coral reef surrounding Weizhou Island is between 6 and 8km^2 and contains the genera Pavona, Porites, Favites, Favia, and Platygyra (Huang et al., 2017). Recent estimations suggest that the fringing reefs surrounding Weizhou Island have experienced a dramatic decline, from 70% live cover in the 1990's to less than 10% at present, due to increased pressures of anthropogenic activity and climate change (Xu et al., 2020).

Corals are also known to exist within the Guangxi and Guandong coasts of the study area, though data on the area cover or specific locations are not reported (Xin-Qing et al., 2013). The western coast of Xuwen county (see Figure 26) is also home to a national coral reef nature reserve (Bai & Hou, 2020), offering a protective reach exceeding 14,000ha (Wang, 2018). The boundary of the nature reserve and the abundance of coral it protects could not be found using generic search terms, suggesting that the information may be highly sensitive. Hughes and colleagues (2012) provide the best available map of coral coverage in the study area (Figure 35).

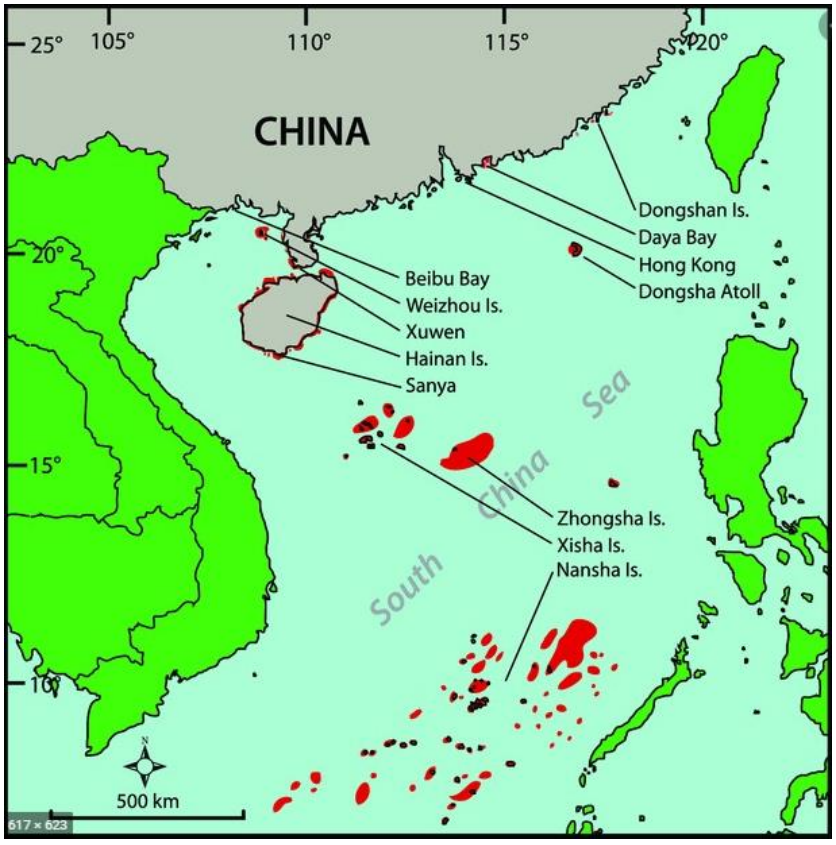

Figure 35. Distribution of coral reefs in the South China Sea, denoted by the red colouration on the map. Figure taken from Hughes et al (2012).

A comprehensive meta-analysis by Latypov Y.Y (2003) provides a long list of coral species found in the east of the gulf but, like most studies, does not specify their location or give estimates on species coverage. It does, however, provide a description and diagrammatic of the two most common reef types found in the gulf: unstructured and structural reefs (Figure 36). The classification of these reef types comes as the typical reef zones exhibited in most parts of the world are more difficult to recognise in the gulf (e.g. lagoons and reef flats). The author relates the composition of unstructured reefs to encrusting reefs, where corallogenic deposits form a thin crust over the underlying substrate. As such, the vertical profile of the reef seems unchanged. Conversely, structural reefs have distinguishable zonality.

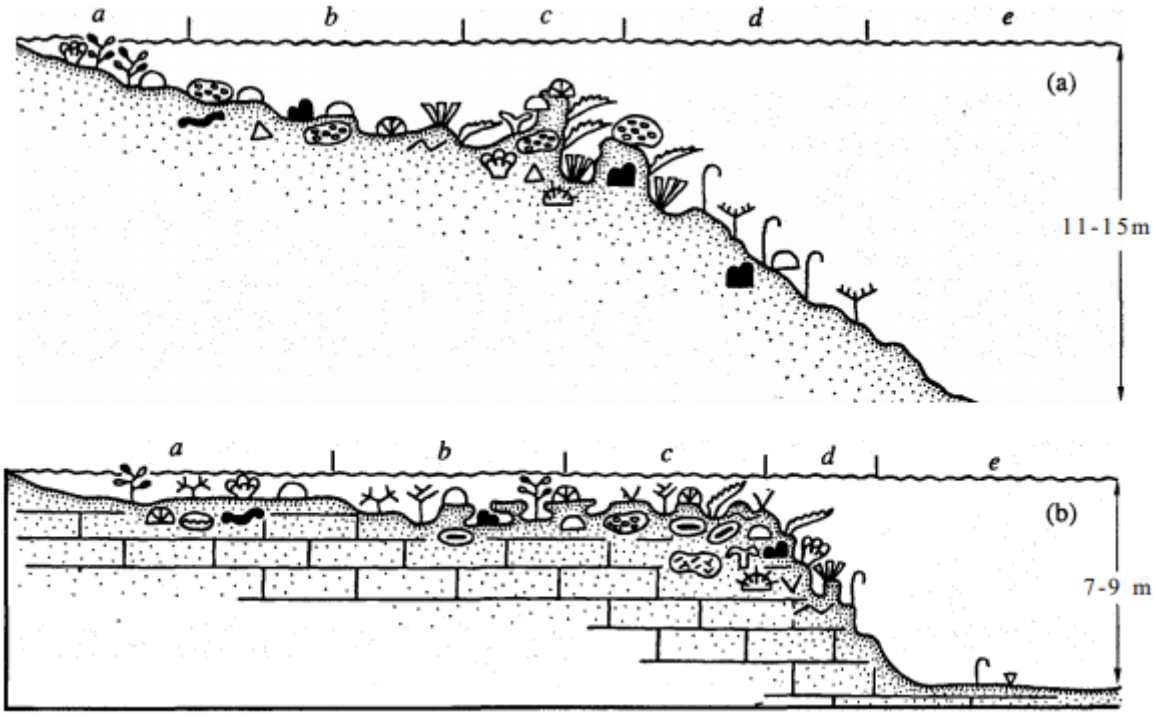

Figure 36. Profile of an unstructured (a) and structural reefs (b) found in the Beibu Gulf, taken from Latypov Y.Y (2003). The segments at the top denote: a - the algal-coral zone, b – multispecific coral settlement zone, c – predominance of one or two coral species, d – reef slope and e – the pre-reef platform.

5.1.3.2 Macroalgae

The review reports Weizhou island to be the only location discussing the presence of macroalgae in the entire study area. The nearshore reef zones are known to support algal communities consisting of red-brown sargasso species, padins and turbinaria (Latypov, 2003). Turf algae also exist in competition with the sclerectinian corals, predominantly *Lobophora variegata* and *Bryopsis pennata* (Liao et al., 2019). The only other seaweed studies that could be found related to species cultivations, such as sea grapes (Long et al., 2019).

5.1.3.3 Mollusc communities

Studies detailing the size and location of reef-building or bed-forming mollusc habitats in the Beibu Gulf remain elusive. The literature searches returned studies that were mostly focused on shellfish aquaculture (e.g. Lim et al., 2020) or inventories of molluscan biodiversity (Lutaenko, 2016).

Just two studies provided the location of oysters in the study area of the Beibu Gulf. The first was a paper stating the Maiowi Sea (see Figure 26 for location) contained ~2340hm^2 of natural spawning and breeding ground for the Jinjiang oyster, *Megallana rivularis* (Yang et al., 2019), a once dominant species that could form reef structures (Quan et al., 2012). The other, a study comparing the genetic variation of wild and cultivated pearl oysters (*Pinctada fucata*) with wild samples collected from the Beibu Bay (Figure 33; Yu & Chu, 2006) – a species known to form beds (Chellam et al., 1983).

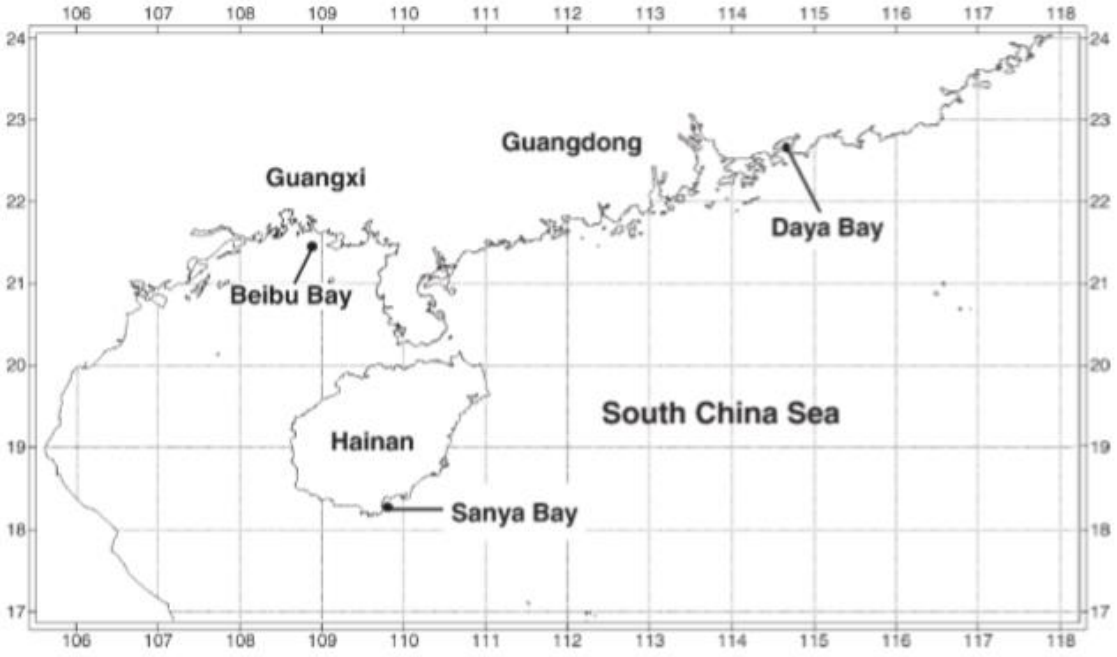

Figure 37. Location of wild and cultured pearl oysters. From Yu & Chu (2006).

Given the high economic value of oysters in an area renowned for intense aquaculture, it's unsurprising that the locations of any large-scale habitats are not published in literature.

5.1.3.4 Seagrasses

There are three main locations within the study area that are reported to contain seagrass beds. These are: Pearl Bay, Hepu Bay and Liusha Bay (see Figure 26 for location). Recent literature suggests there are five species of seagrasses that exist in the Beibu Gulf which, collectively, cover a total area of ~37km^2 (Fortes et al., 2018).

A single seagrass bed comprised of two species is located within Liusha Bay, covering a total area of 900ha (Figure 38). The composition of the bed is reported to contain 98% by the species *Halophila ovalis* and 2% by the species *Halodule uninervis* (Huang, 2008).

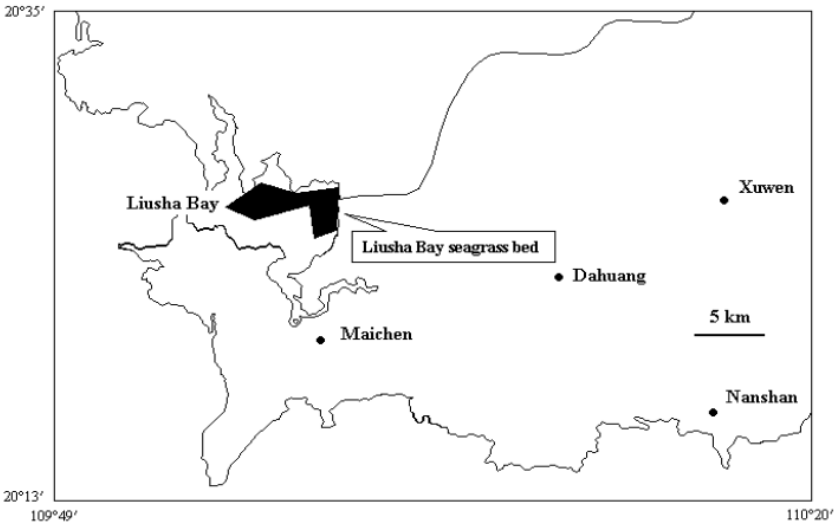

Figure 38. Location of the large seagrass bed in Liusha Bay, Guangdong province. Figure taken from Huang (2008).

Several seagrass beds exist across Hepu Bay (Figure 39) and contain a mixture of *Halophila ovalis* and *Halodule uninervis* (Huang 2006). A third species, *Zostera japonica*, has also been reported in the region, however, its coverage has not been recorded. Each bed ranges between 20-250ha in size, with a collective total of 540ha (Huang, 2008).

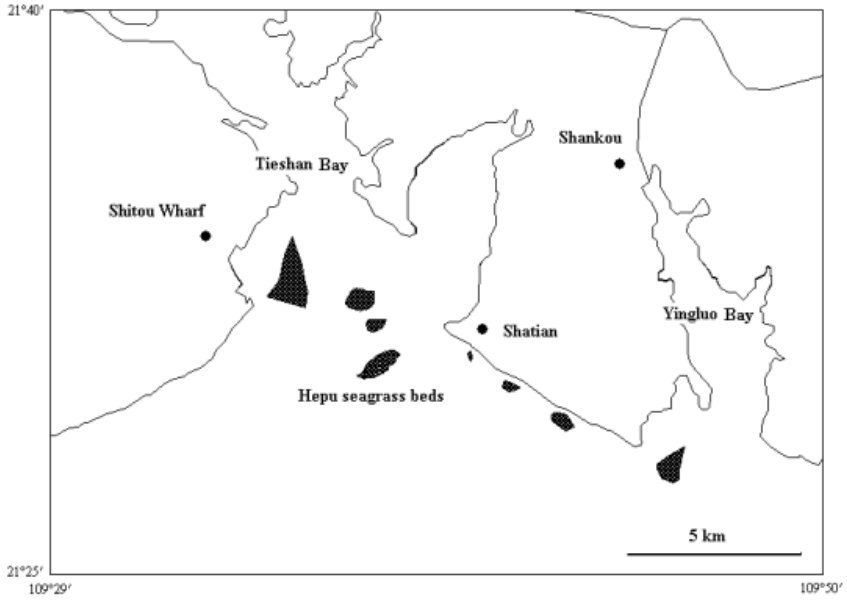

Figure 39. Location of seagrass beds in Hepu Bay, Guangxi province. Taken from Huang (2008).

Seagrass beds are reported in multiple locations across the tidal sand- and mudflats in Pearl Bay (Fan et al., 2017). The largest beds are reported by Huang (2008), comprised of two co-existing species across two separate beds, with *Zostera japonica* as the dominant species and interludes of *Halophila beccarii* (Figure 40). The total area represented by these beds is 150ha (Huang 2006).

Figure 40. Location of seagrass beds in Pearl Bay, Guandong. Taken from Huang (2008).

Smaller beds are reported in a study by Fan and colleagues (2017), which is much closer to the coast. In this study area, it is reported that beds of *H. beccaruii* exist at the edges of the mangrove forests which eventually transition over to Z. japonica beds moving towards the centre of the bay (Figure 41).

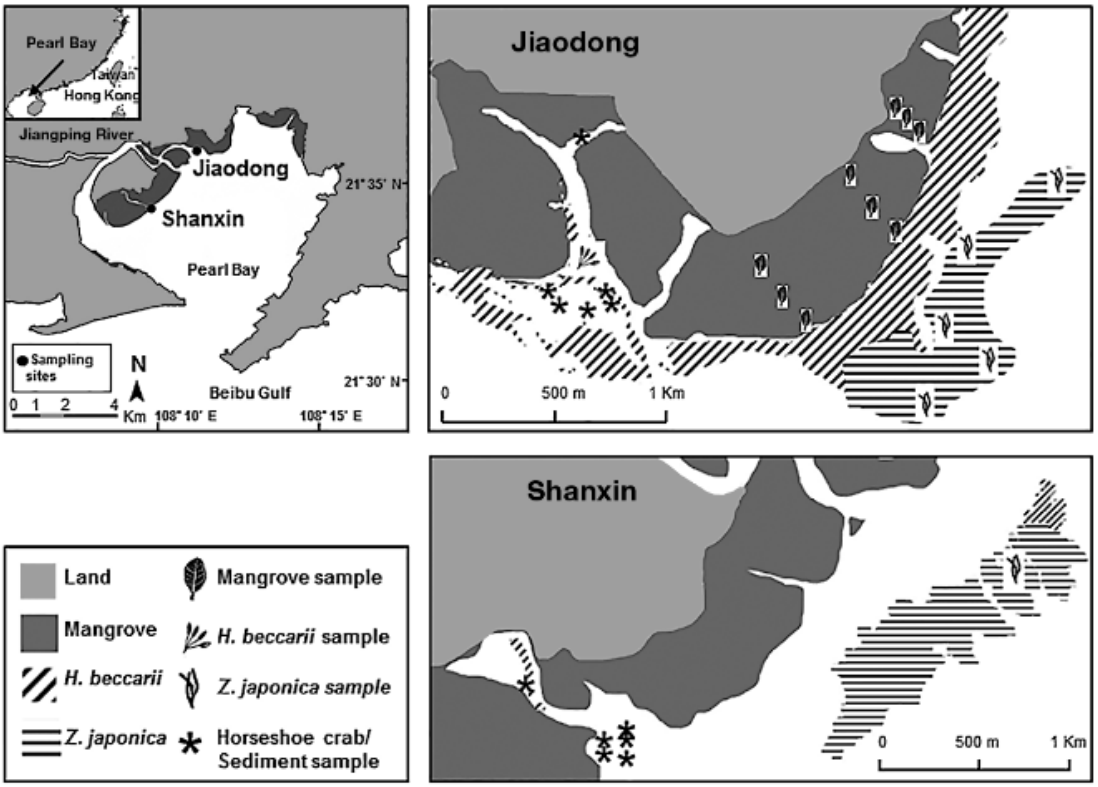

Figure 41. Location of seagrass beds in Pearl Bay, Guangdong province. Figure has been taken from Fan et al., 2017.

5.1.4 Conclusion

In summary, very little habitat mapping activities have occurred in the study area, at least from the literature searches performed in English. Whilst there are extensive studies on the physical conditions exhibited across the Beibu Gulf, information on the distribution of habitats and communities was limited to a handful of papers on corals and seagrass. These papers were only discoverable once the search terms were tailored to specific locations within the gulf and coupled with specific biotopes that were presumed to exist in the study area.

There is still a significant knowledge gap on what other communities may exist in the gulf, evident from the number of papers boasting the gulf for its species richness without supplementary spatial information. Clues as to what communities exist in the gulf are scattered in descriptions of study sites within the Beibu Gulf, (e.g. presence of sponge communities, Liu et al., 2019), but further searches on their abundance and distributions subsequently led to dead ends.

Given the amount of literature pertaining to aquaculture and oil exploration, the mapping of artificial substrates and separate classes for shrimp ponds, shellfish farms and seaweed mariculture should be considered.

5.1.5 References

Bauer A, Radziejewska T, Liang K, Kowalski N, Dellwig O, Bosselmann K, Stark A, Xia Z, Harff J, Böttcher M, Schulz-Bull D, Waniek J (2013) Regional Differences of Hydrographical and Sedimentological Properties in the Beibu Gulf, South China Sea. *Journal of Coastal Research*, 66, pp.49-71. 10.2112/SI_66_5.

Bai S, Hou G (2020) Microbial communities on fish eggs from Acanthopagrus schlegelii and Halichoeres nigrescens at the XuWen coral reef in the Gulf of Tonkin. PeerJ 8:e8517 https://doi.org/10.7717/peerj.8517

Chellam A, Velayudhan T.S, Dharmaraj S, Victor A.C.C, Gandhi A.D (1983) A note on the predation on pearl oyster Pinctada fucata (Gould) by some gastropods. *Indian Journal of Fisheries*, 30(2), pp.337-339.

Chen Z, Qui Y, Jia X, Xu S (2008). Using an Ecosystem Modeling Approach to Explore Possible Ecosystem Impacts of Fishing in the Beibu Gulf, Northern South China Sea. *Ecosystems*. 11, pp. 1318-1334. 10.1007/s10021-008-9200-x.

Chen S, Li Y, Hu J, Zheng A, Huang L, Lin Y (2011a) Multiparameter cluster analysis of seasonal variation of water masses in the eastern Beibu Gulf. *Journal of oceanography*, 67(6), pp.709-718.

Chen Z, Qiu Y, Xu S (2011b) Changes in trophic flows and ecosystem properties of the Beibu Gulf ecosystem before and after the collapse of fish stocks, *Ocean & Coastal Management*, Volume 54, Issue 8, Pages 601-611, ISSN 0964-5691,https://doi.org/10.1016/j.ocecoaman.2011.06.003.

Chen Z, Qiao F, Xia C. et al (2015) The numerical investigation of seasonal variation of the cold water mass in the Beibu Gulf and its mechanisms. *Acta Oceanologica Sinica*. Sin. 34, pp.44–54. https://doi.org/10.1007/s13131-015-0595-x

DanLing Tang, Hiroshi Kawamura, Ming-An Lee, Tran Van Dien (2003) Seasonal and spatial distribution of chlorophyll-a concentrations and water conditions in the Gulf of Tonkin, South China Sea, *Remote Sensing of Environment*,85,(4),pp.475-483, ISSN 0034-4257,https://doi.org/10.1016/S0034-4257(03)00049-X.

Fan H, Chen G, He B, Mo Z (2005) Coastal wetland and management of Shankou Mangroves, 35–89. Beijing: *China Ocean Press*.in Chinese

Fan L.F, Chen C.P, Yang M.C, Qiu G, Liao Y.Y, Hsieh H.L (2017) Ontogenetic changes in dietary carbon sources and trophic position of two co-occurring horseshoe crab species in southwestern China. *Aquatic biology*, 26, pp.15-26.

Fortes M.D, Ooi J.L.S, Tan Y.M, Prathep A, Bujang J.S, Yaakub S.M (2018) Seagrass in Southeast Asia: a review of status and knowledge gaps, and a road map for conservation. *Botanica Marina*, 61(3), pp.269-288.

Huang R, Yu K, Wang Y, Wang J, Mu L, Wang W (2017) Bathymetry of the coral reefs of Weizhou Island based on multispectral satellite images. *Remote Sensing*, 9(7), pp.750.

Huang, M.X (2008) Seagrass in the South China Sea. National Report on Seagrass in the South China Sea – China. Accessed online [20/01/2021]:
http://www.unepscs.org/components/com_remository_files/downloads/National-Report-Seagrass-China.pdf

Huang S.L, Peng C, Chen M, Wang X, Jefferson T.A, Xu Y, Yu X, Lao Y, Li, J, Huang H, Wu H (2019). Habitat configuration for an obligate shallow-water delphinid: The Indo-Pacific humpback dolphin, Sousa chinensis, in the Beibu Gulf (Gulf of Tonkin). *Aquatic Conservation: Marine and Freshwater Ecosystems*, 29(3), pp.472-485.

Huang X, Huang L, Li Y, Xu Z, Fong C.W, Huang D, Han Q, Huang H, Tan Y, Liu S, (2006) Main seagrass beds and threats to their habitats in the coastal sea of South China. Chinese Science Bulletin, 51(2), pp.136-142.

Hughes T.P, Huang H.U.I, Young M.A (2013) The wicked problem of China's disappearing coral reefs. *Conservation Biology*, 27(2), pp.261-269.

Jingsong Gao, Guidan Wu, Hanzheng Ya (2017) Review of the circulation in the Beibu Gulf, South China Sea. *Continental Shelf Research*, 138,pp.106-119, ISSN 0278-4343, https://doi.org/10.1016/j.csr.2017.02.009.

Jingsong Gao, Guidan Wu, Hanzheng Ya, (2017) Review of the circulation in the Beibu Gulf, South China Sea. *Continental Shelf Research*, 138, pp.106-119, ISSN 0278-4343, https://doi.org/10.1016/j.csr.2017.02.009.

Kaiser D, Schulz-Bull D.E, Waniek J.J (2016) Profiles and inventories of organic pollutants in sediments from the central Beibu Gulf and its coastal mangroves. *Chemosphere*, 153, pp.39-47.

Lai J, Jiang F, Ke K, Xu M, Lei F, Chen B (2014). Nutrients distribution and trophic status assessment in the northern Beibu Gulf, China. *Chinese journal of oceanology and limnology*, 32(5), pp.1128-1144.

Latypov, Y.Y (2003). Reef-building corals and reefs of Vietnam: 2. The Gulf of Tonkin. *Russian Journal of Marine Biology*, 29(1), pp.S34-S45.

Liao W, Hu J, Zhou H, Hu J, Peng P, Deng W (2018) Sources and distribution of sedimentary organic matter in the Beibu Gulf, China: Application of multiple proxies*, Marine Chemistry*, 206, pp 74-83, ISSN 0304-4203, https://doi.org/10.1016/j.marchem.2018.09.006.

Lim, Leong-Seng Leong-Seng, Kit-Shing Liew, Tzuen-Kiat Yap, Nai-Han Tan, and Cheng-Kai Shi (2020) Length-weight relationship and relative condition factor of pearl oyster, Pinctada fucata martensii, cultured in the Tieshangang Bay of the Beibu Gulf, Guangxi Province, China. *Borneo Journal of Marine Science and Aquaculture (BJoMSA)* 4, (1), pp. 24-27.

Liu T, Wu S, Zhang R, Wang D, Chen J, Zhao J (2019) Diversity and antimicrobial potential of Actinobacteria isolated from diverse marine sponges along the Beibu Gulf of the South China Sea. *FEMS microbiology ecology*, 95(7), p.fiz089.

Long H, Gu X, Zhu Z, Wang C, Xia X, Zhou N, Liu X, Zhao M (2019) Effects of bottom sediment on the accumulation of nutrients in the edible green seaweed Caulerpa lentillifera (sea grapes). *Journal of Applied Phycology*,32(1) pp.1-12.

Lutaenko K.A (2016) Biodiversity of bivalve mollusks in the western South China Sea: an overview. Biodiversity of the Western Part of the South China Sea. Vladivostok*, Dalnauka*, pp.315-384.

Ma, X., Yan, J. and Fan, F (2014) Morphology of submarine barchans and sediment transport in barchans fields off the Dongfang coast in Beibu Gulf. *Geomorpholog*y, 213, pp.213-224.

Ma, X., Yan, J., Song, Y., Liu, X., Zhang, J. and Traykovski, P.A (2019) Morphology and maintenance of steep dunes near dune asymmetry transitional areas on the shallow shelf (Beibu Gulf, northwest South China Sea). *Marine Geology*, 412, pp.37-52.

Meng X, Xia P, Li Z, Meng, D (2017) Mangrove development and its response to Asian monsoon in the Yingluo Bay (SW China) over the last 2000 years. *Estuaries and Coasts*, 40(2), pp.540-552.

Qiao Y, Chen Z, Lin Z (2008) Changes of community structure of fishery species during spring and autumn in the Beibu Gulf. *Journal of Fishery Sciences of China* (in Chinese), 15(5), pp. 816–821

Quan W, Humphries A.T, Shen X, Chen Y (2012) Oyster and associated benthic macrofaunal development on a created intertidal oyster (Crassostrea ariakensis) reef in the Yangtze River estuary, China. Journal of Shellfish Research, 31(3), pp.599-610.

Shen C, Yan Y, Zhao H, Pan J, T. Devlin A (2018) Influence of monsoonal winds on chlorophyll-α distribution in the Beibu Gulf. *PLoS ONE* 13(1): e0191051. https://doi.org/10.1371/journal.pone.0191051

Shi M, Chen C, Xu Q, Lin H, Liu G, Wang H, Wang F, Yan J (2002) The role of Qiongzhou Strait in the seasonal variation of the South China Sea circulation. *Journal of Physical Oceanography*, 32(1), pp.103-121.

Sun T, Macrander A., Kaiser D (2014) A water movement study in Lianzhou Bay, Guangxi Province, China. Journal of Ocean University of China 13, 13–22. doi:10.1007/s11802-014-1963-4

Tian, Q. and Li, S. (2018) Mangrove recognition and extraction using multispectral remote sensing data in Beibu Gulf. *In Multispectral, Hyperspectral, and Ultraspectral Remote Sensing Technology, Techniques and Applications VII* (Vol. 10780, p. 107800C). International Society for Optics and Photonics.

Tri D.Q, Don N, Ching C, Mishra P.K (2014) September. Utilizing Environmental Sensitive Index Map as a Tool for Oil Spill Response: Case Study of Cat Ba Island, Vietnam. In *Proceedings of the 19th IAHR-APD Congress* (Vol. 21, p. 24).

Wang B (2018) The outlook for the establishment and management of marine protected area network in China. *International Journal of Geoheritage and Parks*, 6(1), pp.32-42.

Wang R, Xu D, Ge Q (2020) Modern modes of sediment distribution and the anthropogenic heavy metal pollution record in northeastern Beibu Gulf, south China sea. *Marine Pollution Bulletin*, 150, pp.110694.

Wang Y, Zhang W, Lin Y, Cao W, Zheng L, Yang J (2014) Phosphorus, Nitrogen and Chlorophyll-a Are Significant Factors Controlling Ciliate Communities in Summer in the Northern Beibu Gulf, South China Sea. PLoS ONE 9(7): e101121. https://doi.org/10.1371/journal.pone.0101121

Wu H, Jefferson T.A, Peng C, Liao Y, Huang H, Lin M, Cheng Z, Liu M, Zhang J, Li S. Wang D (2017) Distribution and habitat characteristics of the Indo-Pacific humpback dolphin (Sousa chinensis) in the northern Beibu Gulf, *Aquatic Mammals* 43(2), pp.219-228 China.

Xiaohua Li, Yi Liu, Chung-Che Wu, Ruoyu Sun, Liugen Zheng, Mahjoor Ahmad Lone, Chuan-Chou Shen (2019) Coral-inferred monsoon and biologically driven fractionation of offshore seawater rare earth elements in Beibu Gulf, northern South China Sea, *Solid Earth Sciences*, 4(4),pp. 131-141, ISSN 2451-912X, https://doi.org/10.1016/j.sesci.2019.09.003.

Xie X, Wu Z, Wang C.C, Fu Y, Wang, X, Xu P, Huang X, Liao Y, Huang S.L, Kwan K.Y (2020) Nursery habitat for Asian horseshoe crabs along the northern Beibu Gulf, China: Implications for conservation management under baseline gaps. *Aquatic Conservation: Marine and Freshwater Ecosystems*, 30(2), pp.260-272.

Xin-Qing Z, Yuan-Chao L, Rong-Cheng L, Wen-Lu L, Jian-Guo D, Xiao-Zhou Y, Wen-Tao N, Xiao-Feng, Ding-Yong H (2013) Coral reef conservation and restoration in Mainland China. Sea, 8, pp.12-14.

Xu S, Yu K, Zhang Z, Chen B, Qin Z, Huang X, Jiang W, Wang Y, Wang Y (2020) Intergeneric Differences in Trophic Status of Scleractinian Corals From Weizhou Island, Northern South China Sea: Implication for Their Different Environmental Stress Tolerance. *Journal of Geophysical Research: Biogeosciences*, 125(5), p.e2019JG005451.

Yang, B., Zhou, J.B., Lu, D.L., Dan, S.F., Zhang, D., Lan, W.L., Kang, Z.J., Ning, Z.M. and Cui, D.Y., (2019) Phosphorus chemical speciation and seasonal variations in surface sediments of the Maowei Sea, northern Beibu Gulf. *Marine pollution bulletin*, 141, pp.61-69.

Yang B, Lan R.Z, Lu D.L, Dan S.F, Kang Z.J, Jiang Q.C, Lan W.L, Zhong Q.P (2019) Phosphorus biogeochemical cycling in intertidal surface sediments from the Maowei Sea in the northern Beibu Gulf. *Regional Studies in Marine Science*, 28, pp.100624.

Yang G, Sun X, Song Z (2020) Trophic level and heavy metal pollution of Sardinella albella in Liusha Bay, Beibu Gulf of the South China Sea*, Marine Pollution Bulletin*, 156, 111204, ISSN 0025-326X, https://doi.org/10.1016/j.marpolbul.2020.111204.

Yu D.A, Chu K.H (2006) Genetic variation in wild and cultured populations of the pearl oyster Pinctada fucata from southern China. *Aquaculture*, 258(1-4), pp.220-227.

Yu Y, Mu Y (2006) The new institutional arrangements for fisheries management in Beibu Gulf, Marine Policy, 30,(3), pp. 249-260, ISSN 0308-597X, https://doi.org/10.1016/j.marpol.2004.12.006.

Zhang L, Zhang S, Guo J, Yu K, Wang Y, Li R (2020a) Dynamic distribution of microplastics in mangrove sediments in Beibu Gulf, South China: Implications of tidal current velocity and tidal range, *Journal of Hazardous Materials*, 399, pp.122849, ISSN 0304-3894, https://doi.org/10.1016/j.jhazmat.2020.122849.

Zhang R, Yu K, Li A, Zeng W, Lin T, Wang Y (2020b) Occurrence, phase distribution, and bioaccumulation of organophosphate esters (OPEs) in mariculture farms of the Beibu Gulf, China: A health risk assessment through seafood consumption. *Environmental Pollution*, 263 (B), pp.114426, ISSN 0269-7491, https://doi.org/10.1016/j.envpol.2020.114426.

Zhou G, Huang J, Yue T, Luo, Q, Zhang G (2015) Temporal-spatial distribution of wave energy: A case study of Beibu Gulf, China. *Renewable Energy*, 74, pp.344-356

5.2 Appendix II: Model Guidance

This document is a guide for creating a seabed habitat map and accompanying confidence map using the EUSeaMap approach, the concepts of which are described in detail in Populus et al., 2017. The method is implemented in the form of ArcGIS™ Model Builder models.

A-CREATING THE SEABED HABITAT MAP

The creation of the seabed habitat map comprises 2 steps that respectively create 1) the biological zone layer, and 2) the seabed habitat layer

A.1–STEP 1: CREATING THE BIOLOGICAL ZONE LAYER

The biological zones are illustrated in Figure 1. We will define the infralittoral as the area in which there is light enough for seagrass or macroalgae species to grow. The circalittoral will start where there is not enough light for these species to grow, and end where the sea bottom is no longer disturbed by wave action. Then will start the deep circalittoral. In the study area of the Beibu Gulf, we will not go deeper than the deep circalittoral because the maximum depth (around 50m) does not reach the bathyal.

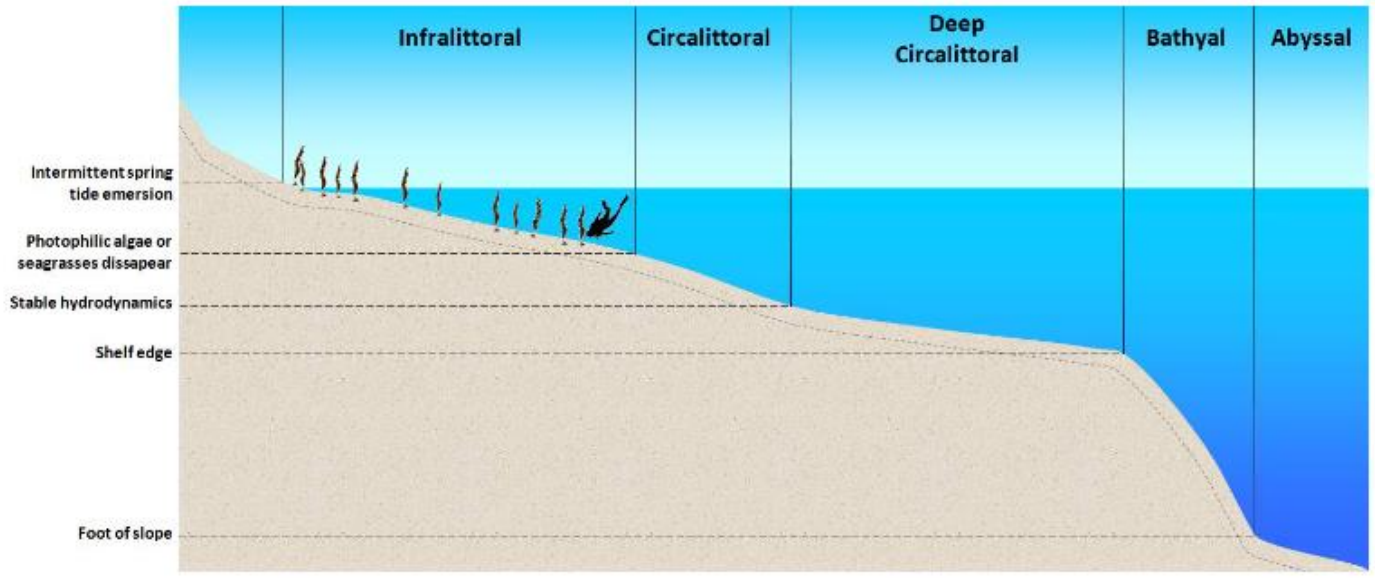

Figure 1. The biological zones and their meaning.

For the infralittoral/ circalittoral boundary we will use the variable 'fraction of light at the seabed' (Fr), which is calculated by intersecting a KdPAR (coefficient of light attenuation in the water column) raster and a bathymetry raster using the equation $Fr = e^{-hxKdpar}$, where h is the depth. Values are in

the range [0-1], 0 meaning 0% of the surface light reaches the seabed, 1 meaning 100% of the surface light reaches the seabed. We will consider that the infralittoral is where Fr ≥ 0.01 (i.e. there is light enough for seagrass or macroalgae species to grow when Fr ≥ 0.01).

For the circalittoral /deep circalittoral boundary we will use the bathymetry and consider that below a depth of -30m, the seafloor is no longer affected by wave action.

A.2‑STEP 2: CREATING THE SEABED HABITAT LAYER

The habitat map is created by combining the habitat descriptors layers. Here, 2 habitat descriptors will be considered: the biological zones and the seabed substrate. The biological zone layer is produced in step 1 (see section A.1). The seabed substrate layer is provided ready-to-use as input. Each habitat descriptor layer has one field in which the values are 2-digit codes, each code being representative of a habitat descriptor class, coded as described in tables 1 and 2.

Table 1. Seabed substrate codes.

2-digit code	Name
10	Mud
20	Sand
30	Coarse sediment
40	Mixed sediment
50	Sandy mud
60	Muddy sand
70	Rock
72	Tropical coral reef

Table 2. Biological zone codes

2-digit code	Name
10	Infralittoral
20	Circalittoral
30	Deep circalittoral

The 2 habitat descriptor layers are combined using a geometric intersection. As a result, a seabed habitat polygon layer is created. In that layer, a field contains values of seabed substrate types and another one contains values for biological zones. For each polygon the values contained by these 2 fields are summed in a new field using the following formula: (biozone x 1000) + substrate. As a result, the field contains a 4-digit code that is representative of a unique combination of a biozone and a seabed substrate type: the 2 first digits from the right correspond to the seabed substrate and the 2 last digits from the right correspond to the biological zone (e.g. 1040 means biological zone = 10 and substrate = 40).

The last step comprises joining the seabed habitat layer and the look-up table, which is that table that crosswalks the abovementioned 4-digit habitat codes and the habitat classes described in the habitat classification that is used for the study area.

A.3-ARCGIS™ MODEL BUILDER MODELS

2 model builder models are available, one for each above-mentioned step. They will require the following inputs:

- A fraction of light at the seabed layer
- A bathymetry layer
- A seabed substrate layer
- A look-up table

Test datasets are provided for a European study area. They were all produced as part of EMODnet. The seabed substrate layer was slightly modified: in order for all the seabed substrate types found in the Beibu Gulf to be represented, some false tropical coral reef polygons were added. All the datasets are in the 'input' folder. The models will create all the outputs in the 'output' folder.

A.3.1 -CREATING THE BIOLOGICAL ZONE LAYER

ArcGIS™ Model Builder Model name	Toolset *A_Seabed_Habitat_Map* Model *1_create_biological_zones*
Descr.	Creates a polygon shapefile for biological zones. It will contain 3 biological zones: infralittoral and circalittoral. Infralittoral will be assigned the code 10, circalittoral will be assigned the code 20, and deep circalittoral will be assigned the code 30. To separate between infralittoral and circalittoral, a raster of fraction of surface light reaching the seabed (value in the range [0-1], 0 meaning 0% of the surface light reaches the seabed, 1 meaning 100% of the surface light reaches the seabed) is used. The threshold value used is 0.01 (i.e., 1% of light reaching seabed): values above the threshold are classified as infralittoral, values below are classified as circalittoral. To separate between circalittoral and deep circalittoral, a raster of bathymetry is used. The threshold value used is -30m: values above that depth threshold are classified as circalittoral, values below are classified as deep circalittoral. The raster calculator is used to classify the raster of fraction of surface light reaching the seabed and bathymetry into the relevant biological zones (a, b, c). As a result, one categorical raster is produced for each biological zone. These rasters are then merged into a single raster (d), in which infralittoral pixels have value 10, circalittoral pixels have value 20, and deep circalittoral pixels have value 30. The raster is then converted to a polygon shapefile (e), in which the field with biozone values is named 'grid code'. A field with a more appropriate name ('biozone') is created (f), values of grid code are copied in that field (g), and the field 'grid code' is deleted (h).
Inputs	

Model Variable name	Type	Description
Infralittoral / Circalittoral boundary variable	Raster dataset	The raster for the variable that is used to model the boundary between infralittoral and circalittoral. It is a raster of fraction of surface light reaching at the seabed (value in the range [0-1], 1 meaning 100% of the surface light reaches the seabed)
Infralittoral / Circalittoral boundary threshold value	Float	The threshold value of light fraction at the seabed that is used to separate between infralittoral and circalittoral. The value is 0.01

	Circalittoral / Deep circalittoral boundary variable	Raster dataset	The raster for the variable that is used to model the boundary between circalittoral and the deep circalittoral. It is a raster of depth
	Circalittoral / Deep circalittoral boundary threshold value	Float	The threshold value of depth that is used to separate between circalittoral and deep circalittoral. The value is -30m
	Infralittoral code	Integer	The code that will be assigned to infralittoral polygons (i.e. 10)
	Circalittoral code	Integer	The code that will be assigned to circalittoral polygons (i.e. 20)
	Deep circalittoral code	Integer	The code that will be assigned to deep circalittoral polygons (i.e. 30)
Output	**Model Variable Name**	**Type**	**Description**
	Biozone polygons	Feature class	The shapefile of biological zones, with one field, 'biozone', the value of which is 10 (for infralittoral), 20 (for circalittoral) or 30 (for deep circalittoral)
Main ArcGIS™ tools used	•Raster calculator (spatial analyst tools) •Mosaic to new raster (data management) •Raster to Polygon (Conversion)		

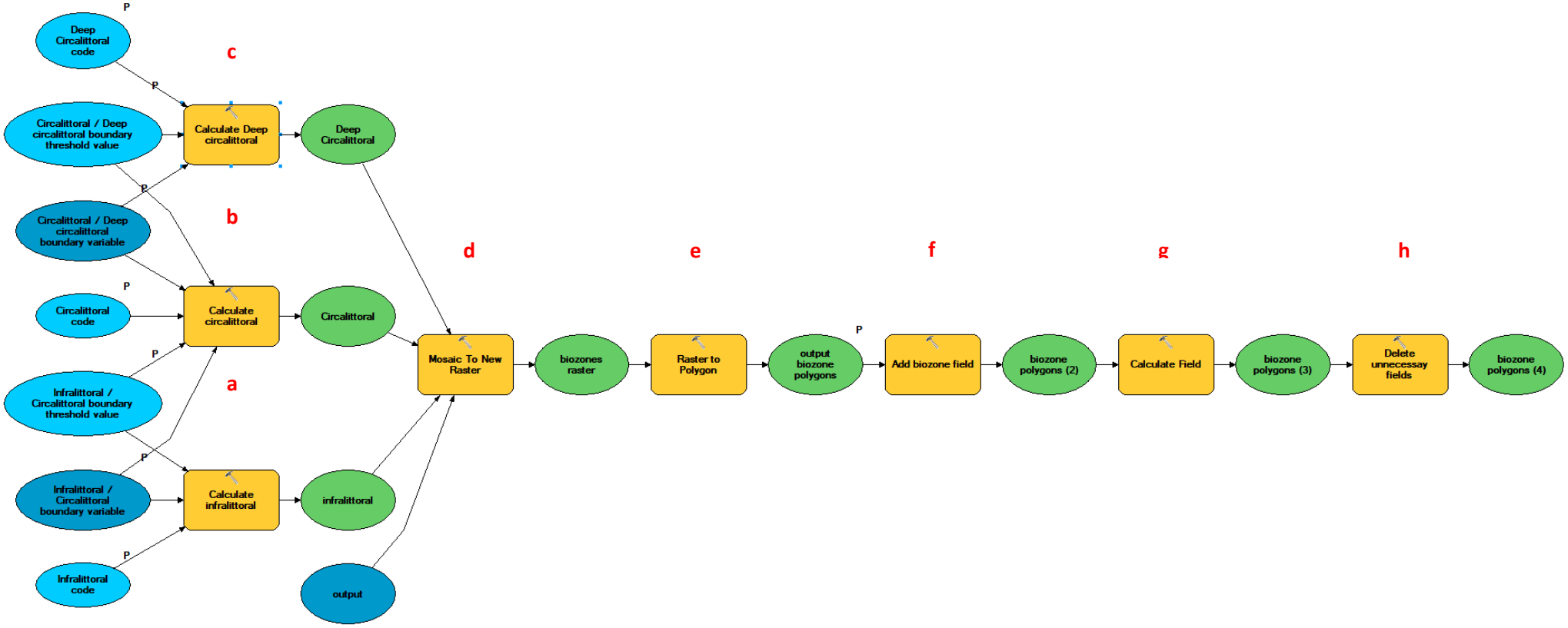

The project “International Ocean Governance: Strengthening international ocean data through the EU’s ocean diplomacy with China” is financed by the European Commission EuropeAid/139904/DH/SER/CN.

A.3.2–Creating the seabed habitat layer

<table>
<tr><td>ArcGIS™ Model Builder Model name</td><td>Toolset A_Seabed_Habitat_Map
Model 2_create_seabed_habitat_map</td></tr>
<tr><td>Descr.</td><td>Creates the habitat shapefile as a result of the combination of the biological zones (created using the model described in section A.3.1) and the seabed substrate shapefiles. The shapefiles are first spatially intersected (a). As a result, a shapefile is created in which each polygon is the intersection of a polygon of substrate and a polygon of biological zone. The output shapefile has one field for the substrate type (named ‘substrate’) and another one for the biological zone (named ‘biozone’). Then a field ‘hab_code’ is created (b), in which a habitat code is calculated using the following formula (c): biozone*1000 + substrate, so that the 2 first digits from the right correspond to the seabed substrate and the 2 last digits from the right correspond to the biological zone (e.g. 1040 means biological zone = 10 and substrate = 40). Then unnecessary fields are deleted (d). Finally (e), the shapefile is joined to a look-up table that crosswalks each individual habitat code with its corresponding habitat of the habitat classification.</td></tr>
<tr><td>Inputs</td><td>
<table>
<tr><th>Model Variable name</th><th>Type</th><th>Description</th></tr>
<tr><td>Seabed substrate</td><td>Feature class</td><td>A shapefile of seabed substrates. It contains a field ‘substrate’, the values of which are: 10 (Mud), 20 (Sand), 30 (Coarse sediment), 40 (Mixed sediment), 50 (Sandy mud), 60 (Muddy sand), 70 (Rock), 72 (Tropical coral reef)</td></tr>
<tr><td>Biozones</td><td>Feature class</td><td>A shapefile of biological zones. It contains a field ‘biozone’, the values of which are: 10 (infralittoral), 20 (circalittoral), 30 (deep circalittoral)</td></tr>
<tr><td>Look-up table</td><td>Table</td><td>A table (dbase file) that crosswalks each individual habitat code with its corresponding habitat of the habitat classification. It contains:
•a field ‘code’, the values of which are in the form of a4-digit code that describes a habitat type (2 first digits from the right correspond to the biological zone, the 2 last digit from the right correspond to the seabed substrate). e.g. 1040 means biological zone = 10 and substrate = 40
•a field ‘habitat’, that is the habitat name in the habitat classification</td></tr>
</table>
</td></tr>
<tr><td>Output</td><td>
<table>
<tr><th>Model Variable name</th><th>Type</th><th>Description</th></tr>
<tr><td>Seabed habitats</td><td>Feature class</td><td>The seabed habitat shapefile</td></tr>
</table>
</td></tr>
<tr><td>Main ArcGIS™ tools used</td><td>•Intersect (Analysis tools)
•Join field (data management)</td></tr>
</table>

The project “International Ocean Governance: Strengthening international ocean data through the EU’s ocean diplomacy with China” is financed by the European Commission EuropeAid/139904/DH/SER/CN.

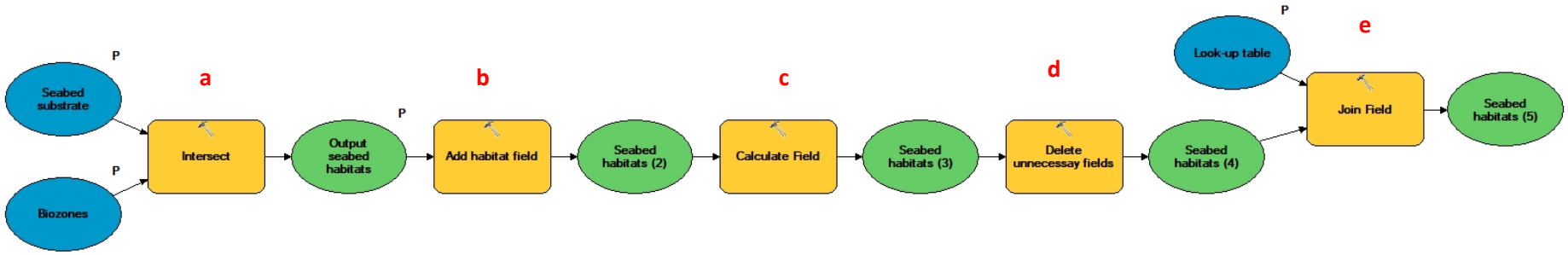

The project “International Ocean Governance: Strengthening international ocean data through the EU’s ocean diplomacy with China” is financed by the European Commission EuropeAid/139904/DH/SER/CN.

B-CREATING THE SEABED HABITAT CONFIDENCE MAP

An instrumental part of the EUSeaMap approach is being able to communicate the overall uncertainty of the habitat map to its users, achieved through the application of a confidence assessment. To assess confidence, we use the method developed by EMODnet Seabed habitats for the product EUSeaMap, described in Populus et al., 2017. To simplify the text and make it more reader-friendly, the confidence assessment resulting from the application of the EUSeaMap method will be referred to as "EUSeaMap confidence" in this document.

As illustrated in figure 2, the method results in a hierarchy of confidence assessments: confidence assessments are initially performed on the continuous physical datasets (e.g., kDPAR, Bathymetry), which inform the confidence assessments of the classified habitat descriptors (e.g., biological zones), which in turn inform the overall confidence assessment of the seabed habitat map. It is important to mention that confidence scores are not a mathematical definition, such as sensitivity, specificity of kappa scores calculated in species distribution modelling, but are qualitative measure for users to readily compare the reliability of datasets – assigning labels of low, medium, or high.

The way confidence in continuous physical variables (figure 2, box 1) is assessed is dependent on the nature of the variable. For Bathymetry, we use here the quality index that is used by EMODnet Bathymetry (EMODnet, 2017). For the kdPAR, we consider the number of remote sensing images used to generate the average values recorded in each grid cell, and assume that the more images used, the better the confidence. The way confidence in habitat descriptor layers is assessed (figure 2, box 2) is dependent on the nature of the habitat descriptor. For the **biological zone** habitat descriptor, confidence is an aggregation of i) the fuzziness in the thresholds used to delineate between two classes, accounting for the natural transition between one biological zone to its adjacent one and ii) the confidence in the continuous physical variables used as input to the biological zone layer calculation. For the **seabed substrate** habitat descriptor, we use the combined confidence index developed by EMODnet Geology (Kaskela et al., 2019). Finally, the habitat class confidence (figure 2, box 3) is a spatial combination of each habitat descriptor confidence layer, i.e. here of the biological zone and the seabed substrate confidence layers.

All confidence assessments are carried out in raster mode, with each raster cell being assigned a value in the EUSeaMap confidence scoring system, i.e. a score of 1 (low confidence), 2 (moderate confidence) or 3 (high confidence).

The project "International Ocean Governance: Strengthening international ocean data through the EU's ocean diplomacy with China" is financed by the European Commission EuropeAid/139904/DH/SER/CN.

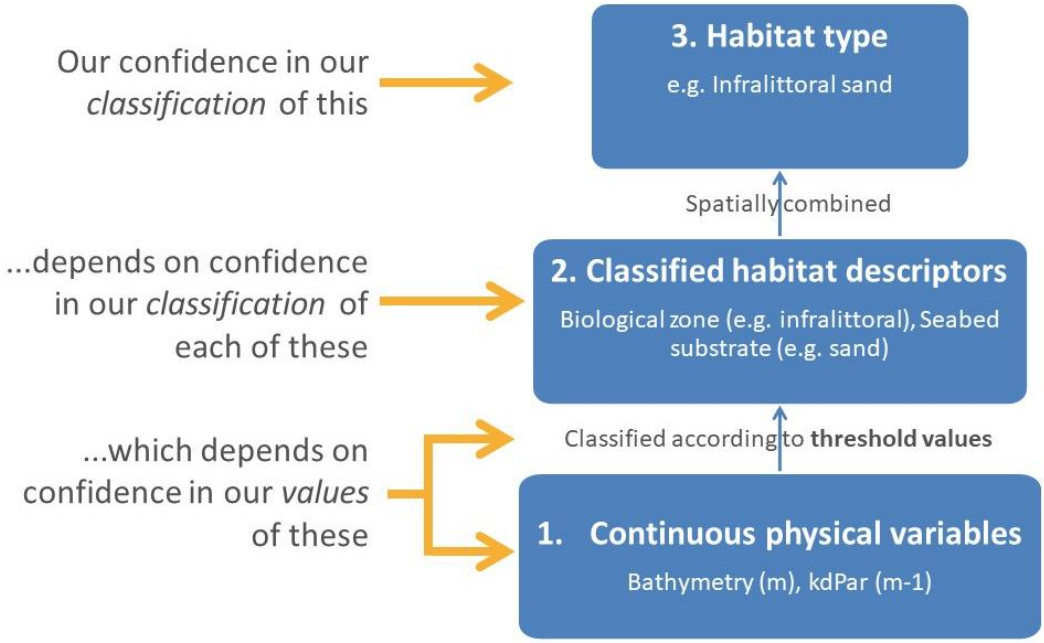

Figure 2. Diagram summarising the three levels of data involved in building the habitat map and how confidence in each layer relates to the confidence of the others (adapted from Populus et al, 2017).

B.1–STEP 1: PREPARING CONTINUOUS PHYSICAL VARIABLE CONFIDENCE

Two continuous variables are involved in the calculation of the biological zone layer: fraction of light at the seabed and bathymetry. As a result, the confidence in these two variables needs to be assessed.

Bathymetry: EMODnet Bathymetry provides a measure of the quality for all datasets that are used to build the digital terrain model (DTM). This is made available in the form of a polygon layer, in which polygons are the spatial extent of the datasets used and a column contains the quality score. As the EUSeaMap confidence assessment is performed in raster mode, the first step is to convert the polygon layer into a raster layer of quality score. The EMODnet Bathymetry quality score is a value in the range [0-100], that we translate into low, medium and high confidence using the thresholds 40 and 70 (table 3).

Table 3. criteria used for categorising the EMODnet Bathymetry quality index (QI) in EUSeaMap qualitative confidence score.

Confidence	Criteria
1 (low)	QI < 40
2 (moderate)	40 ≤ QI < 70
3 (high)	70 ≤ QI

Fraction of light at the seabed: that variable is calculated by intersecting KdPAR (coefficient of light attenuation in the water column) and bathymetry. For KdPar, the number of remote sensing images used to generate the average values recorded in each grid cell is used; the number is translated translate into low, medium and high confidence using the thresholds 29 and 39 (table 4).

Table 4. criteria used for categorising the number of remote sensing images in EUSeaMap qualitative confidence score.

Confidence	Criteria
1 (low)	Number of images < 29
2 (moderate)	29 ≤ Number of images < 39
3 (high)	39 ≤ Number of images

B.2–STEP 2: CREATING BIOLOGICAL ZONE CONFIDENCE MAP

The confidence in the biological zone habitat descriptor is an aggregation of i) the fuzziness in the thresholds used to delineate between two classes and ii) the confidence in continuous physical variables used as input to the biological zone layer calculation.

Using fuzzy membership functions

There are multiple techniques to express the uncertainty around the threshold values that are used to classify continuous physical variables into the various biological zone classes (infralittoral, circalittoral etc.). All techniques are discussed in Populus et al., 2017. We use here fuzzy membership functions. Figure 3 illustrates the fuzzy membership function used to calculate the infralittoral membership, for which a fraction of light threshold value of 0.01 is used to delineate the lower boundary (see section A). The fuzzy membership function shape used is governed by 2 values: X_0=0.001, below which the infralittoral membership is 0, and X_1 = 0.019, above which the infralittoral membership is 1. Between X_0 and X_1, the infralittoral membership increases linearly from 0 to 1.

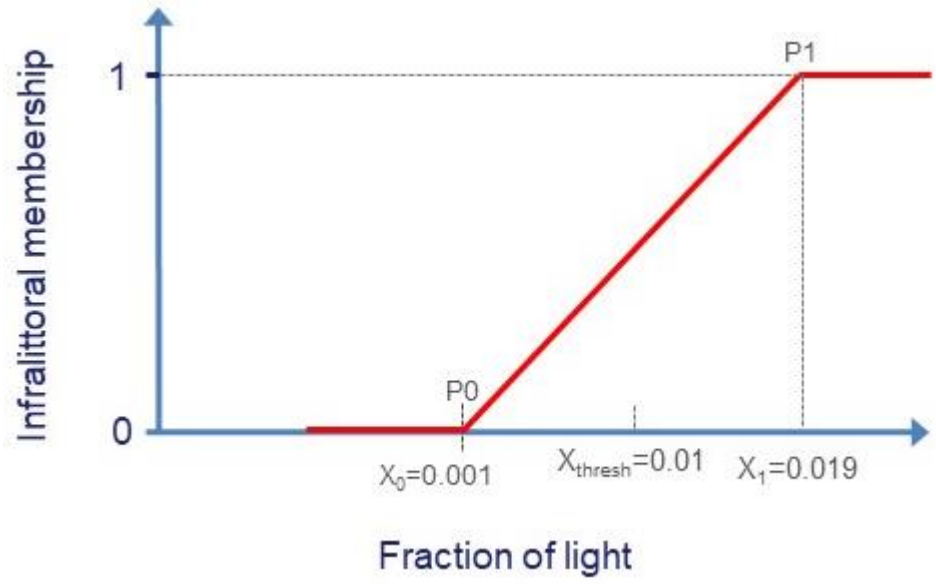

Figure 3. fuzzy membership function used for calculating the infralittoral membership. The shape of the curve is governed by 2 control points, P0 (X_0,0) and P1(X_1,1). X_{thresh} is the threshold value used for creating the biological zone layer (see section A).

Figure 4 illustrates the fuzzy membership functions used to calculate the circalittoral membership. Unlike the infralittoral, which has one boundary only (the one with the circalittoral), the circalittoral zone has two boundaries (an upper one, which is its boundary with the infralittoral, and a lower one which is its boundary with the deep circalittoral). As a result, two fuzzy membership functions are used: i) one for the upper boundary, where circalittoral occurrence is defined by a value of fraction of light at the seabed (the fuzzy membership function is governed by the same values as for the infralittoral, but the other way around as the circalittoral membership decreases with light availability between X_1=0.001 and X_0=0.019), and ii) one for the lower boundary where circalittoral occurrence is defined by a depth value (membership decreases with depth between X_1=-25m and X_0=-35m).

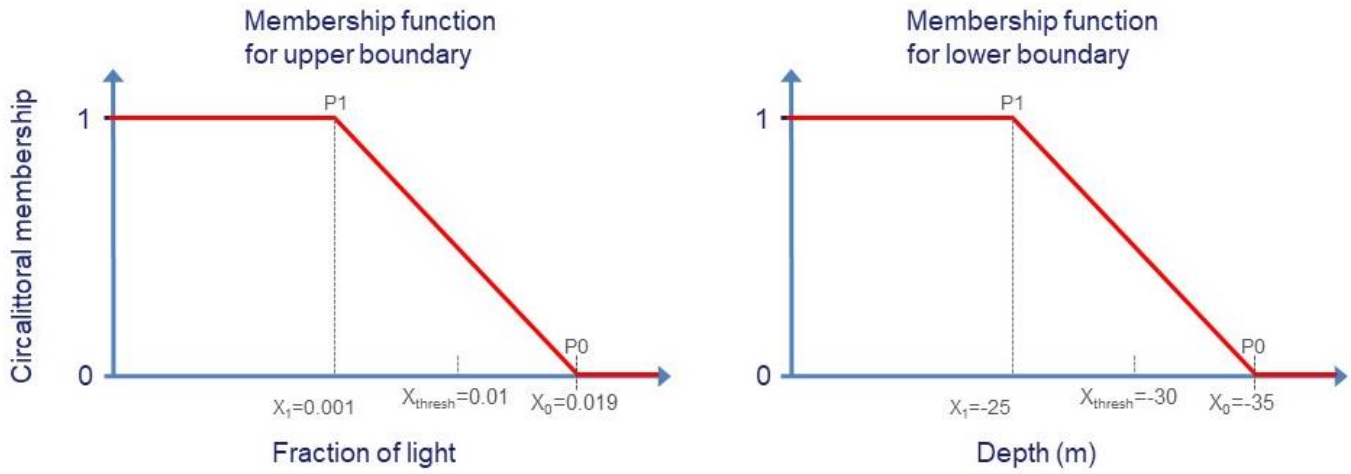

Figure 4. fuzzy membership functions used for calculating the circalittoral membership nearby the upper boundary (left) and the lower boundary (right) of the circalittoral. The shape of the curves is governed by 2 control points, P0 (X_0,0) and P1(X_1,1). X_{thresh} is the threshold value used for creating the biological zone layer (see section A).

Figure 5 illustrates the fuzzy membership function used to calculate the deep circalittoral membership. As the maximum depth of the study in the Beibu Gulf is 50m, the deep circalittoral has only one boundary, the upper one, which is the boundary shared with the circalittoral. As a result, only one fuzzy membership function is used, governed by the same values as for the lower boundary of the circalittoral, but the other way around as the deep circalittoral membership increases with depth between X_0=-25m and X_1=-35m).

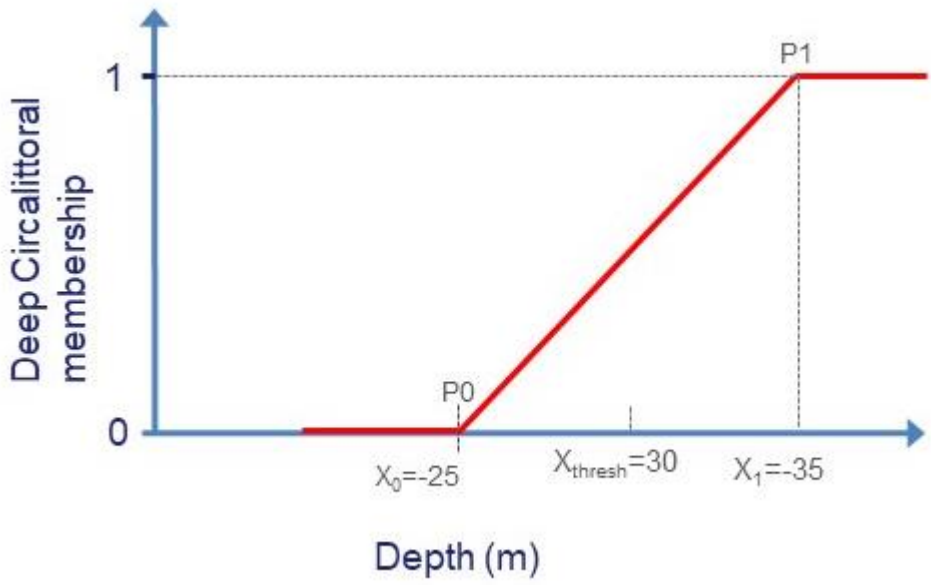

Figure 5. fuzzy membership function used for calculating the deep circalittoral membership nearby the upper boundary. The shape of the curve is governed by 2 control points, P0 (X_0,0) and P1(X_1,1). X_{thresh} is the threshold value used for creating the biological zone layer (see section A).

Classifying fuzzy membership continuous raster into EUSeaMap confidence categorical raster

The raster with continuous values in the range [0-1] which results from the fuzzy membership-based confidence assessment is then classified into the low, moderate and high categories of the EUSeaMap confidence scoring system. Table 5 describes the set of membership thresholds that are used for the classification.

Table 5. criteria used for categorising the fuzzy membership in EUSeaMap qualitative confidence score.

Confidence	Criteria
1 (low)	0.5 ≤ Membership < 0.6
2 (moderate)	0.6 ≤ Membership < 0.8
3 (high)	0.8 ≤ Membership ≤ 1

Calculating overall confidence by combining confidence based on fuzzy membership and confidence in physical variables

In a last step, one single overall confidence raster is created by combining the raster of confidence in physical variables and the fuzzy membership-based confidence raster. This is done for each habitat descriptor class boundary, hence for the circalittoral the combination is done for the upper boundary

(combination of fuzzy membership-based confidence and confidence in variable 'light fraction at the seabed') and the lower boundary (combination of fuzzy membership-based confidence and confidence in variable 'bathymetry'). The logic used for the combination is described in table 6, and can be implemented using the following conditional expressions:

```
If (fuzzy membership confidence = H and physical variables confidence = L) then overall confidence = M

Else if (fuzzy membership confidence = M and physical variables confidence = L) then overall confidence = L

Else overall confidence = fuzzy membership confidence
```

Table 6. Logic used for combining confidence based on fuzzy membership and confidence in physical variables (adapted from Populus et al., 2017)

		Confidence in physical variables		
		H	**M**	**L**
Confidence based on fuzzy membership	**H**	H	H	M
	M	M	M	L
	L	L	L	L

B.3–STEP 3: CREATING SEABED SUBSTRATE CONFIDENCE MAP

Unlike biological zones, the seabed substrate type habitat descriptor has no continuous physical variables involved. The confidence assessment is made at polygon level, following a method used by EMODnet Geology (Kaskela et al., 2019) that considers remote sensing coverage, amount of sampling and distinctiveness of class boundaries. To each polygon of the seabed substrate layer is assigned a total confidence score from 0 to 4. To comply with the EUSeaMap confidence assessment method, the polygon layer is first converted into a raster of seabed substrate confidence score. Then the seabed substrate confidence score is translated in the EUSeaMap confidence score using the rules defined in table 7.

Table 7. criteria used for translating the seabed substrate confidence score in the EUSeaMap confidence score.

Confidence	Criteria
1 (low)	Seabed substrate confidence score < 1
2 (moderate)	1 ≤ Seabed substrate confidence score ≤ 2
3 (high)	2 < Seabed substrate confidence score

B.4–STEP 4: CREATING SEABED HABITAT CONFIDENCE MAP

To obtain a single confidence map for the seabed habitat map, the biological zone and the seabed substrate confidence raster layers are combined, keeping the minimum value of the two layers.

B.5-ARCGIS™ MODEL BUILDER MODELS

4 model builder models are available, one for each above-mentioned step.

Test datasets are provided for a European study area. All the datasets are in the 'input' folder. The models will create all the outputs in the 'output' folder.

B.5.1 - PREPARING CONTINUOUS PHYSICAL VARIABLE CONFIDENCE

<table>
<tr><td>ArcGIS™ Model Builder Model name</td><td colspan="3">Toolset B_Seabed_Habitat_Confidence_Map
Model 1_prepare_continuous_physical_variable_confidence</td></tr>
<tr><td>Descr.</td><td colspan="3">Creates confidence rasters for the bathymetry and the light fraction at the seabed variables.

Bathymetry: converts the bathymetry quality score polygon dataset into a raster (a) and translates the raster into EUSeaMap confidence assessment score (b) according to the criteria mentioned in table 3.

Light fraction at the seabed: translates into EUSeaMap confidence assessment score the number of satellite images (c) according to the criteria mentioned in table 4, and creates the light at the seabed confidence layer (d) by combining bathymetry and kdPAR confidence layers using the average (rounded to the nearest integer). Average values having a decimal part of 5 are rounded up (e.g. 2.5 is rounded to 3).</td></tr>
<tr><td>Inputs</td><td>Model Variable name</td><td>Type</td><td>Description</td></tr>
<tr><td></td><td>Master raster</td><td>Raster dataset</td><td>Raster used as reference by the model for creating new rasters. All output rasters have the same cell size as the master raster, are snapped onto the master raster, and have the same spatial extent as the master raster. Note that the master raster used here was created based on the bathymetry raster.</td></tr>
<tr><td></td><td>Bathymetry Quality polygon layer</td><td>Feature class</td><td>Shapefile containing, for each dataset used to create the DTM raster, a [0-100] combined quality score. The quality values are in the column 'combined'.</td></tr>
</table>

	kdpar image observation number	Raster dataset	The raster containing the number of satellite images used to generate the average kdPAR values.
Output	**Model Variable Name**	**Type**	**Description**
	Bathymetry confidence raster	Raster dataset	Bathymetry confidence raster, with scores in the EUSeaMap confidence scoring system, i.e. a rating of 1 (low confidence), 2 (moderate confidence) or 3 (high confidence).
	Light at seabed confidence raster	Raster dataset	Light at the seabed confidence raster, with scores in the EUSeaMap confidence scoring system, i.e. a rating of 1 (low confidence), 2 (moderate confidence) or 3 (high confidence).
Main ArcGIS™ tools used	•Raster calculator (spatial analyst tools) •Raster to Polygon (Conversion)		

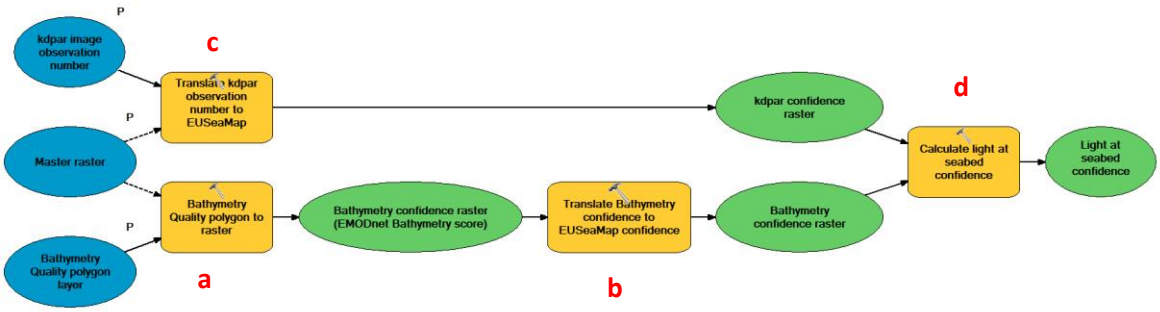

B.5.2 - CREATING BIOLOGICAL ZONE CONFIDENCE MAP

<table>
<tr><td>ArcGIS™ Model Builder Model name</td><td>Toolset B_Seabed_Habitat_Confidence_Map
Model 2_create_biological_zone_confidence</td></tr>
<tr><td>Descr.</td><td>Creates a confidence raster for the biological zone map.

First a fuzzy membership raster is calculated for each biological zone boundary, i.e. for the infralittoral lower boundary (a), the circalittoral upper boundary (b) and circalittoral lower boundary (c), dans the deep circalittoral boundary (d). The minimum and maximum values used for the fuzzy membership functions are those referred to as, respectively, X0 and X1 in figures 3, 4 and 5. These 4 fuzzy membership rasters are then classified into the EUSeaMap confidence scoring system (i.e. 1 for low confidence, 2 for moderate confidence and 3 for high confidence) using the criteria mentioned in table 5 (e,f,g,h). Then for each biological zone boundary, the overall confidence, i.e. the confidence that accounts for both the confidence fuzzy membership-based confidence and the confidence in the relevant physical variable, is calculated: the infralittoral lower boundary and circalittoral upper boundary fuzzy membership-based confidence rasters are combined with the light at the seabed confidence raster (i and j), while the circalittoral lower boundary and deep circalittoral upper boundary fuzzy membership-based confidence rasters are combined with the bathymetry confidence raster (k and l). The circalittoral lower boundary and upper boundary overall confidence rasters are then merged into a single circalittoral overall confidence raster (m). Finally, the infralittoral, circalittoral and deep circalittoral overall confidence rasters are merged into a single biological zone confidence raster (n).</td></tr>
<tr><td>Inputs</td><td>
<table>
<tr><th>Model Variable name</th><th>Type</th><th>Description</th></tr>
<tr><td>Infralittoral / Circalittoral boundary variable</td><td>Raster dataset</td><td>The raster for the variable that is used to model the infralittoral lower boundary and the circalittoral upper boundary. It is a raster of fraction of surface light reaching at the seabed (value in the range [0-1], 1 meaning 100% of the surface light reaches the seabed)</td></tr>
<tr><td>Infralittoral lower boundary membership1 value</td><td>Float</td><td>The fuzzy membership function maximum value used for the infralittoral lower boundary. This value is 0.019</td></tr>
</table>
</td></tr>
</table>

	Infralittoral lower boundary membership0 value	Float	The fuzzy membership function minimum value used for the infralittoral lower boundary. This value is 0.001
	Circalittoral upper boundary membership1 value	Float	The fuzzy membership function maximum value used for the circalittoral upper boundary. This value is 0.001
	Circalittoral upper boundary membership0 value	Float	The fuzzy membership function minimum value used for the circalittoral upper boundary. This value is 0.019
	Circalittoral / Deep circalittoral boundary variable	Raster dataset	The raster for the variable that is used to model the circalittoral lower boundary and the deep circalittoral upper boundary. It is a raster of depth
	Circalittoral lower boundary membership1 value	Float	The fuzzy membership function maximum value used for the circalittoral lower boundary. This value is -25m
	Circalittoral lower boundary membership0 value	Float	The fuzzy membership function minimum value used for the circalittoral lower boundary. This value is -35m
	Deep circalittoral upper boundary membership1 value	Float	The fuzzy membership function maximum value used for the circalittoral lower boundary. This value is -35m
	Deep circalittoral upper boundary membership0 value	Float	The fuzzy membership function minimum value used for the circalittoral lower boundary. This value is -25m
Output	**Model Variable Name**	**Type**	**Description**
	Biozone overall confidence	Raster dataset	The biological zone confidence raster
Main ArcGIS™ tools used	• Fuzzy membership (spatial analyst tools) • Raster calculator (spatial analyst tools) • Mosaic to new raster (data management)		

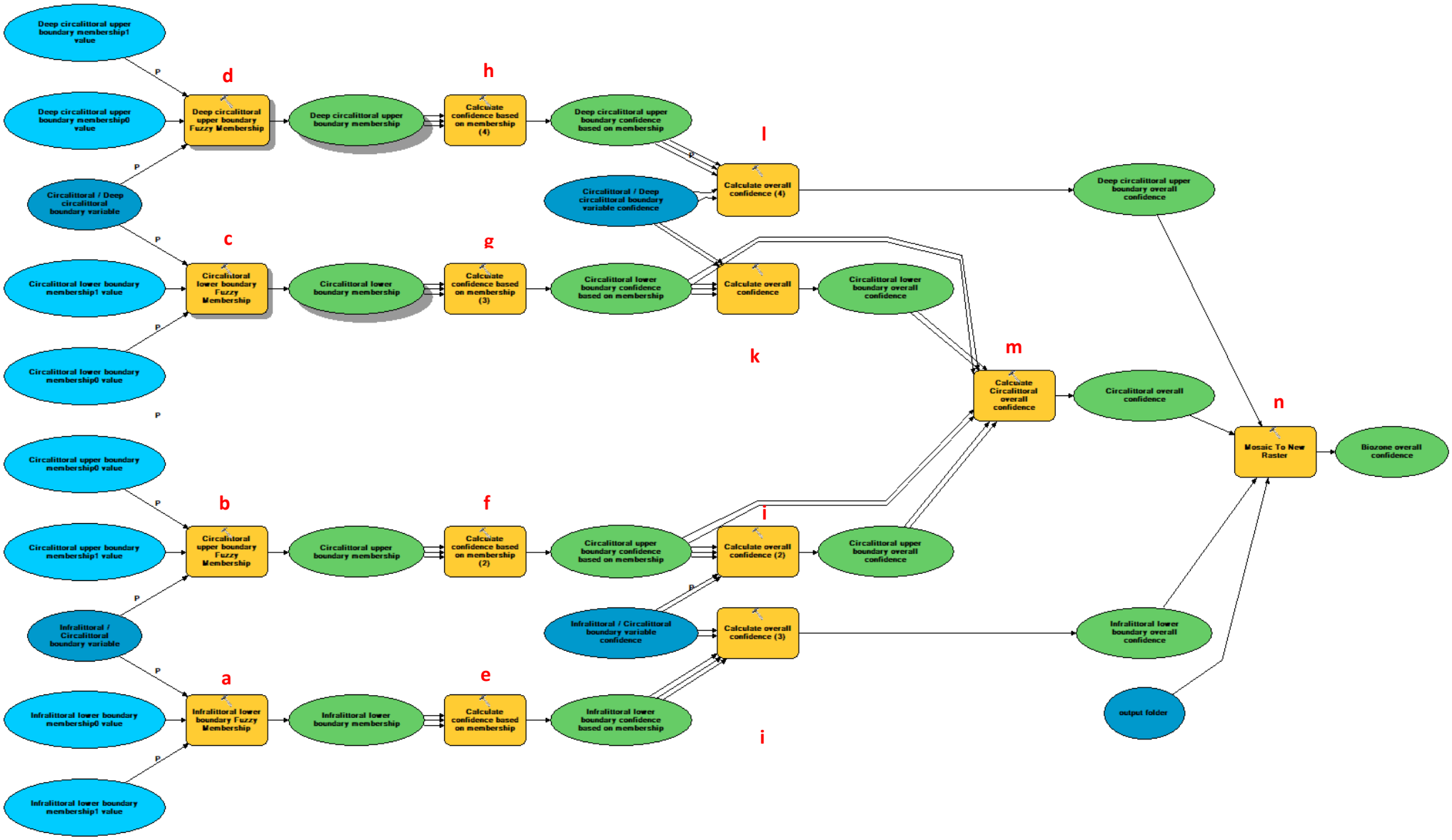

The project “International Ocean Governance: Strengthening international ocean data through the EU’s ocean diplomacy with China” is financed by the European Commission EuropeAid/139904/DH/SER/CN.

B.5.3 - CREATING SEABED SUBSTRATE CONFIDENCE MAP

<table>
<tr><td>ArcGIS™ Model Builder Model name</td><td colspan="3">Toolset B_Seabed_Habitat_Confidence_Map
Model 3_create_seabed_substrate_confidence</td></tr>
<tr><td>Descr.</td><td colspan="3">Creates a confidence raster for the seabed substrate map.
The input polygon layer, a column of which contains seabed substrate confidence expressed in the EMODnet Geology confidence scoring system (i.e. a value in the range [0,1,2,3,4]), is converted into a confidence raster (a). Then the seabed substrate confidence score is translated into the EUSeaMap confidence score using the rules defined in table 7 (b).</td></tr>
<tr><td>Inputs</td><td>Model Variable name</td><td>Type</td><td>Description</td></tr>
<tr><td></td><td>Master raster</td><td>Raster dataset</td><td>Raster used as reference by the model for creating new rasters. All output rasters have the same cell size as the master raster, are snapped onto the master raster, and have the same spatial extent as the master raster. Note that the master raster used here was created based on the bathymetry raster.</td></tr>
<tr><td></td><td>Seabed Substrate polygon layer</td><td>Feature class</td><td>Shapefile class in which a [0,1,2,3,4] EMODnet Geology confidence score is assigned to each seabed substrate polygon. The confidence values are in the column ‘CONF_TOT’.</td></tr>
<tr><td>Output</td><td>Model Variable Name</td><td>Type</td><td>Description</td></tr>
<tr><td></td><td>Seabed Substrate confidence raster</td><td>Raster dataset</td><td>Seabed Substrate confidence raster, with scores in the EUSeaMap confidence scoring system, i.e. a rating of 1 (low confidence), 2 (moderate confidence) and 3 (high confidence)</td></tr>
<tr><td>Main ArcGIS™ tools used</td><td colspan="3">•Raster calculator (spatial analyst tools)
•Raster to Polygon (Conversion)</td></tr>
</table>

The project “International Ocean Governance: Strengthening international ocean data through the EU’s ocean diplomacy with China” is financed by the European Commission EuropeAid/139904/DH/SER/CN.

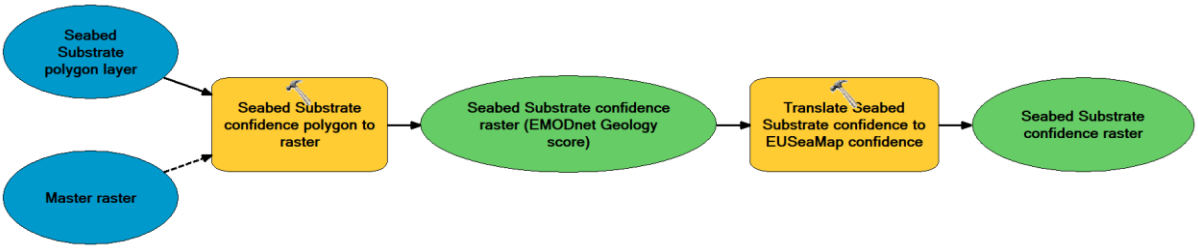

B.5.4 - CREATING SEABED HABITAT CONFIDENCE MAP

ArcGIS™ Model Builder Model name	Toolset *B_Seabed_Habitat_Confidence_Map* Model *4_create_seabed_habitat_map_confidence*		
Descr.	Creates the confidence raster for the seabed habitat map. The biological zone and the seabed substrate confidence raster layers are combined, keeping the minimum value of the two layers.		
Inputs	**Model Variable name**	**Type**	**Description**
	Seabed Substrate Confidence	Raster dataset	The seabed substrate confidence raster created in B.5.3
	Biological Zone Confidence	Raster dataset	The biological zone confidence raster created in B.5.2
Output	**Model Variable Name**	**Type**	**Description**
	Seabed Habitat Confidence	Raster dataset	Seabed habitat confidence raster, with scores in the EUSeaMap confidence scoring system, i.e. a rating of 1 (low confidence), 2 (moderate confidence) and 3 (high confidence)
Main ArcGIS™ tools used	•Cell statistics (spatial analyst tools)		

The project "International Ocean Governance: Strengthening international ocean data through the EU's ocean diplomacy with China" is financed by the European Commission EuropeAid/139904/DH/SER/CN.

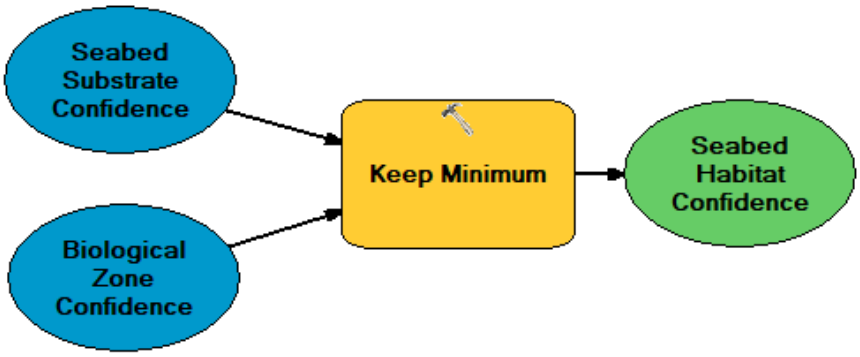

5.2.1 References

EMODnet, 2017. High Resolution Seabed Mapping WP1: Data provider contribution - Completing metadata elements for the generation of the Quality Index for the EMODnet DTM. Service Contract No. EASME/EMFFM2016/005

Kaskela, A.M., Kotilainen, A.T., Alanen, U., Cooper, R., Green, S., Guinan, J., van Heteren, S., Kihlman, S., Van Lancker, V., Stevenson, A., the EMODnet Geology Partners, 2019. Picking Up the Pieces—Harmonising and Collating Seabed Substrate Data for European Maritime Areas. Geosciences 9, 84. https://doi.org/10.3390/geosciences9020084

Populus, J., Vasquez, M., Albrecht, J., Manca, E., Agnesi, S., Al Hamdani, Z., Andersen, J., Annunziatellis, A., Bekkby, T., Bruschi, A., Doncheva, V., Drakopoulou, V., Duncan, G., Inghilesi, R., Kyriakidou, C., Lalli, F., Lillis, H., Mo, G., Muresan, M., Salomidi, M., Sakellariou, D., Simboura, M., Teaca, A., Tezcan, D., Todorova, V., Tunesi, L., 2017. EUSeaMap. A European broad-scale seabed habitat map. https://doi.org/10.13155/49975

5.3 Appendix III: EMODPACE/ CEMDNET Joint activities

5.3.1 Joint activities related to Task 4.1: Seabed habitat mapping.

The following joint activities were carried out as part of the EMODPace /CEMDNet collaboration:

JA 4.1.1 Literature review

a. NMDIS and EU partners discuss options and decided on a study area.

b. NMDIS mainly focused on reviewing Chinese literature of what work has gone before and ecology of the area, i.e. which benthic communities or biogenic habitats occur there and what are the environmental factors and seabed substrate that drive the distribution of the communities.

c. JNCC mainly focused on reviewing English language literature of what work has gone before and ecology of the area, i.e. which benthic communities or biogenic habitats occur there and what are the environmental factors and seabed substrate that drive the distribution of the communities.

d. NMDIS and EU partners jointly prepared a short report based on literature review (see Deliverable 4.1).

JA 4.1.2 Data collation and preparation – depth to the seabed

a. NMDIS provided an inventory of best available depth to the seafloor (bathymetry) data and data products available to Task 4.1, including details on use restrictions and metadata;

b. Ifremer provided specification for the bathymetry data in the area of interest.

c. NMDIS collated best available bathymetry data and data products for the area of interest, even if restricted for use by EU partners;

d. SHOM and EOMAP investigated available of other source of bathymetry data for the area of interest and provide the data;

e. NMDIS (with assistance from SHOM and EOMAP where required) created a full-coverage gridded dataset of bathymetry for the basin of interest, using the best available data at 200m resolution.

In addition, NMDIS with EU partners support tested the satellite derived bathymetry methods to improve bathymetry maps quality in very shallow waters.

JA 4.1.3 Data collation and preparation – seabed substrate.

a. NMDIS provided an inventory of substrate (rock, sediment) and biogenic habitat data and data products available to Task 4.1, including details on use restrictions and metadata.

b. NMDIS/JNCC/Ifremer and GTK defined on a list of biogenic habitat data to include in the substrate maps .

c. NMDIS collated best available substrate data and data products for the area of interest;

d. JNCC/ NMDIS and GTK investigated availability of biogenic (JNCC) and non-biogenic (GTK) sources of substrate data for the area of interest from global repositories and other sources.

e. NMDIS with the support of GTK and JNCC worked with available data from NMDIS and global sediment/coral data products to deliver a harmonized substrate map of the study area with the maximum coverage possible.

JA 4.1.4 Data collation and preparation – optical properties -PAR (photosynthetically active radiation) and KdPAR (PAR diffuse attenuation coefficient).

a. Ifremer provided specifications for the required datasets;

b. EOMAP worked with available Sentinel satellite data to deliver a gridded dataset of PAR at the sea surface and a gridded dataset of KdPAR for the area of interest and associated confidence layers.

a. NMDIS combined KdPAR dataset produced by EOMAP with the bathymetry data to produce a full-coverage gridded dataset of PAR average at the seabed for the area of interest, with assistance from ifremer.

JA 4.1.5 Data collation and preparation – biological observations and other explanatory variables

a. NMDIS provided an inventory of biological data and data products available to Task 4.1, including details on use restrictions and metadata;

b. SMHI/Ifremer/AZTI/ JNCC/NMDIS jointly reviewed data available and progress and decided what biological data to use for thresholds based on expert knowledge of NMDIS colleagues, literature review and outcomes of task 4.1.5a and 4.1.5b;

c. SMHI Created a script and guidelines for NMDIS to use the script to extract benthic species observation data from the OBIS repository – if data because available in the future. The script can be adapted to be run in other areas, where species data can be extracted.

JA 4.1.6 First draft report on choice of test areas

a. JNCC prepared, with the support of all partners, a short summary report summarizing choice of test areas, identification of data requirements and list of required data and data already gathered and NMDIS to review.

JA 4.1.7 Identify ecologically-relevant thresholds for classifying the explanatory variables

a. We planned that depending on outcomes of Task 4.1.5, SMHI/Ifremer/AZTI and JNCC would run statistical models to fit thresholds using statistical methods when feasible and data would allow it, for each habitat descriptor category. However biological data was not suitable for the task and we used values from literature and expert judgement of NMDIS colleagues.
b. Ifremer shared guidance and R code on statistical analysis that NMDIS could apply in the future once/if data become available.

JA 4.1.8 Classify input data products and combine classified outputs into a single broad-scale habitat map

a. Ifremer (with JNCC support) provided guidance, adapted the coded NMDIS on d he use of the broad-scale model.

b. NMDIS (with Ifremer support) adapted the GIS workflow provided and model, and run it to produce a biological zone and a broad-scale habitat for the study area;

c. Ifremer (with JNCC support) provided guidance and model code on methodology for confidence assessment, based on final choice if input layers.

d. NMDIS provided information (quantitative or qualitative data) helped assess confidence on input datasets (substrate, bathymetry, and relevant explanatory variables).

e. NMDIS delivered a confidence map for the input data products (substrate, bathymetry, and relevant explanatory variables) and the output data products (biological zones and -if relevant- other habitat descriptors, and the final broad-scale habitat map);

g. JNCC liaised with WP1 colleagues and published the Open data products on the EMODpace/CEMDNET JNCCportal. NMDIS to liaise with colleague to publish and managed WMS services for the final substrate, biological zone and habitat map (and associated confidence map).

JA 4.1.09 Draft report ((Deliverable 4.2)

a. JNCC, with NMDIS and EU partners input, produced a draft joint report on methodologies used (Deliverable 4.2) , listing and describing input data for the first draft of the broad-scale habitat map in the Beibu Gulf.

JA 4.1.10 Assess the EU habitat mapping method and suitability of the EUNIS classification in basin of interest

a. NMDIS, and EU partners had a remote workshop where suitability of the broad-scale habitat mapping method to a Chinese sea was discussed.

JA 4.1.11 Draft report (Deliverable 4.4)

a. JNCC led on, and all contributed to a final report (Deliverable 4.4.) describing the mapping method and the suitability of EUNIS approach to China, showing a single sea basin as an example.

5.3.2 Joint deliverables

All deliverables were prepared jointly by EU partners and NMDIS. The deliverable writing is jointly led by one EU partner and NMDIS. The leading EU partner will initiate the writing with a frame of each deliverable.

The deliverables are:

- Deliverable 4.1. Internal work document Short summary report summarizing choice of test areas, identification of data requirements and list of required data and data already gathered (Due M12) JNCC, NMDIS, Ifremer, AZTI, SMHI, SHOM, EOMAP, GTK.

- Deliverable 4.2. Internal work document Draft report describing the mapping method and the suitability of EUNIS approach to China, showing a single sea basin as an example (Due M24) JNCC, NMDIS, Ifremer, AZTI, SMHI, SHOM, EOMAP, GTK .

- Deliverable 4.4. Public - Final report describing the mapping method and the suitability of EUNIS approach to China, showing a single sea basin as an example (Due M.30) (JNCC, NMDIS, Ifremer, AZTI, SMHI, SHOM, EOMAP, GTK.

- An extra joint deliverable was agreed in May 2022 - Public Guide for creating a seabed habitat map and accompanying confidence map using the EUSeaMap approach)- NMDIS lea, EU partners contributed.